Characterization and Dynamics of Pyrene and Gamma-Cyclodextrin Complexes of Multiple Stoichiometries

by

Andria Sara Marie Dyck
B.Sc., University of Saskatchewan, 1998

A Thesis Submitted in Partial Fulfillment of the
Requirements for the Degree of

Master of Science

in the Department of Chemistry

We accept this thesis as conforming
to the required standard

[redacted]

Dr. Cornelia Bohne, Supervisor (Department of Chemistry)

[redacted]

Dr. Thomas M. Fyles, Departmental Member (Department of Chemistry)

[redacted]

Dr. Richard Keeler, Outside Member (Department of Physics and Astronomy)

[redacted]

Dr. David A. Harrington, External Examiner (Department of Chemistry)

Supervisor: Dr. Cornelia Bohne

Abstract

The pyrene/ γ-CD supramolecular guest/ host system was characterized using several photophysical techniques, and the dynamics were investigated using the stopped-flow technique with fluorescence detection. This study was undertaken in order to better understand the dynamics involved in supramolecular systems containing complexes of multiple stoichiometry. In addition, the methodologies used in this study may be employed in future studies investigating the dynamics of other guest: CD supramolecular systems containing multiple stoichiometric complexes.

The techniques used to characterize the system included absorption spectroscopy, fluorescence emission and excitation spectroscopy, quenching of the excited state using the iodide ion, and time-resolved spectroscopy. Results from these various techniques indicate that the supramolecular pyrene: γ-CD complexes that are present are the 1:1, 1:2, and 2:2 complexes. Using a step-wise formation mechanism, the equilibrium constants are found to be 325 ± 25 M^{-1}, 110 ± 30 M^{-1}, and (1.5 ± 0.5) x 10^{6} M^{-1} for these complexes, respectively (at 20 ° C).

The dynamics of the pyrene: γ-CD system were found to be quite complex. At lower host concentrations and at shorter time-bases, i.e. less than ~ 10 x 10^{-3} M γ-CD and around 200 ms, respectively, the kinetics were semi-quantitatively explained by a dimerization model. The association rate constant for this process is found to be of the order of 10^{7} $M^{-1}s^{-1}$, whereas the dissociation rate constant is approximately 10 to 10^{2} s^{-1}. At higher host concentrations, the kinetics were more complex at longer time-scales, i.e.

> 100 ms to the minute time-scale. This was qualitatively found to be a result of the dynamics of the 1:2 complex.

Examiners:

[redacted]

Dr. Cornelia Bohne, Supervisor (Department of Chemistry)

[redacted]

Dr. Thomas M. Fyles, Departmental Member (Department of Chemistry)

[redacted]

Dr. Richard Keeler, Outside Member (Department of Physics and Astronomy)

[redacted]

Dr. David A. Harrington, External Examiner (Department of Chemistry)

TABLE OF CONTENTS

PRELIMINARY PAGES

LIST OF TABLES

LIST OF FIGURES

LIST OF SCHEMES

List of Abbreviations

a_i	pre-exponential factor of component, i
Å	Ångstrom (1×10^{-10} m)
CD	cyclodextrin
c_n	final equilibrium concentration of species, n
Δc_n	change in concentration of species, n
ε	molar absorption coefficient (M^{-1} cm^{-1})
f	fluorescence
h	hour
HOMO	highest occupied molecular orbital
h	Plank's constant (6.626×10^{-34} Joule seconds)
I	intensity
I, III	peak 1 (0-0 transition) and peak 3, respectively, in the pyrene fluorescence emission spectrum
I^-	iodide ion
IC	internal conversion
IRF	instrument response function
ISC	intersystem crossing
k_o	intrinsic decay rate constant
k^o_f	rate constant for natural fluorescence
k_{obs}	observed rate constant
k^o_r	natural radiative rate constant

k_q	quenching rate constant
k_+	association rate constant
k_-	dissociation rate constant
K_{eq}	equilibrium constant
$K_{n:n}$	equilibrium constant for n:n guest: host complex
K_{SV}	Stern-Volmer constant
λ	wavelength (nm)
λ_{em}	emission wavelength
λ_{ex}	excitation wavelength
LUMO	lowest unoccupied molecular orbital
M	mole/litre
MCA	multichannel analyzer
$[M^*]$	concentration of excited state molecule, M
n	non-bonding
nr	non-radiative
n:n	stoichiometry of guest: host complex
PMT	photomulitiplier tube
PPO	2,5- Diphenyloxazole
Py	pyrene
Q	quencher
ϕ_f	fluorescence quantum yield
r	radiative
R_m	monomer intensity ratio

R(I/III)	ratio of emission intensities of peaks I and III in pyrene's fluorescence emission spectrum
s	second
S_o	singlet ground state
S_n	n^{th} excited singlet state
SPC	single-photon counting or single-photon counter
t	time
TAC	time-to-amplitude converter
T_n	n^{th} excited triplet state
τ	lifetime (photophysics terminology) or relaxation time (relaxation kinetics terminology)
$<\tau>$	average lifetime
τ_o	intrinisc lifetime (in the absence of quencher in Stern-Volmer analysis)
τ_{obs}, τ_i	observed lifetime (of component, i)
τ^o_r	natural radiative lifetime
ν	frequency (s^{-1})

ACKNOWLEDGEMENTS

I would like to express thanks to several people who assisted me throughout the undertaking of this thesis. My gratitude goes out to Cornelia Bohne, my supervisor, who guided and motivated me in my research; other members of the research group, including Luis Netter, for their ideas and support; to special friends and family members who supported me in both words and actions.

1. Introduction

1.1 Photophysics

The interaction of light with matter has the potential to alter the nature of the material. For example, it may induce a chemical reaction or change the quantum states of a molecule. The former case is referred to as photochemistry, whereas the latter is photophysics. Knowledge of the photophysics of molecules, or how light interacts and alters the quantum states, may lead to information not only on the mechanism of photochemical reactions, but may also allow one to study the chemical nature of complex systems.

1.1.1 Photophysical processes

Molecules undergo photophysical processes upon the interaction with light of certain energy. Depending on the energy of the light used, different transitions are possible. The energy of light most commonly used to induce electronic transitions in organic molecules is that in the ultra-violet (UV) and visible regions of the electromagnetic spectrum. Smaller amounts of energy are required for rotational and vibrational transitions. The specific interaction between a particular molecule with light occurs only if the light energy, or quantized packet called a photon, equals the difference in electronic energy levels of the molecule. As indicated by Equation 1-1, this change in energy is related to *h*, Plank's constant (6.626×10^{-34} J x s); ν, the frequency of the light (s^{-1}); c, the speed of light (3.0×10^{8} m/s); and λ, the wavelength of the light.

$$\Delta E = h\nu = {}^{hc}/_{\lambda}$$

Equation 1-1

When absorption of light occurs, the electron in the lower energy level ground-state is promoted or energized to a higher energy level. In closed-shell organic molecules, the ground-state energy level, which is the highest occupied molecular orbital (HOMO), is often a bonding σ, π or non-bonding (n) orbital. The upper energy level, which is the lowest unoccupied molecular orbital (LUMO), is usually an anti-bonding σ^* or π^* orbital[1]. The most common transition for alkenes, alkynes, and aromatic molecules is the $\pi \rightarrow \pi^*$ transition, whereas compounds containing a carbonyl group often undergo $n \rightarrow \pi^*$ transitions. Upon the absorption of light, or the promotion of electron(s) to higher energy levels, deactivation back to the ground state may occur through a number of processes, including radiative or non-radiative decay (Figure 1-1). Which of these processes occurs depends on factors including the aforementioned specific electronic state of the individual molecule, solvent interactions, or the presence of other molecules.

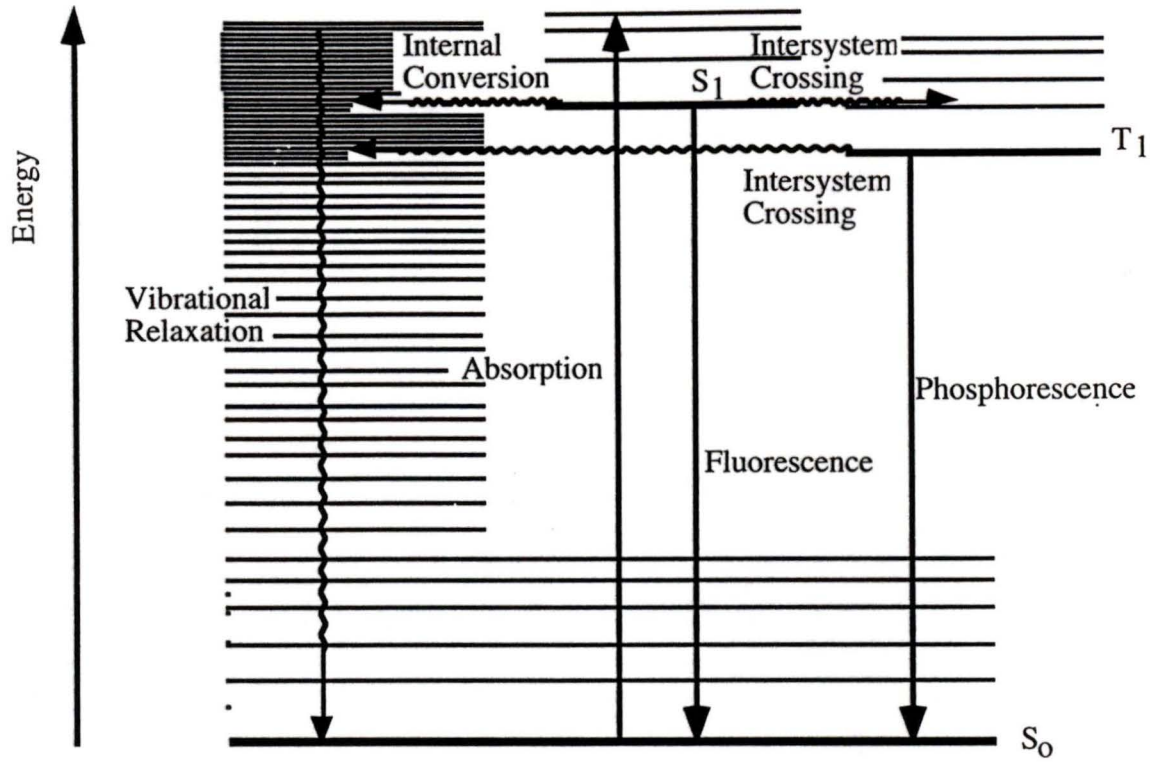

Figure 1-1: Jablonski Energy Diagram: Radiative processes include absorption, fluorescence, and phosphorescence; non-radiative processes include internal conversion, intersystem crossing, and vibrational relaxation.

All of the processes depicted in Figure 1-1 are unimolecular in nature. The radiative transitions are absorption, fluorescence, and phosphorescence, and will be discussed in more detail in the next section. The non-radiative processes include vibrational relaxation, internal conversion and intersystem crossing. Vibrational relaxation occurs between vibrational levels of the same electronic state, e.g. between v = 2 → v = 0 of S_0. In solution, this occurs very rapidly ($<10^{-11}$ s)[2] due to collisions with solvent. Internal conversion occurs between different electronic states of the same multiplicity, e.g. $S_1 \rightarrow S_0$. Intersystem crossing is a forbidden non-radiative process that occurs between different electronic states of different multiplicity, e.g. $T_1 \rightarrow S_0$.

1.1.2 Steady state measurements of unimolecular processes

1.1.2.1 Absorption spectra

The probability for light absorption to occur is related to factors such as the exact energy of the light and the strength of the transition, i.e. there is a larger probability of absorption to occur for an allowed transition than a forbidden transition. The likelihood of absorption also depends on the polarizability of the molecule, or how well the electron density is distortable. This is because as light interacts with the molecule it induces a dipole moment in the electron cloud, i.e. "promotes" an electron from one type of orbital to another. The probability of the transition is expressed in the molar absorption coefficient, ε, which is included in the Beer-Lambert absorption law used when experimentally measuring absorption (Equation 1-2). The other terms involved in the equation include I_o, the intensity of incident light; I, the intensity of transmitted light; c, the concentration of the absorbing species; l, the pathlength through which the light travels.

$$A = -\log(I_o/I) = \varepsilon c l$$

Equation 1-2

The absorption spectrum is related to the difference between the molecule's excited state and ground state structures, the molecule's rigidity, and solvent interactions. According to the Frank-Condon principle, the strongest electronic transition is where there is the largest overlap of vibrational wavefunctions between the ground and excited

states. The energy at which this occurs depends on the difference between a molecule's ground and excited state structure. For example, this occurs at a lower energy if there is little change in nuclear configuration between the two structures as opposed to if they differ considerably. A second factor influencing the spectrum is the molecule's rigidity. A rigid molecule, having fewer vibrations and therefore fewer ground state configurations, is more likely to have a vibrationally structured absorption spectrum when compared to a flexible molecule. However, the absorption spectra of solutions often do not have vibrational fine structure due to de-population of the vibrational excited states as a result of the interactions between solvent and the excited state molecule.

1.1.2.2 Fluorescence emission spectra

Fluorescence is a radiative deactivation process that occurs between electronic states of the same multiplicity, e.g. $S_1 \rightarrow S_0$ (Figure 1-1). This opposes phosphorescence which occurs between electronic states of different multiplicity, e.g. $T_1 \rightarrow S_0$. The former process is allowed whereas the latter deactivation transition is forbidden according to spin selection rules, although it does occur due to spin-orbit coupling. As a result, phosphorescence is a much weaker transition than fluorescence, and occurs over a much longer time period making it experimentally more challenging to measure.

Experimentally, fluorescence emission is measured by keeping a constant excitation energy and monitoring the intensity at various emission wavelengths. Fluorescence emission most often occurs from the lowest vibrational level of the excited electronic state because vibrational relaxation to this level is a very fast process. The result of fast vibrational relaxation in the excited electronic state is that emission occurs

at a lower energy, i.e. longer wavelength, than its corresponding absorption energy (see Figure 1-1). Radiative decay from $v = 0$ of S_1, for example, may drop the electron to any of the vibrational levels of S_0. As such, the emission spectrum may contain vibrational fine structure. A shift in the peak maxima of absorption and emission spectra, also known as the Stokes shift, indicates the difference in nuclear location or overall structure between the ground state and excited state species. For example, a large Stokes shift usually indicates that the structure of the excited state is very different from that in the ground state.

1.1.2.3 Fluorescence excitation spectra

Excitation spectra differ from fluorescence spectra in that the former monitors excitation wavelength or energy as a function of constant emission wavelength, whereas the latter monitors emission energy as a function of constant excitation energy. In other words, by monitoring a particular emission wavelength, the probability of absorption or excitation of a molecule to an excited state capable of emitting at that frequency of radiation is related to the intensity in the excitation spectrum. Excitation spectra are useful in determining whether more than one species are present in solution. This differentiation between species can only occur, however, when the emission spectra of the two species differ in energy. By monitoring different emission wavelengths, i.e. unique to each species, one obtains a simulated absorption spectrum which is the excitation spectrum of that particular species. This differs from the absorption spectrum which always corresponds to the sum of the absorption of the two species.

1.1.3 Kinetics of unimolecular processes

1.1.3.1 Lifetimes

The absorption of light occurs very rapidly. Deactivation kinetics, however, commonly occur on the nanosecond to microsecond time scale, which is experimentally measureable using several instruments. The time taken for deactivation to occur is an important source of information about the molecule's reactivity and the environment around it.

The time taken for the concentration of an excited species to fall to 1/e of its initial value is known as its lifetime, τ. The "natural" radiative lifetime is the time taken for radiative decay of an excited species to occur in the absence of any other competitive process, such as internal conversion and intersystem crossing. Its disappearance is a first order process, i.e. depends on the first power of $[M^*]$ (Equation 1-3)[1].

$$\frac{-d}{dt}[M^*] = k_r^o[M^*]$$

Equation 1-3

The radiative rate constant, k_r^0, may indicate either one of the radiative processes, i.e fluorescence or phosphorescence. The "natural" radiative lifetime, τ_r^0, measured in seconds, is the inverse of k_r^0 (s^{-1}).

The experimentally determined deactivation kinetics involves all processes of the system, including both radiative (r) and non-radiative (nr) decay pathways. That is, the "intrinsic" decay rate constant, k_0, is given by Equation 1-4.

$$k_o = k_r^o + k_{nr}$$

Equation 1-4

If the radiative process is fluorescence, and the non-radiative processes are intersystem crossing (ISC) and internal conversion (IC), the rate law for the disappearance of [M*] is given in Equation 1-5.

$$\frac{-d}{dt}[M^*] = (k_f^o + k_{ISC} + k_{IC})[M^*] = k_o[M^*]$$

Equation 1-5

Integration of Equation 1-5 leads to Equation 1-6 where $[M^*]_0$ is the initial concentration of the excited species.

$$[M^*] = [M^*]_o \exp^{-k_o t}$$

Equation 1-6

The measured fluorescence lifetime (Equation 1-7) is the inverse of the intrinsic decay rate constant, k_0. For most organic molecules, this value is on the nanosecond time scale.

$$\tau_o = \frac{1}{(k_f^o + k_{ISC} + k_{IC})} = \frac{1}{k_o}$$

Equation 1-7

1.1.3.2 Quantum Yields

The fluorescence quantum yield, ϕ_f, is given as the number of photons emitted as fluorescence relative to the total number of photons absorbed. In terms of rate constants, this may be presented as Equation 1-8.

$$\phi_f = \frac{k_f^o}{(k_f^o + k_{nr})} = k_f^o \tau_o$$

Equation 1-8

1.1.4 Time resolved fluorescence emission measurements: Single photon counting

Fluorescence lifetimes are measured using the time-correlated single photon counting technique. This is a measure of fluorescence in the time domain, rather than the energy domain as in steady state fluorescence measurements. It is a very informative technique, as it is highly sensitive and differentiation between species is possible. This is especially useful in supramolecular systems which are quite heterogeneous, as it is possible to differentiate between species with similar steady-state emission spectra but different lifetimes. A schematic diagram of a single photon counter is shown in Figure 1-2.

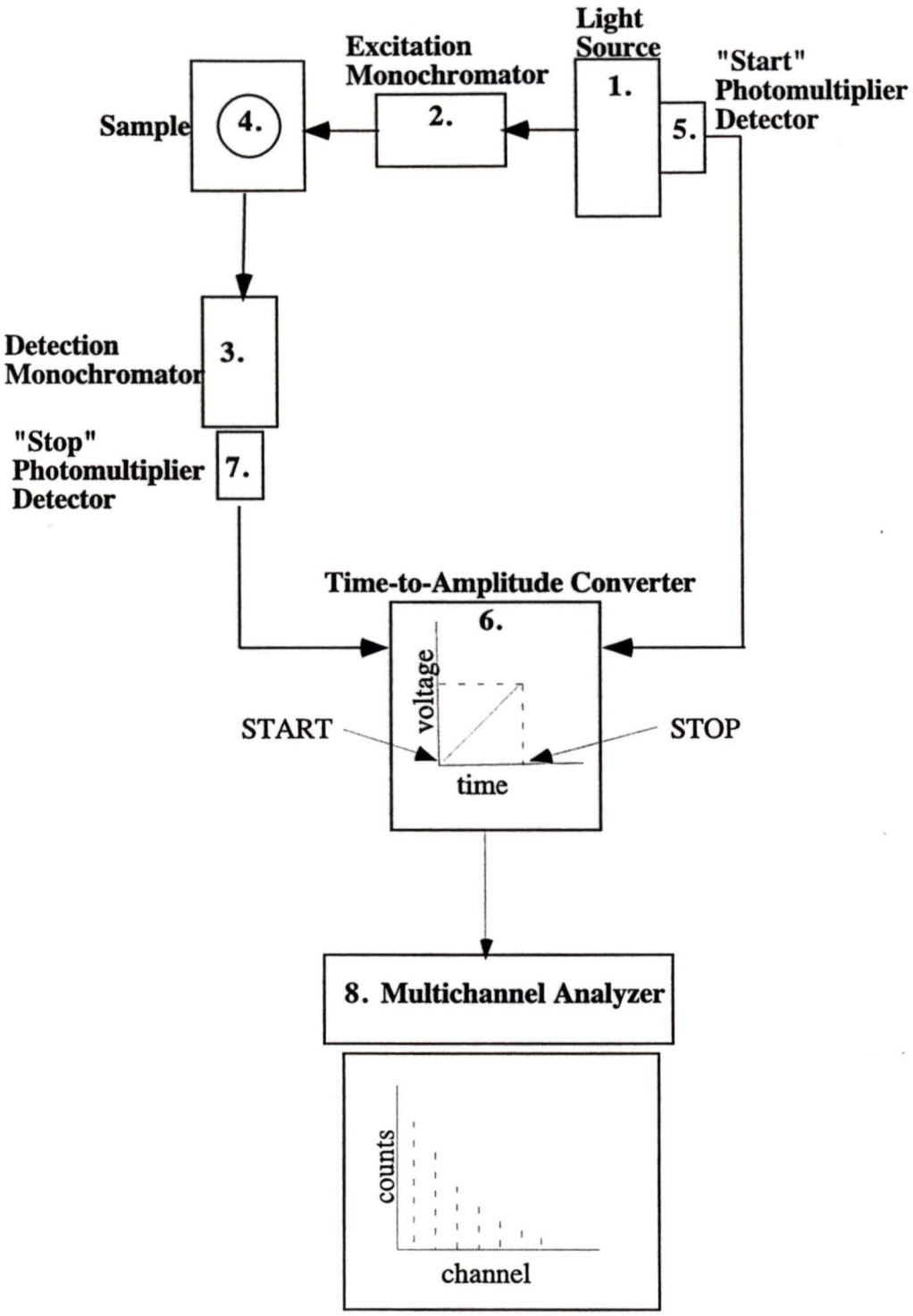

Figure 1-2: A schematic representation of a single photon counter adapted from reference 3. See text for explanation of parts corresponding to the appropriate number as illustrated in the figure.

The light source (1.) in a single photon counter is often a flash lamp that uses various gases, such as N_2 or H_2. The duration of the pulse is around 2 ns. This is an important limiting factor in determining the time resolution of measureable lifetimes using this technique. The excitation and emission wavelengths used are set using two different monochromators (2. and 3.). Upon excitation of the sample (4.), the photomultiplier (PMT) detector attached to the excitation source (5.) is simultaneously triggered resulting in an electrical signal which is sent to the time-to-amplitude converter (TAC) (6.). Once the 'start' trigger is detected by the TAC, a voltage ramp that is linear with time begins. Emission of the first photon from the sample is then detected by a second PMT (7.). This sends a 'stop' signal to the TAC, and the voltage difference between the start and stop triggers is related to a time delay. A count is then stored in the pre-calibrated multichannel analyzer, MCA (8.) in the appropriate channel that corresponds to the time delay between the 'start' and 'stop' pulses as received from the TAC. The accumulated distribution of counts stored in each channel of the MCA then represents the time dependence of the fluorescence emission of the sample from which lifetime information is obtainable. It is important that only single photons are detected so that the counts distribution in the MCA follows a Poisson statistical distribution. This is achieved when the rate of photons counted is less than 2% of the rate at which excitation pulses are generated[3]. Further, for accurate lifetime analysis to be possible, a minimum of 10,000 counts should be collected in the channel of maximum counts.

As indicated by Equation 1-6, first order decay processes are exponential in nature. Thus, when more than one species is present in solution, lifetime fitting is done using a sum of exponentials equation, Equation 1-9, where I(t) is the intensity or number

of counts (as a function of time); a_i is a pre-exponential factor of component, i; t is time; and τ_i is the fluorescence lifetime of component, i.

$$I(t) = \sum_{i=1}^{n} a_i \exp(-t/\tau_i)$$

Equation 1-9

It is important when fitting the exponential decay curve to account for the shape of the lamp pulse as it is not finite. Thus, after some molecules have already decayed, the tail end of the excitation pulse may still be exciting other molecules. The non-finite lamp pulse can be accounted for by measuring the instrument response function (IRF) using a scattering sample irradiated at the same excitation wavelength as the sample. Upon fitting the experimental decay curve, this lamp profile is deconvoluted out of the simulated decay curve. It is the best fit of this simulated curve to the experimental data that is used to extract lifetimes. The parameters, as well as their acceptable values used in determining best fits, are described in Chapter 2, section 2.3.3.2 (Single photon counting).

1.1.5 Bimolecular photophysical processes

Bimolecular processes are those requiring the interaction between two species, such as A + B → 2C, where the rate law is given by Equation 1-10[4].

$$-d[A]/dt = -d[B]/dt = \frac{1}{2} d[C]/dt = k[A][B]$$

Equation 1-10

However, most bimolecular processes are experimentally pseudo-first order, where one of the reagents is present in excess. This simplifies the rate law significantly, because if [B]>>[A], [B] can be considered constant and Equation 1-11 applies. In this case, k_{obs} = k x [B].

$$-d[A]/dt = k_{obs}[A]$$

Equation 1-11

Integration of Equation 1-11 leads to Equation 1-12, which follows first order kinetics.

$$[A] = [A]_o \exp(-k_{obs}t)$$

Equation 1-12

1.1.5.1 Quenching

Quenching is a deactivation pathway for excited state molecules in addition to those previously discussed in sections 1.1.1 and 1.1.3. As quenching provides an additional deactivation pathway, it reduces the measured lifetime of the excited state molecule. This is especially useful to study microheterogenous systems, e.g. supramolecular systems, where molecules may be present in various environments. That is, because quenching is bimolecular in nature: $M^* + Q \rightarrow M + Q$, the change in lifetime

upon the addition of quencher can indicate the degree of protection the molecule, M^*, has from Q, thereby indicating what sort of environment it is in.

The rate for the disappearance of M^* in the presence of quencher is given by Equation 1-13, where k_0 is defined generally in Equation 1-4 and specifically to fluorescence measurements in Equation 1-5.

$$\frac{-d}{dt}[M^*] = k_o[M^*] + k_q[M^*][Q]$$

Equation 1-13

Quenching studies are commonly done under pseudo-first order conditions where $[Q] >> [M^*]$. As such, the observed rate constant may be obtained as a first-order exponential function as is the case for unimolecular radiative lifetime measurements using single photon counting. In the presence of quencher, the observed lifetime, τ_{obs}, decreases by a factor $k_q[Q]$ as depicted in Equation 1-14, where k_0 is the intrinsic rate constant (s^{-1}) and k_q is the quenching rate constant ($M^{-1}s^{-1}$).

$$\tau_{obs} = \frac{1}{k_o + k_q[Q]}$$

Equation 1-14

Quenching may occur through a number of mechanisms, including energy transfer, electron transfer, or charge transfer. Further, the interaction may be collisional in nature, i.e. dynamic quenching, occur upon complexation of probe and quencher

before excitation, i.e. static quenching, or may occur over long ranges. A combination of the dynamic and static quenching mechanisms are represented in Scheme 1-1.

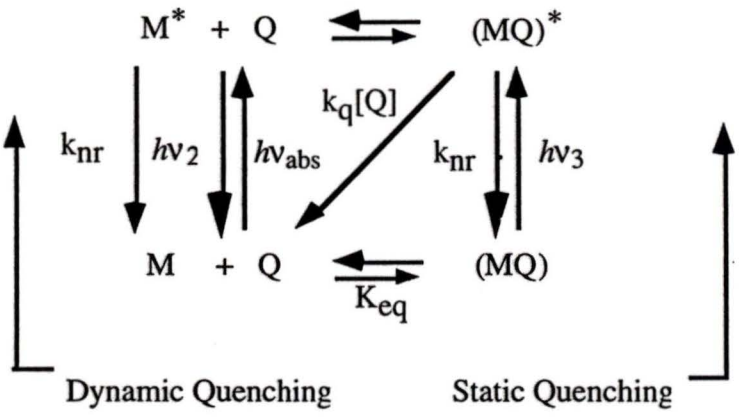

Scheme 1-1: Combined dynamic and static quenching mechanisms by quencher, Q, on molecule, M.

1.1.5.2 Stern-Volmer analysis

The kinetics of dynamic quenching, as depicted in Scheme 1-1, are given as a lifetime in Equation 1-14. Upon separation of terms and using the inverse relation of τ and k (Equation 1-7), one arrives at Equation 1-15 where τ_o is the lifetime of the probe in the absence of quencher, Q; τ_{obs} is the observed lifetime in the presence of quencher; and k_q is the quenching rate constant.

$$\frac{1}{\tau_{obs}} = \frac{1}{\tau_o} + k_q[Q]$$

Equation 1-15

After multiplying Equation 1-15 by τ_o, one arrives at the ratio:

$$\frac{\tau_o}{\tau_{obs}} = 1 + \tau_o k_q [Q]$$

Equation 1-16

where the product $\tau_o k_q$ is known as the Stern-Volmer constant, K_{SV}. A similar expression can be arrived at for steady state fluorescence measurements (Equation 1-17). This is possible as the intensity of fluorescence emission is proporptional to the fluorescence quantum yield[1], which in turn is proportional to the lifetime (Equation 1-8).

$$\frac{I_o}{I} = \frac{\tau_o}{\tau_{obs}} = 1 + \tau_o k_q [Q]$$

Equation 1-17

The Stern-Volmer constant may be determined experimentally by plotting the intensity or lifetime ratios (I_o/I or τ_o/τ) versus the quencher concentration. The slope of such a plot reveals K_{SV}. It is important to note that Equation 1-17 is only valid for the dynamic quenching mechanism. When this is the case the Stern-Volmer plot is linear. When static quenching is involved, the fluorescence emission intensity decreases as fewer fluorophores are available to emit light. However, the lifetime of the fluorophore remains unchanged, as the additional (quenching) deactivation route is essentially instantaneous and the unquenched fluorophores remain unperturbed[5], resulting in $\tau_o/\tau_{obs} = 1$. As such, steady state fluorescence emission measurements and time-resolved data are both required to fully determine the quenching mechanism.

In microheterogeneous systems, such as supramolecular systems, where time-resolved data are often multi-exponential, it is still important to compare the lifetime data to steady-state experiments to determine whether the quenching process is dynamic, static, or a combination of the two. The degree of static quenching involved in supramolecular systems becomes an important consideration when one wants to determine the accessibility of the quencher to the probe molecule, i.e what sort of environment the probe is in. This is because only the dynamic quenching mechanism reveals the degree of protection from an external quencher. In order to relate steady-state and time-resolved data, the integrated fluorescence emission spectrum, which is the sum of all emitting species, must be related to an average of the multiple lifetimes. The average lifetime, $<\tau>$, is given by Equation 1-18[6]. The denominator in Equation 1-18 is equal to 1, as the sum of all pre-exponential factors is normalized to 1 when fitting the lifetime data.

$$<\tau>=\frac{\sum_i a_i\tau_i}{\sum_i a_i}$$

Equation 1-18

The use of this "amplitude average lifetime" is favored over the weighted "intensity average lifetime" (Equation 1-19), as the latter emphasizes the longer lived component(s), which is dangerous when static quenching occurs[7,8].

$$<\tau>=\frac{\sum a_i\tau_i^2}{\sum a_i\tau_i}$$

Equation 1-19

Static quenching may be indicated by a very fast decay component in the time-resolved analysis, rather than only a non-radiative decay component as indicated for static quenching in Scheme 1-1. As such, this fast decay component would be underestimated when using Equation 1-19 [8]. However, even if a fast component is not detected, Equation 1-18 represents the total integrated area under the decay trace, which is related to the area under the steady-state spectrum[6-8]. If there is a component of static quenching involved, $<\tau_0>/<\tau>$ (using "amplitude average" lifetimes) is expected to lie below I_0/I in a Stern-Volmer plot[6].

1.1.5.3 Excimer formation

The formation of excimers, or *excited dimers*, is another mechanism of quenching, as it provides an additional deactivation pathway for an excited state monomer species (Scheme 1-2):

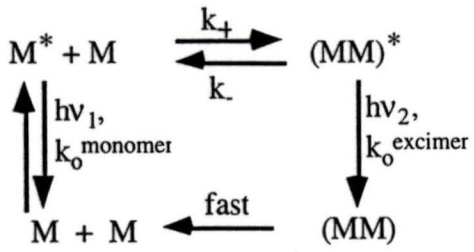

Scheme 1-2: Mechanism of excimer formation and a representation of excimer kinetics.

In the above scheme, a molecule, M, is excited into its singlet state and is followed by a collisional interaction with a ground state species of the same molecule[1,9]. The resulting species, formed through a bimolecular reaction with a rate constant k_+, is an entity unique from either the individual ground state or excited state monomer. The excimer is present only in the excited state. It has its own photophysical properties, i.e. fluorescence emission spectrum, $h\nu_2$, and lifetime, $\tau_o^{excimer}$, which is equal to the inverse of the excimer emission radiative rate constant, $k_o^{excimer}$. This is equivalent to monomer kinetics as defined in Equation 1-7. Once the excimer decays to the ground state it immediately dissociates into two (ground-state) monomer species. The absorption spectrum of a solution containing excimers is not altered from its corresponding excimer-free solution, indicating that excited dimers are indeed dissociated in the ground state[9].

Evidence of excimer formation is provided using steady-state and time-resolved fluorescence emission spectroscopy. Steady-state excimer emission is characterized by a broadened, red-shifted emission band, i.e. relative to the monomer emission band. The reason for this characteristic emission may be seen from the excimer potential energy diagram in Figure 1-3. As excimer formation brings two molecules closer together, the excimer emission is to a higher energy level on the ground state surface than the emission

of the individual monomer molecules. Excimer emission is therefore of lower energy or longer wavelength than the monomer emission. A further consequence is that the vibrational levels at this point are so closely spaced that they are nearly a continuum. This results in a lack of vibrational fine structure in the excimer emission. Monomer emission, however, which may fall to the ground state surface where the vibrational levels are discrete may contain vibrational fine structure.

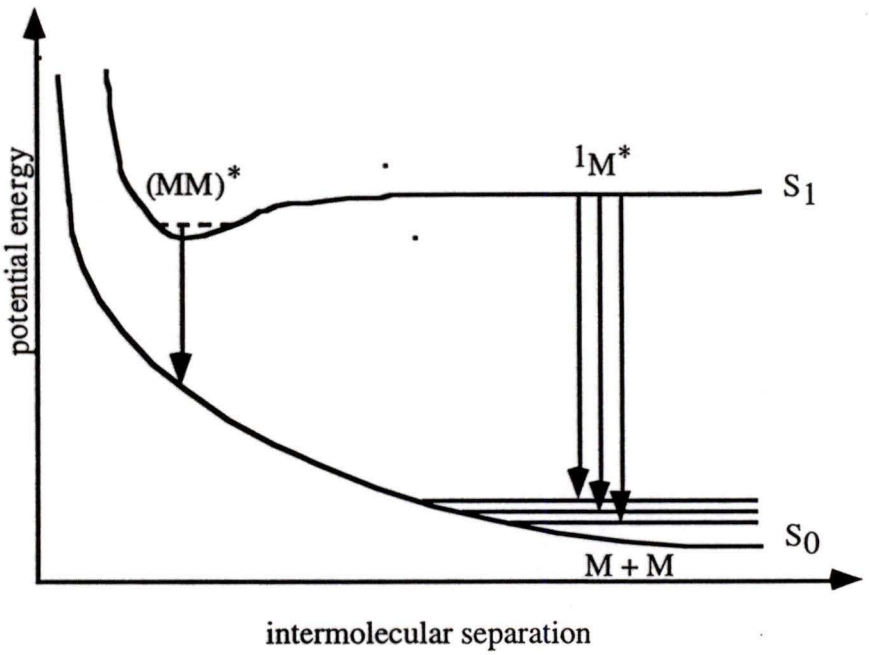

Figure 1-3: Potential energy diagram of monomer and excimer emission (adapted from reference 1).

Time-resolved fluorescence measurements also reveal information regarding excimer formation. As excimer formation is essentially a quenching mechanism for the monomer species, an additional deactivation rate constant is added to the denominator as in Equation 1-14, and the observed lifetime of the monomer is decreased. This additional

quenching mechanism, i.e. excimer formation, is seen as the top equilibrium of Scheme 1-2.

Time-resolved measurements at the excimer emission wavelength also provide information on excimer formation kinetics and the excimer lifetime. As the excimer is not formed instantaneously upon excitation, i.e. a collision between a ground state molecule and an excited state molecule must occur, there is an initial growing in of excimer emission after the excitation pulse. This initial growth corresponds to excimer formation kinetics as does the fast decay component of the monomer lifetime. As such, these two rate constants should correspond with one another. The monomer and excimer emission kinetics are fitted to the sum of two exponentials, and the two exponential factors are related to the monomer and excimer lifetimes, as well as the association ($k_+[Py]$) and dissociation (k_-) processes[9].

1.2 Stopped Flow

Stopped flow, also referred to as a concentration- jump technique, is used to study the kinetics of reactions on the millisecond to minute time scale. The technique is based on a mixing process of two solutions that results in a perturbation of the initially equilibrated chemical system(s), and the relaxation to the new equilibrium state is monitored and analysed as a function of time. As such, the fastest kinetic measurements this techinique can monitor are for those systems in which the re-equilibration is slower than the time required for the mixing process and for transport of the solution to the detection system to occur. On a modern stopped-flow apparatus, this is typically done within 2 ms. Absorption and fluorescence spectroscopy are two dectection methods that

the stopped flow technique can use to measure the re-equilibration as a function of time. A schematic representation of a stopped-flow apparatus is shown in Figure 1-4.

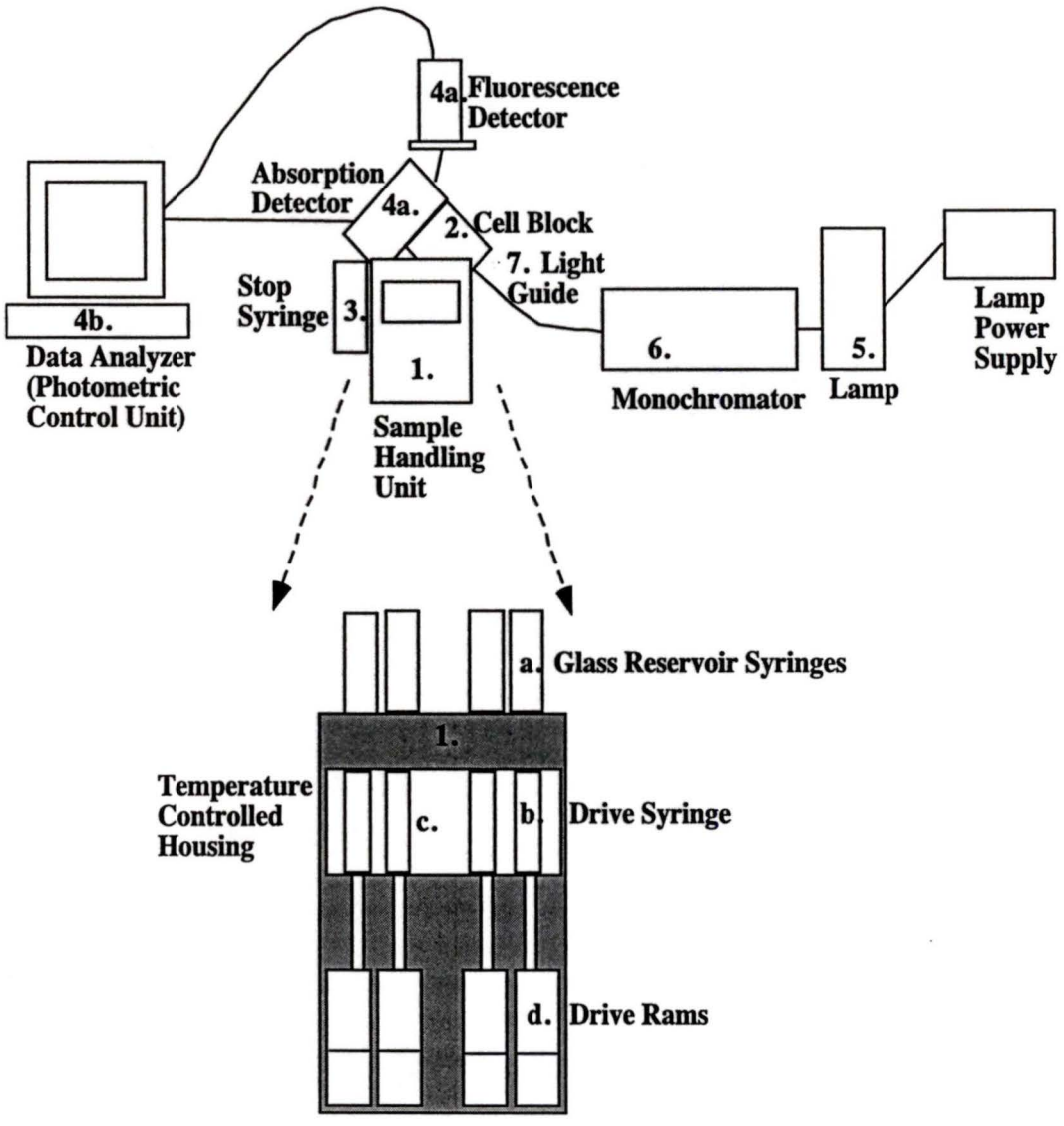

Figure 1-4: Schematic diagram of a stopped-flow apparatus. See text for explanation of parts corresponding to the appropriate number in the figure.

The two solutions to be mixed are held in glass reservoir syringes (1a.) that are screwed into the sample handling unit (1.), and fill the drive syringes (1b.) that are

contained within a controlled thermostat bath (1c.). Below these drive syringes is the drive ram (1d.) which is operated using compressed gas. The solutions are mixed together rapidly (usually within 0.5 ms) right after the drive ram (1d.) pushes the drive syringes (1b.) up. The solutions flow through the tubing to the mixing chamber or cell block (2.), and on to the stop syringe (3.). The total volume of solution moving through the system can be controlled at the stop syringe. Once the set volume of mixed solution has filled the stop syringe, the flow of solution is instantly stopped and the computer is triggered to start data collection (4a.,4b.). The time taken for the mixed solution to reach the optical cell and for the solution to stop flowing is known as the dead-time, and is typically 1.5 ms. As the solutions are mixed before data collection, stopped-flow measures the re-equilibration of the newly perturbed system as opposed to the mixing or the dilution of the initial systems.

A continuous light source (5.) is used for the excitation energy in the stopped-flow apparatus. The monochromator (6.) sets the absorbance/ excitation wavelength, and the light reaches the cell block via a fibre optic light guide (7.). The emission may be measured using either a second monochromator or an emission cut-off filter. As with regular absorption and fluorescence specroscopic measurements, absorbance is detected 180° from the light source, while fluorescence detection is 90° to the excitation light.

1.3 Cyclodextrins

1.3.1 Structure and properties

Cyclodextrins are cyclic oligomers containing α-D-glucopyranose units that are covalently linked through glycosidic 1,4 bonds, as labelled in Figure 1-5.

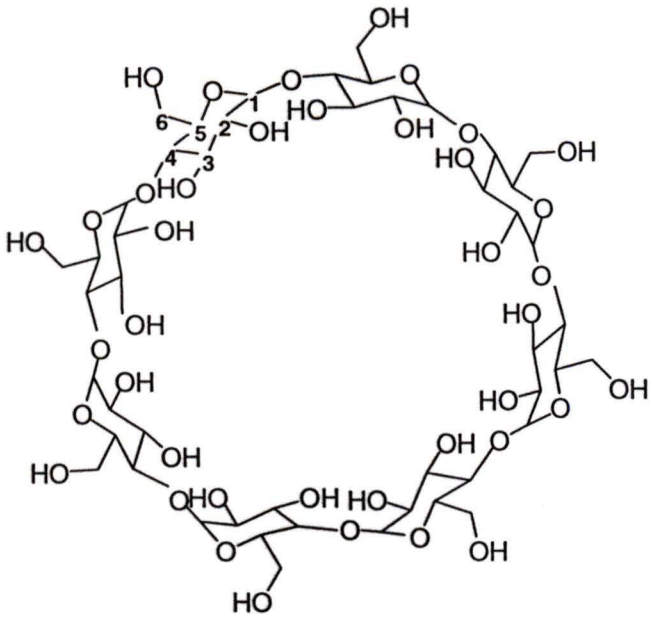

Figure 1-5: End-on view of γ-cyclodextrin showing the numbering of the carbon atoms in each glucose unit. (Diagram adapted from reference 10.)

The three most common cyclodextrins (CDs) are α, β, and γ-CD. They differ in the number of glucose units they contain, i.e. 6, 7, and 8, respectively, and therefore their cavity sizes vary. The CDs are essentially cone shaped, the larger diameter end containing 2n secondary hydroxyl groups and the narrow end containing n primary hydroxyl groups, where n is the number of glucose units. As such, the cavity diameters range from 4.7 – 5.2 Å for α-CD, 6.0 – 6.4 Å for β-CD, and 7.5 – 8.3 Å for γ-CD[10]. The heights of the cavities are constant for all three CDs, at 7.9 – 8 Å[10].

The interior of the CD cavity is quite hydrophobic whereas its exterior is relatively hydrophilic, owing to the several hydroxyl groups lining the rims. The opposing polarities make CDs useful as hosts for inclusion complexes, as they may host

hydrophobic guest molecules in polar media. This is especially useful when studying biological systems as an aqueous medium allows for the best simulation of the actual environment. The various sizes of the CDs allow molecules of different sizes to be included into each of the three cavities. It should be noted, however, that the CD cavity is not a rigid structure and different conformations are possible[11], which may alter the expected inclusion capability of the CDs.

An interesting difference between the CDs is the difference in their water solubility levels. The solubility limit of β-CD is well below that of the other two CDs (Table 1-1). This significant difference is one indication that generalities made between CDs, including complex formation comparisons, must be made with caution as the differences in properties among CDs may not be as simple as merely size variations[11].

Table 1-1: The aqueous solubility limits and the pK_a of the various CDs at 25°C. Data taken from reference 11.

Cyclodextrin	**Solubility in water (mol/L @ 25°C)**	**pKa (25°C)**
α-CD	0.1211	12.33
β-CD	0.0163	12.20
γ-CD	0.168	12.08

1.3.2 Complexation of organic molecules to cyclodextrins

Supramolecular complexes are those that form from several individual molecules through specific non-covalent interactions. For example, inclusion of certain guest molecule(s) within CD cavities form host-guest complexes that are stabilized through non-covalent interactions. The driving forces for the formation of such complexes have been deduced based on experimental data. Such driving forces include: 1) the release of 'high-energy' water from the CD cavity; 2) hydrophobic interactions; 3) hydrogen bonding between the guest and CD; and 4) induction forces (e.g. dipole- induced dipole)[11]. In general, it has been proposed that the stability of the CD inclusion complex varies in relation to how much of the hydrophobic part of the guest molecule is included within the hydrophobic CD cavity[12]. That is, a complex that incorporates a large portion of the hydrophobic moiety of guest into the hydrophobic CD host will be more stable than a complex that incorporates a hydrophilic moiety and/or leaves a hydrophobic part outside the CD cavity. Further, stability is thought to increase as the amount of free space within the included cavity decreases[11]. This latter conclusion is based on many studies that involve the addition of a third space-filling molecule, such as alcohols, that result in the formation of three or four component complexes of increased stability[13-16].

1.3.2.1 Determination of species present in equilibrium in CD systems

Host-guest systems involving CDs may be quite complex, involving several species of various stoichiometries. Techniques used to determine the number of species present and their stoichiometries include absorption spectroscopy, steady-state and time-resolved fluorescence measurements, together with quenching experiments.

The presence of isosbestic point(s) in the absorption spectra of a probe molecule with the addition of host is a good indicator that two species are present in equilibrium. That is, if the two species present in equilibrium, A and B, have the same molar absorption coefficient, ε, at an absorbing wavelength, λ, then the absorption spectrum will go through the same point under all conditions, i.e. as the equilibrium shifts. This is because the only terms that vary in the experimental absorption equation are the concentrations of the two species which shift as the equilibrium shifts. However, the sum of the concentrations does not vary. Alternatively, the absence of an isosbestic point indicates that more than two species are likely present[17,18]. As the number of different absorbing species increases, the chances of them all having the same ε at a certain absorbing wavelength is very small and therefore no isosbestic point would be observed. It should be noted, however, that the lack of an isosbestic point is not solid evidence for the presence of more than two species, as the two complexes may not have the same ε at any absorbing wavelength.

The quenching of an excited state probe is a useful methodology in determining the species present in CD systems. The principle of this methodology is based on the fact that the inclusion within a CD complex acts as a shield to protect the probe molecule from quenching. Thus, as quencher is added, an included species will be shielded to a larger degree relative to a more exposed probe. Experimentally, these species can be differentiated as the emission intensity of the protected species will remain higher and its lifetime will remain longer than for the exposed probe. In steady-state emission measurements, a Stern-Volmer plot (see section 1.1.5.2) of a system with more than one type of complex present which have different degrees of exposure will lead to a non-

linear plot. For example, in a study of pyrene in β-CD[16], the Stern-Volmer plot of pyrene being quenched by tryptophan resulted in an intially linear plot which then levelled off at higher quencher concentrations. This result was a good indication that a more protected pyrene/ CD complex was present, such as a 1:2 pyrene: β-CD complex.

The addition of a quencher to the supramolecular system also results in a bigger difference between lifetimes for excited states located in different environments. After quencher is added, the more protected probe will not change its lifetime to the same degree as will the more exposed probe. As such, whereas before the addition of quencher the lifetimes of the various species may be quite similar and therefore not distinguishable, the various lifetimes will become substantially different after quencher is added.

1.3.2.2 Determination of equilibrium constants in multiple stoichiometric systems

Equilibrium constants may be determined by using any physical or photophysical property of the host or guest that changes on the formation of the complex[12]. These include chemical shifts in NMR spectra[19,20], changes in absorption spectra[21-24], changes in steady-state fluorescence spectra[13,14,17-19,25-27], or lifetime data[15,28]. A larger change in the physical property being measured allows K_{eq} to be determined more precisely. The computational method by which these changes are analyzed to extract K_{eq} will vary, however, based on the number and stoichiometry of complexes present. In the case where only a 1:1 host:guest complex is present, K_{eq} is often evaluated using the Benesi-Hildebrand method[29]. However, in the case where several different species are present simultaneaously, in particular when two probes enter one or two CDs, this method is not

applicable. Rather, the (photo)physical change seen on complexation is multivariable and a different analysis technique is used.

When more than one probe molecule is involved in the complex, excimer emission may be observed. The change in excimer emission intensity on CD addition (and therefore complexation) is related to the concentration of the complex. However, as the emission quantum yield of the complex is not known, its exact concentration is not known. As such, the emission intensity values are normalized at a certain CD concentration. The experimental values of excimer concentration are then compared to calculated values, based on a particular model for complex formation and various equilibrium constants. The equilibrium constants are then taken as the values used in the calculation for which the best comparison between experimental and calculated values were obtained. (See Chapter 3 for the calculation equations and the corresponding model for complex formation of the pyrene/ γ-CD system.) This method has been used by several authors to study the complexation of various probes to CDs, including 2-naphthyl-1-ethanol to β-CD [19], 1-cyanonaphthalene to β-CD [27], and 2-methylnaphthalene to β-CD and γ-CD[17]. In the first of these examples, the presence of a 1:1 and 2:2 complex was assumed. In the latter three examples, comparisons were made using calculated values based on the multi-probe complex consisting of a 2:1 probe: CD complex as well as a 2:2 complex. As the fits for the 2:1 complex could not fit to the experimental data within reasonable error, the excimer emission was concluded to come from a 2:2 complex. Representative equilibrium constants for several probe molecules to β-CD and γ-CD with multiple stoichiometry are listed in Table 1-2.

Table 1-2: Equilibrium constants for various multiple stoichiometric probe: CD systems.

Probe	**CD**	**Temp (°C)**	**$K_{probe:\ CD}$ / M^{-1}**	**reference**
Naphthalene	β-CD	25	$K_{1:1}$ = 685 $K_{2:2}$ = 4000	30
1-Methylnaphthalene	β-CD	25	$K_{1:1}$ = 340± 40 $K_{2:2}$ = 5820	18
1-Ethylnaphthalene	β-CD	25	$K_{1:1}$ = 630 ± 70 $K_{2:2}$ = present but not reported	18
2-Methylnaphthalene	β-CD	25	$K_{1:1}$ = 1190 ± 40 $K_{2:2}$ = 1400	17
2-Ethylnaphthalene	β-CD	25	$K_{1:1}$ = 2000 ± 200 $K_{2:2}$ = 3370	18
Pyrene	β-CD	room temp.	$K_{1:1}$ = 120 - 260 $K_{1:2}$ = 70 - 280 $K_{1:1}$ x $K_{1:2}$ = 3 x 10^4 (M^{-2})	26 $K_{1:2}$ found by (0.5-2)x $K_{1:1}$
Pyrene	β-CD	20	$K_{1:1}$ = 354.5 $K_{1:2}$ = 177 - 709 $K_{1:1}$ x $K_{1:2}$ = 3.74 x 10^4 (M^{-2})	25 $K_{1:2}$ found by (0.5-2)x $K_{1:1}$
1-Cyanonaphthalene	β-CD	25	$K_{1:1}$ = 120 ± 10 $K_{2:2}$ = 7 x 10^4	27
2-Methylnaphthalene	γ-CD	25	$K_{1:1}$ = 9 ± 3 $K_{2:2}$ = 3.38 x 10^6	17
Sodium 4-pyren-1-ylbutyrate	γ-CD	25	$K_{1:1}$ = 1300 $K_{2:2}$ = 5.2 x 10^4	21

Pyrene	γ-CD	25	$K_{1:1} = 300$ $K_{1:2} = 170$ $K_{2:2} = 1.3 \times 10^6$	31
Pyrene	γ-CD	ambient temp	$K_{1:1} = 35$ $K_{1:2} = 310$ $K_{2:1} = 1.9 \times 10^7$ $K_{2:2} = 1.1 \times 10^8$	32
Pyrene	γ-CD	25	$K_{1:1} = 20$ $K_{1:2} = 200$ $K_{2:1} = 5 \times 10^6$	13

1.3.2.3 Dynamics of CD systems

Contrary to the large number of reports available on the stability of cyclodextrin complexes, significantly fewer studies have looked into the dynamics of these systems. The techniques used to study the dynamics of the systems are quite variable, and the rates that have been reported vary by orders of magnitude. For example, for various 1:1 naphthylazobenzenes: α-CD complexes, the association rate constant varied from 2.8 $M^{-1}s^{-1}$ to 5.2×10^7 $M^{-1}s^{-1}$ [33]; however, values of association rate constants for large organic molecules in aqueous CD solutions forming 1:1 probe: CD complexes have also been reported as being as large as $(1\text{-}5) \times 10^8$ $M^{-1}s^{-1}$ [19,33] to "diffusion controlled"[34]. The dissociation rate constants have also been found to vary significantly for the 1:1 naphthylazobenzenes: α-CD complexes, from 0.01 s^{-1} to 1.3×10^5 s^{-1} [33]. The dissociation rate constants of other 1:1 systems involving β-CD as the host, including excited triplet xanthone, pyrene, and naphthalene, vary from $(8.4 \pm 0.7) \times 10^6$ s^{-1} [35], 5×10^4 s^{-1} [36], and 1×10^5 s^{-1} [36], respectively.

The dynamics of multiple stoichiometric CD systems have also been studied to a small extent. Several of these systems have shown slow kinetics, occuring on the millisecond time scale. For example, the 2:2 2-naphthyl-1-ethanol: β-CD complex was found to have a dissociation rate constant of (0.2 – 2.5) x 10^3 s^{-1} [19], whereas the dissociation rate constant from the 1:1 complex was found to be (1.8 ± 0.7) x 10^5 s^{-1} [19]. In other multiple stoichiometric systems, the slow dissociation is reported as being due to the 2:1 guest: CD complex whereas the 2:2 complex is believed to be relatively fast, i.e. beyond the time resolution of the measuring technique. For example, for Tropaeolin 000 No. 2 in γ-CD, the rate constants for the slow 2:1 system were found to be (2.27 ± 0.61) x 10^9 $M^{-1}s^{-1}$ for association and (1.35 ± 0.23) x 10^3 s^{-1} for dissociation[37].

1.3.3 Cyclodextrin applications

Due to their low toxicity, biodegradibility, and relatively low cost, cyclodextrins are favorable hosts for many applications. For example, cyclodextrins have been used to improve the aqueous solubility of several hydrophobic drug molecules thereby providing simpler drug formulations and improved up-take of the drug[12]. Conversely, the encapsulation may slow down the rate of release of certain molecules, which is important in the case of reducing the smell or taste of undesirable aromatic compounds[12].

Cyclodextrins have also been used to separate guest molecules from a mixture by acting as the stationary phase in column chromatography. That is, a strong interaction between the stationary host CD and mobile guest will result in good separation of guest from the mixture. This is because the guest will be maintained in the column, i.e. in the CD, while the other non- interacting molecules move out of the column[12].

Organic synthesis also takes advantage of CD cavities, as they may be used as reaction vessels. For example, the close proximity between two molecules when they are both included in one CD cavity increases the probability and facility for a reaction to occur[12]. It is important to note that in all of the above examples the strength of the interaction and the association and dissociation kinetics between CD as host and the guest molecule(s) are important factors in the various applications of the CDs.

1.4 Pyrene

1.4.1 Physical properties

Pyrene is a polycyclic aromatic hydrocarbon, with a molecular structure as shown in Figure 1-6.

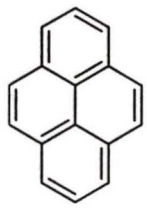

Figure 1-6: Molecular structure of pyrene

The dimensions of pyrene are reported as being 10.4 Å long and 8.2 Å wide[25,38]. The thickness of the molecule could be approximated as being equal to that of benzene, 3.4 Å[39,40].

The aqueous solubility of pyrene is very low. Its limit in water is reported as being 1.6×10^{-6} M[15,32]. If the molecule is not thoroughly dissolved, pyrene microcrystals

can form which may lead to pyrene excimer formation, as seen by excimer fluorescence[9]. This leads to inconsistent and inaccurate experimental results due to the variation of free aqueous pyrene concentration in solution. Pyrene also tends to adsorb onto glass surfaces, which can lead to experimental uncertainty. For these reasons extreme care must be taken when preparing pyrene solutions.

1.4.2 Photophysical properties

Pyrene is a well studied photophysical probe molecules due to its many favorable and informative photophysical characteristics. These include highly sensitive and revealing fluorescence emission characteristics based on the polarity of its microenvironment, its ability to form excimers at high concentrations in numerous solvents or when in confined media, a very long singlet lifetime, and a high fluorescence quantum yield.

The fluorescence lifetime of molecules is inversely proportional to the absorption oscillator strength, or the probability for light to be absorbed[41]. As pyrene's lifetime is relatively long, its $S_0 \rightarrow S_1$ transition probability is quite weak. As such, the strong absorption of the $S_0 \rightarrow S_2$ transition (maximum near 335 nm) is often used to excite the pyrene molecule. In solution, internal conversion from S_2 to S_1 is faster than the lifetime of pyrene, which allows radiative processes from the S_1 state to be studied.

1.4.2.1 Solvent polarity effects

The fluorescence emission spectrum of pyrene is very structured, consisting of five vibronic peaks in the 370 nm to 400 nm wavelength region. The relative intensity of

these peaks varies, depending on the polarity of pyrene's environment. In particular, the emission of the first peak (0-0 transition at ~371 nm) is the most sensitive, increasing in intensity with the polarity of the solvent. Alternatively, peak III at 383 nm varies the least with solvent polarity. The reason for this sensitivity to solvent polarity is related to the Ham effect, as seen for benzene where the intensity of the forbidden vibronic band is enhanced with solvent polarity[42].

By taking the relative intensity ratio of peak I (371 nm) and peak III (383 nm) in the pyrene emission spectrum, one can determine the degree of polarity of pyrene's microenvironment. A representative sample of R(I/III) ratios for pyrene in various solvents is shown in Table 1-3. It should be noted that the ratio is sensitive to experimental conditions and may therefore be different for experiments performed in different laboratories.

Table 1-3: Dependence of R(I/III) of pyrene on solvent polarity, as exemplified in various solvents.

Solvent	**R(I/III)**
water	1.50[(a)] ; 1.64 ± 0.02 (3)[(b-ii)]
acetone	1.47[(a)]
ethanol	1.10[(a)]
cyclohexane	0.60[(a)] ; 0.49[(b-i)]

a) Values taken from reference 40; b-i) Values obtained under our experimental conditions; b-ii) [pyrene] = 5.0 x 10^{-7} M, T = 20.0 ± 0.02 °C, excitation and emission slits = 3.0 nm. The error is the standard deviation of three trials.

Environment sensitive probes are very useful in the study of supramolecular systems, including host-guest and micellar complexes[42], as well as in bile salt aggregates[43]. They help indicate the location of the probe within the non-covalent structure, and may offer information as to the stoichiometry of the host-guest complex formed (see also section 1.4.3).

1.4.2.2 Excimer formation

At a high enough pyrene concentration, pyrene forms excimers. This is evident in the fluorescence spectra of increasing pyrene concentration where the excimer emission intensity increases at the expense of the monomer intensity. The fluorescence emission of pyrene excimer is quite red-shifted relative to the monomer emission. In cyclohexane

and ethanol, the wavelength of maximum intensity for the excimer emission is 480.8 nm. This is a significant red-shift relative to the pyrene monomer, which is at 371.7 nm and 373.8 nm in the above solvents, respectively[9].

1.4.2.3 Fluorescence quantum yields and lifetimes

The quantum yield of fluorescence for the pyrene monomer is quite high, making it a favorable probe molecule, as only a small concentration is required to give significant and sensitive fluorescence measurements. The lifetime of singlet-state pyrene is also very long, even when compared to other organic probe molecules (Table 1-4). A probe molecule with a long fluorescence lifetime is advantageous in studying supramolecular systems, as the decrease in lifetime upon quenching of the fluorophore within the supramolecular complex, can be measured using a time-resolved single-photon counting apparatus.

Table 1-4: Comparison of fluorescence quantum yields and lifetimes of pyrene and naphthalene in various solvents (de-aerated, unless otherwise specified).

Compound	Solvent	Quantum yield of fluorescence, ϕ_f	Lifetime (ns)
pyrene[a)]	Cyclohexane	0.65	450
	Ethanol	0.65	475
	95% ethanol	0.44	290
	Acetone	0.50	330
pyrene	Water (aerated)	--	130[b)]; 128[c)]
naphthalene[a]	Cyclohexane	0.19	120
	95% ethanol	0.12	52

a) Data from reference 9. Measurements taken at room temperature. b) Data from reference 26; aerated solution; c) Data from reference 16; aerated solution.

1.4.3 Complex formation with cyclodextrins

Pyrene is a well-studied photophysical probe in the absence and presence of CDs. It has been studied in the presence of α, β, and γ-CD using several spectroscopic methods, including absorption spectroscopy, steady-state and time-resolved fluorescence spectroscopy. However, results among various authors are not consistent, both in the stoichiometry of the equilibria proposed and the equilibrium constants evaluated for the systems. The proposed complexes formed are shown in Scheme 1-3.

$$py + CD \underset{}{\overset{K_{1:1}}{\rightleftharpoons}} py\text{-}CD \qquad K_{1:1} = \frac{[py - CD]}{[py][CD]}$$

$$py\text{-}CD + CD \underset{}{\overset{K_{1:2}}{\rightleftharpoons}} CD\text{-}py\text{-}CD \qquad K_{1:2} = \frac{[CD - py - CD]}{[py - CD][CD]}$$

$$py\text{-}CD + py \underset{}{\overset{K_{2:1}}{\rightleftharpoons}} py\text{-}py\text{-}CD \qquad K_{2:1} = \frac{[py - py - CD]}{[py - CD][py]}$$

$$py\text{-}CD + py\text{-}CD \underset{}{\overset{K_{2:2}}{\rightleftharpoons}} CD\text{-}py\text{-}py\text{-}CD \qquad K_{2:2} = \frac{[CD - py - py - CD]}{[py - CD][py - CD]}$$

Scheme 1-3: Various proposed equilibria and their corresponding equilibrium constants based on the above model of step-wise complex formation between pyrene (py) and cyclodextrin (CD). The complexes reported vary per study and on the CD used.

1.4.3.1 Pyrene in γ-Cyclodextrin

As metioned in section 1.4.1, a reason for the inconsistent literature results in pyrene/ CD complexation is due to pyrene's very low aqueous solubility. Further, the formation of microcrystals leading to excimer emission not related to the excimer emission due to the complexation within the confined CD cavity is another source of experimental error. As such, some authors have moved to use more soluble pyrene derivatives, such as the charged 4-pyren-1-ylbutyrate ion[15,21] to study inclusion complexation with CDs. In this case, the absorption spectrum shifted 180 cm^{-1} to the red (longer wavelength, lower energy) upon the addition of γ-CD. As no change in the absorption spectrum was seen on the addition of individual glucose units, the shift was concluded to be due to the inclusion of the pyrene derivative into the CD cavity, and not

due to complexation to its exterior[21]. This red-shift in the absorption spectrum is commonly seen upon the addition of CDs to pyrene solutions[31]. Isosbestic points have also been reported in the absorption spectra for pyrene in the presence of γ-CD (below 5 x 10^{-3} M) at 322 nm, 327nm, and 336 nm[31]. This would indicate that only two species are present in equilibrium below 5 x 10^{-3} M γ-CD.

The fluorescence emission spectrum of pyrene changes in the presence of γ-CD. An increase in excimer fluorescence emission with increasing γ-CD indicates the presence of a 2:1 or a 2:2 pyrene: γ-CD complex, since no excimer emission is present in the absence of γ-CD. The characteristic excimer emission of pyrene has only been seen in the presence of γ-CD, the largest CD.

Another feature in the absorption spectrum of the pyrene that occurs upon the addition of γ-CD is broadening of the red-shifted tail[31]. The loss of absorption resolution and an increase in excimer fluorescence emission intensity upon the addition of the CD indicates interactions between ground state pyrene molecules. That is, these spectroscopic results support the formation of a ground state pyrene dimer within the γ-CD cavity (or cavities).

To determine the mechanism that leads to pyrene excimer emission in the presence of γ-CD, other spectroscopic information is useful. This includes excitation spectra as well as the relative monomer to excimer intensities at different excitation wavelengths. In the former, a shift or broadening of the excitation spectrum indicates that a species other than the pyrene monomer is being excited. In the formal excimer formation mechanism, the excitation spectrum of excimer emission should yield the same spectrum as that monitoring the monomer emission. This is because one must excite the

monomer before the excimer is formed. If, however, another species is being excited to yield excimer emission, the excitation spectra will differ. This is what has been seen for pyrene in γ-CD[44]. The dependence on excitation wavelength of the emission spectrum, i.e. relative excimer to monomer emission intensities, is related to the above argument. If the excimer is formed from a ground state dimer, the emission intensity in the excimer region will increase relative to the monomer emission at longer excitation wavelengths where the dimer absorbs, i.e. in the broadened red-shifted area in the absorption spectrum. This is because a larger percentage of dimer is being excited. This also has been reported for the pyrene/ γ-CD system[44].

There is a change in the intensities of the pyrene monomer vibronic emission bands on the addition of the CD. Not only is there an overall decrease in monomer emission (up to 5 x 10^{-3} M γ-CD) due to the formation of excimer, but the relative intensities between peaks I and III also vary. That is, the R(I/III) ratio decreases as the γ-CD concentration increases. The change in the R(I/III) ratio with γ-CD concentration has been used to extrapolate equilibrium constants. However, this method has not proven successful, as in deriving the equations the assumption that only one pyrene monomer complex is present is often made[38,45] and is not valid.

The lifetime of pyrene has also been shown to increase on the addition of γ-CD. For example, the lifetime of pyrene monomer increases from around 130 ns in aerated water[26,46] to 215 ns [47], 213 ns[14], and 250 ns [44] in the presence of 10 x 10^{-3} M γ-CD.

The presence of excimer emission has led to the proposal of various equilibria (Scheme 1-3) between pyrene and γ-CD, including 2:1 and 2:2 stoichiometries. Various experiments have been designed to verify which of the stoichiometries is present in

solution. Hamai proposed that if the pH of the excimer containing solution was higher than the pK_a of the hydroxyl groups of γ-CD (12.08, see Table 1-1), the excimer emission intensity should decrease if the stoichiometry of the complex was a "barrel-type"[31] 2:2 complex. This would occur as the facing deprotonated hydroxyl groups of the two CDs would repel one another causing the complex to fall apart. The results of the experiment indicated that the complex was indeed a 2:2 complex, as the excimer emission intensity decreased substantially above pH = 11.5. A second experiment involving pyrene-appended γ-CD units was performed[48,49] that also led to the conclusion that the excimer emission was due to the formation of a doubly encapsulated pyrene dimer, based on data including a pH experiment. Upon acidification of the highly basic system (pH > 12.70), the pyrene excimer emission was recovered[48]. The use of increasing basicity to determine that the stoichiometry of the excimer emitting species was from a 2:2 complex has been done with other probes, including 2-methylnaphthalene in β-CD[17], 1-methylnaphthalene in β-CD[18], 2,2': 5', 2''- terthiophene in γ-CD[50], and 2, 5-diphenyloxazole in γ-CD[51]. In this last case, the excimer emitting species was proposed to arise from linear aggregates of 2, 5- diphenyloxazole within γ-CD, i.e. of stoichiometry greater than 2:2.

1.4.3.2 Pyrene in β-Cyclodextrin

As indicated in Table 1-2, literature results of the equilibrium constants for pyrene: β-CD are inconsistent and imprecise. Although this is the case, the proposed stoichiometries of the species present are consistent. That is, several studies conclude

that a 1:1 and a 1:2 complex forms[16,25,26]. The lack of excimer emission was used to indicate that no 2:2 or 2:1 pyrene: β-CD complexes formed.

The inconsistent and imprecise values obtained for equilibrium constants in the pyrene: β-CD system is primarily a result of the data analysis method used. As mentioned above, the use of the R(I/III) value to extract equilibrium constants has proven quite unsuccessful as the calculation often assumes the presence of only one species [38,45]. When a step-wise formation mechanism for the formation of a 1:1 complex followed by a 1:2 pyrene: β-CD complex was proposed, the variation in $K_{1:2}/K_{1:1}$ was very broad, 0.5-2[25,26], when the R(I/III) values were used for the analysis.

R(I/III) ratios have been used to qualitatively support other evidence as to the degree of protection a CD gives the fluorophore, and therefore the possible stoichiometry of the complex. For example, quenching pyrene with tryptophan in the presence of β-CD yielded an overall decrease in R(I/III) until a plateau was reached. This indicated only a very well protected (monomer) species was left unquenched in a quite hydrophobic environment, such as the previously proposed 1:2 pyrene: β-CD complex[16]. It is important to note that the use of R(I/III) for determining the stoichiometries of the species present is only possible with the addition of quencher. This is because the degree of change in R(I/III) with the addition of CD only may only indicate the degree of complex formation, i.e. a faster drop in R(I/III) ratio may not indicate the presence of a more hydrophobic 1:2 complex, but rather a favorable 1:1 complex equilibrium.

1.4.3.3 Pyrene in α-Cyclodextrin

A study of pyrene with the smallest CD indicated that no complex forms between the host and guest, as relatively insignificant changes in the absorption and fluorescence spectra were seen upon the addition of α-CD[44]. This was rationalized in terms of the sizes of the structures, with pyrene being too large to be included within the small CD cavity. However, a second study proposed the formation of a 1:1 followed by a 1:2 pyrene: α-CD complex[26]. The R(I/III) value was reported as being closer to the value in water than when in the presence of the larger CDs. This was thought to be due to the large pyrene molecule unable to be fully encapsulated by the smaller (two) α-CD cavities, and was therefore in a more polar, i.e. aqueous environment, than if it were more fully encapsulated by the hydrophobic CD cavity.

1.5 Objectives of thesis

Several cyclodextrin studies have centered around the characterization and the stability of the inclusion complexes formed within CD cavities, as discussed in section 1.3.2. A significantly fewer number of studies have looked into the dynamics of the formation and dissociation of the inclusion complexes. Several examples were given in section 1.3.2.3. The rate constants varied considerably for different systems. In particular, the study of 2-naphthyl-1-ethanol in the presence of β-CD[19] indicated that the dissociation rate constant of the 2:2 probe: CD complex was two orders of magnitude slower than the dissociation rate constant of the 1:1 complex. The reason for this difference, however, is unclear. One hypothesis is that the slow dissociation dynamics are a result of structural features of the guest(s) which leads to particularly stable

inclusion complex containing more than one CD. A second hypothesis for the slow dynamics is that CDs aggregate independently of guest(s) to form stable multiple stoichiometric systems, regardless of the probe molecule(s). Thus, the rate limiting step in the complexation kinetics would be the dissociation of the CD oligomers. The goal of this work was to study other guest: CD systems with multiple stoichiometry to help differentiate between these models. That is, we wanted i) to characterize guest: CD complexes where species of multiple stoichiometries are present. The characterization must be done first so that a model for the dynamic mechanism may be proposed and validated; ii) to look at the dynamics of the guest: CD systems and to formulate the dynamic mechanism of the system. We would see whether the dissociation dynamics were slow, and if so, examine the relationship between the guest(s) structure and guest: host stoichiometries with the observed dynamics. The results could have considerable impact on how CDs are used in practical applications, as well as their use as models of supramolecular complexes.

The probe and cyclodextrin used in this study were pyrene and γ-CD. As the characterization of the system proved to be quite difficult, no other probe: CD systems were investigated. However, the methodologies used for the characterization of the system will be used as a model for future studies.

2. Experimental

2.1 Materials

Pyrene (py) (Polysciences Inc. or Aldrich, 99%) was recrystalized once from 95% ethanol. An aerated aqueous solution of 5.0×10^{-7} M pyrene gave a monoexponential fluorescence decay curve with a lifetime of 131 ns, which is comparable to literature results[46]. The absence of a fast decay component in the decay trace indicates the absence of any impurity capable of quenching pyrene, as such a decay was previously observed for impure pyrene samples. The lack of a fast component also indicates the lack of excimer formation at the low pyrene concentration employed, as this too would appear as a fast decay component due to quenching of the excited pyrene molecule by a ground-state pyrene.

γ-Cyclodextrin (γ-CD), a generous gift from Cerestar (Lot E 8056 or F 8025-12), was used as received. Sodium iodide (NaI, 99% BDH, or 99+% Aldrich,), tetrabutylammonium iodide (Sigma-Aldrich ion-pair reagent), ethanol (95%), methanol (99.8% spectrograde ACP), acetonitrile (min 99.8% HPLC grade CALEDON), potassium hydroxide (KOH, min 85% ACP), sodium hydroxide (NaOH, min 97.0% ACP), 2-propanol (min. 99.5% CALEDON) were also used as received. The water used for all aqueous solutions was deionized through the SYBRON Barnstead system. The buffers used to calibrate the pH meter were pH = 7.00 ± 0.02 and pH = 10.00 ± 0.02 (at 25°C) (Fischer Scientific Instrument Company buffer solution).

The glassware and stir bars used for pyrene solutions were soaked in a base bath (KOH, iso-propanol, ethanol, water) for less than 1 h, followed by soaking in soap water

and tap water for about 2 h each, and then rinsing vigorously in deionized water and methanol before solution preparation. The rigorous cleaning method was necessary to prevent pyrene adsorbed on the glassware from previous solutions to contaminate fresh solutions.

2.2 Sample preparation

2.2.1 Preparation of aqueous pyrene solutions

Aqueous pyrene solutions (0.25×10^{-6} M, 0.50×10^{-6} M, and 1.0×10^{-6} M) were prepared by diluting a methanolic pyrene stock solution ($2.5\text{-}3.5 \times 10^{-3}$ M) into deionized water. Gastight glass syringes were used for injection. The aqueous solutions were allowed to stir overnight to fully dissolve the pyrene. Due to its low aqueous solubility, pyrene has been known to aggregate and form excimer emitting microcrystals in water solutions[15]. The absence of pyrene microcrystals in the solutions used was evident from the lack of excimer fluorescence emission and any excimer decay kinetics at the low pyrene concentrations used. For further dilutions of the aqueous pyrene solution, the appropriate amount of the aqueous stock solution was dispensed with an eppendorf pipette, diluted with water, and allowed to shake or stir over night.

2.2.2 Preparation of pyrene/ γ-CD solutions

Pyrene/ γ-CD solutions were prepared by either of two methods. In one method, the methanolic pyrene stock solution (2.5×10^{-3} M - 3.5×10^{-3} M) was diluted to the desired concentration by injection directly into a previously prepared aqueous γ-CD (2.0×10^{-3} M - 10×10^{-3} M) solution. The second method used to prepare pyrene/ γ-CD

solutions was to first make an aqueous pyrene stock solution (0.25×10^{-6} M, 0.50×10^{-6} M, or 1.0×10^{-6} M) as described above. The appropriate amount of solid γ-CD (1.0×10^{-3} M - 40×10^{-3} M) was then diluted with the aqueous pyrene solution and allowed to stir over night. As pyrene's solubility in water increases in the presence of γ-CD, the latter method of solution preparation is preferred[52], however, data obtained by the two methods of sample preparation were comparable. All experiments were done in aerated solutions.

2.2.3 Preparation of solutions for quenching studies

Iodide was used as the quenching agent in all quenching experiments. For aqueous quenching studies, a concentrated aqueous stock solution of known concentration of sodium iodide (NaI) was prepared (~ 2 M), of which 10 μL increments (up to 60 μL) were added to the aqueous pyrene or pyrene/ γ-CD solutions. Gastight glass syringes were used for injection of the quencher into the solutions. The purity of NaI (for the absence of other quenchers) was confirmed by comparing the Stern-Volmer constant (K_{sv}) of the steady- state ($K_{sv} = 169 \pm 5\ M^{-1}$, 4 trials) and time- resolved fluorescence ($K_{sv} = 154\ M^{-1}$, 1 trial) quenching data of an aqueous pyrene solution to previous results ($141\ M^{-1}$ [43]).

Tetrabutylammonium iodide was used as the quenching agent for quenching studies in the organic solvent, acetonitrile. A concentrated stock solution of tetrabutylammonium iodide (~1 M) was prepared from which a 20 μL portion was added to the concentrated pyrene (in acetonitrile) solution. Gastight glass syringes were used for injection of the quencher into the solutions. The pyrene in acetonitrile solution (~10 x

10^{-3} M) was prepared by dissolving a weighed amount of pyrene by the appropriate volume of solvent.

2.2.4 Preparation of solutions for pH study

An aqueous sodium hydroxide solution (0.257 M, pH = 13.06 at 22.4°C) was used to increase the pH in the pH-dependent study. Increments of 10 μL to 50 μL of the base were added to the pyrene/γ-CD solution (prepared as described in section 2.2.2) using a gastight glass syringe.

2.3 Instrumentation

2.3.1 pH measurements

pH measurements were taken using a Cole-Parmer® digital benchtop pH meter. Measurements were taken in the pH/autolock mode. Temperatures of the solutions were measured using an ATC temperature probe. The temperature of the solutions was 23.0 ± 0.5°C. The instrument was dual point calibrated before use using pH = 7.00 ± 0.02 and 10.00 ± 0.02 buffers.

2.3.2 UV-Vis absorption spectroscopy

UV-Vis absorption spectra were taken on a Varian Cary 5 spectrophotometer at room temperature. The slits were set to a bandpass of 2.0 nm, while the scan rate was 200 nm/min over 200 nm to 450 nm. Baseline correction with air was always used. Correction of spectra was done by subtracting the absorption spectrum of solvent

(including γ-CD) after setting each spectrum to zero at a wavelength where both solutions do not absorb light.

2.3.3 Fluorescence spectroscopy

2.3.3.1 Steady state fluorescence

Steady state fluorescence measurements were made on a Photon Technology International® QuantaMaster™ (QM-2) Luminescence spectrophotometer. The program ran using FeliX™ software. The excitation source was a Xenon lamp (75 W). The temperature of the sample cell compartment was held at 20.0 ± 0.2 °C using a Haake F3 temperature control unit. Emission and excitation slit widths were set such that each bandpass was 3 nm. The step size and integration time were usually 0.5 nm and 0.25 s, respectively. Measurements of the solutions were taken using either 1 cm x 1 cm (exact dimensions) quartz fluorescence cells or with 1 cm x 1 cm (approximate dimensions) quartz cells. The latter cells were not employed for quantum yield measurements for which it is necessary to know the exact pathlength. For fluorescence emission spectra, the excitation wavelength was usually 331 nm, while emission was monitored from 345 nm to 550 nm. Fluorescence excitation spectra were scanned and monitored at various wavelengths. Corrected spectra were obtained by subtracting a spectrum of the solvent (including γ-CD where required) from the desired fluorescence spectrum. Data analysis was performed using the Kaleidagraph ™ (version 3.08) program.

Time-based scans were run on the PTI® spectrophotometer to simulate fluorescence detected stopped flow experiments at long collection times. The excitation wavelength was 331 nm, while the emission wavelengths were either 400 nm or 473 nm.

The excitation slit widths were set to a bandpass of 3 nm which is comparable to the bandpass used on the stopped flow, while the emission slit widths were set to a bandpass of 20 nm which is comparable to the interference filter (380 nm - 420 nm) and sharp cut-off filter (transmitting at ≥ 455 nm) employed in the stopped-flow experiments. The temperature was maintained at 20.0 ± 0.2 °C. To simulate the stopped flow experiments, the two solutions were first allowed to equilibrate at the correct temperature by sitting one solution in the cell sample compartment and the other in temperature bath for 10 min before mixing. The solutions were then mixed in a 1:1 ratio (1000 μL volumes) using an eppendorf pipette, and shaken vigorously. The dependence of the emission intensity with time of the newly mixed solution was monitored within 30 s of initial mixing. A control experiment was run in which two solutions, both containing the final concentrations of pyrene and γ-CD of the simulated stopped flow mixture, were mixed in a 1:1 ratio. This was done for two reasons; first, the control verified that the change in emission intensity over time was not due to a temperature effect, as the emission of the control mixture did not change as did the experimental mixing scans under the same temperature conditions. Secondly, the final concentration of the controls allowed one to see whether the mixture had come to equilibrium, i.e. to the final concentration over the duration of the kinetic scan. The kinetic scans were run for a duration of up to 1 h.

2.3.3.2 Time-correlated single photon counting (SPC)

Fluorescence lifetime measurements were done on a Photon Technology International® LS-1™ time-correlated single photon counter. The excitation source (nanosecond lamp) used hydrogen as the plasma gas. The excitation wavelength for

aqueous pyrene and pyrene/ γ-CD system was 331 nm, while the emission wavelength was 383 nm or 473 nm for the monomer or excimer decay, respectively. The temperature of the sample cell compartment was maintained at 20.0 ± 0.1 °C using the Lauda® Super RMS-6 temperature control unit. Slit widths were set to 6.5 mm for a bandpass of 26 nm for the aqueous pyrene solutions, and between 8.0 nm and 10.0 nm for the solutions of pyrene in organic solvent. The maximum number of counts per channel collected varied depending on the intensity of the emission. When reasonably possible, 10,000 counts were collected in the channel of maximum intensity. For close-up decays (i.e. relatively short time bases), 100 to 500 counts were collected, as these kinetic traces were used for qualitative rather than quantitative analysis. The solutions were held in home-made Supracil quartz cells. The scattering sample was an aqueous silica gel solution. The excitation and emission wavelengths to collect the scattered light were 331 nm. The scatterer is used to scatter light from the lamp to get the finite lamp profile. This profile is deconvoluted out of the decay curve upon analysis, as this deconvolution process accounts for the re-excitation of probe molecules that occurs as a result of the finite excitation pulse. The lifetime(s) of the various species present in solution are extracted at the same time as the deconvolution process. Lifetime analysis and fitting was done using the PTI software. Fits were considered acceptable based on the following criteria: i) Durbin- Watson Parameter (DW) greater than 1.7, 1.75, and 1.8 for single, double, and triple exponential decays, respectively; ii) Runs Test (Z) Parameter, which indicates a satisfactory fit at the 95% confidence level for $Z > -1.96$; iii) χ^2 in the range of 0.9 - 1.2. Visual inspection of residuals and autocorrelation also helped deem data fitting

acceptable, as these latter two criteria require random fluctuation around the centre line and any pattern in fluctuation indicates a poor fit.

2.3.4 Stopped Flow

2.3.4.1 Experimental conditions

Kinetic measurements were made with a BioSequential DX-17MV Sequential Stopped-Flow ASVD Spectrofluorimeter (Applied Photophysics) base system, using updated SX.18 MV software and several hardware parts. The upgrades included a more sensitive PMT detector, and non-reactive PEEK (polyetheretherketone) sample flow circuit tubing. Measurements were made with the single mixing mode, where two solutions are mixed in a 1:1 ratio. The light source was a Xenon Arc lamp (150 W). Temperature was controlled using a Haake D8 temperature control unit, and was maintained at 20.0 ± 0.8 °C. Entrance and exit slits of the excitation monochromator were set to 0.5 mm to 0.6 mm (corresponding to a 2.33 nm to 2.79 nm bandpass). The excitation wavelength was 331 nm. Fluorescence was detected using interference or sharp cut-off filters. The fluorescence of the pyrene monomer region was monitored using an interference filter with transmission between its full width half maximum (FWHM) coordinates of 385 nm and 423 nm, and a central wavelength of transmission of 404 nm (at 23.0°C) (Melles Griot, Lot # 13637). Pyrene excimer emission was monitored using a sharp glass cut-off filter that transmits light above 455 nm (Melles Griot, Schott glass type GG 455, Product Number 03FCG463). The PMT was set by running the most emissive sample through the stopped flow apparatus first. Setting the initial voltage to the highest possible value allows the PMT voltage to be maximized while ensuring it

does not become saturated throughout the experiment. The off-set was then set between 3 V to 4 V to bring the initial signal near 0 V to keep the entire trace on the screen. Experimental changes in voltage signal were usually between 0.100 and 1.50 V. The drive rams were operated with nitrogen as the compressed gas, with a pressure set to 120 psi. Glass syringes of 10 mL volume were used to hold the solutions. To ensure that no air bubbles were in the mixing tubing system before the cell compartment, the solution was manually pushed through the drive syringe several times until bubbles were no longer seen coming up out of the drive syringe. The solutions were then allowed to sit in the drive syringes within the temperature controlled housing for 10 min to reach the recorded temperature (20.0 ± 0.8°C) before traces were taken.

2.3.4.2 Data analysis

The stopped flow traces were composed of an average of 1 to 10 runs, each of which contained 1000 data points. The data were analysed using the SX.18MV software which utilizes the curve fitting procedure based on the Marquardt algorithm ("based on the routine Curfit in P.R. Bevingtons Data Reduction and Error Analysis for the Physical Sciences 1969 McGraw-Hill" as described in the Sx.18MV Software section in the Applied Photophysics SX.18MV Stopped-Flow Reaction Analyser User Handbook, Dec.15, 1999). Where valid, data were fit to either a single exponential equation (Equation 2-1) or a double exponential equation (Equation 2-2) where I is intensity, A is total change in amplitude, k_{obs} is the observed rate constant, t is time, and b is the intensity of the endpoint. The numbers 1 and 2 in Equation 2-2 refer to the individual components of the bi-exponential fit.

$$I = A\exp(-k_{obs}t) + b$$

Equation 2-1

$$I = A_1\exp(-k_{obs1}t) + A_2\exp(-k_{obs2}t) + b$$

Equation 2-2

It was not possible to fit some kinetic traces to these simple equations, but they were used for qualitative analysis. These included the very slow kinetics (t ~ 2 s to 1000 s) of pyrene in the presence of high γ-CD concentrations (i.e. > 10 x 10^{-3} M).

3. Characterization of the pyrene/ γ- Cyclodextrin system

3.1 Results

3.1.1 Absorption spectroscopy

The absorption spectrum of pyrene in the presence of γ-CD is slightly red-shifted relative to that of aqueous pyrene (Figure 3-1). This is an indication that pyrene in the presence of γ-CD is in a different environment from that in homogeneous solution.

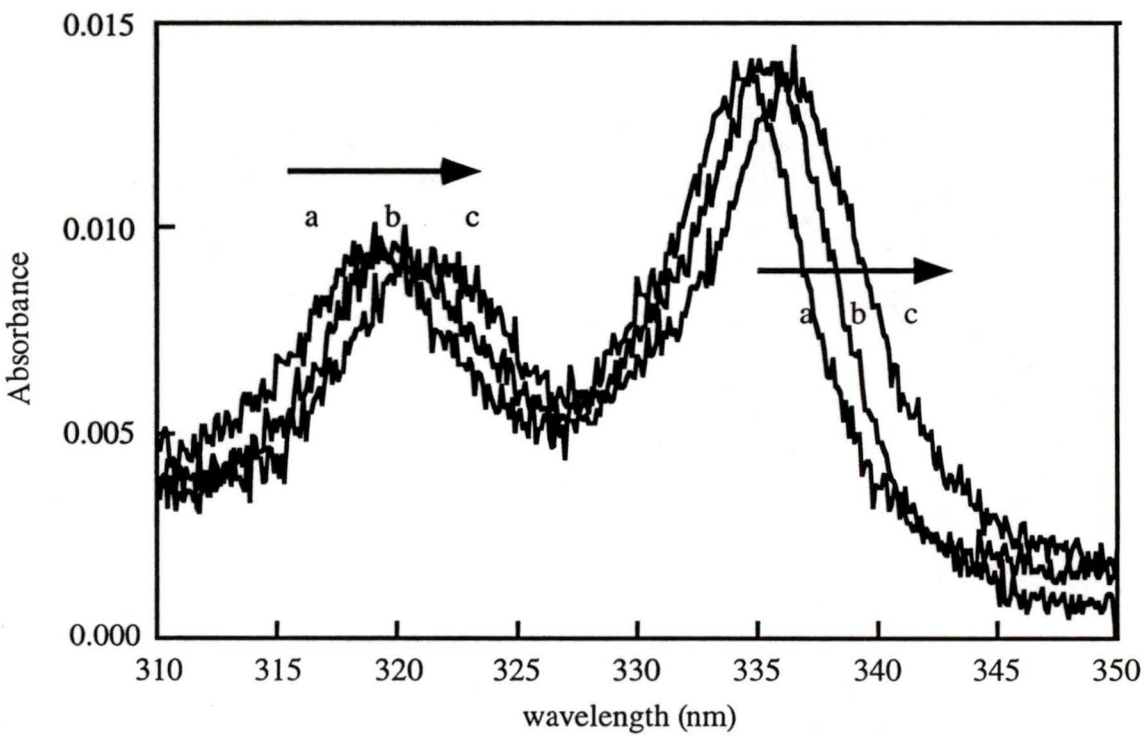

Figure 3-1: Absorption spectra of pyrene (5.0×10^{-7} M) in water, (a); and in the presence of 2.0×10^{-3} M, (b); and 10×10^{-3} M, (c) γ-CD.

There are likely more than two species present in equilibrium as no clear isosbestic points are present in the absorption spectra. This contradicts Hamai's results, as he reports the presence of isosbestic points in the pyrene/ γ-CD system at γ-CD concentrations below 5 x 10^{-3} M[31]. This discrepancy may be a result of errors due to the very low absorption readings, as well as the difference in sample preparation methods between this work and that of Hamai. As Hamai took measurements immediately after solution preparation, the pyrene/ γ-CD system may not have fully equilibrated. Therefore, only a relatively insignificant amount of the multiple stoichiometric complex(es) may have been present at low CD concentrations at the time of measurement. However, the broadening of the red-shifted tail in the presence of high γ-CD concentration was seen in both this and Hamai's[31] studies, and is an indication that a new pyrene species is present. This is attributed to the formation of a ground state pyrene dimer (also see fluorescence data below).

3.1.2 Steady state fluorescence spectroscopy

3.1.2.1 Emission in the presence of γ-cyclodextrin

In aqueous solution, the fluorescece spectrum of pyrene shows five fine structured vibronic peaks between 350 nm and 420 nm corresponding to the emission of pyrene monomer. Upon the addition of γ-CD, a broad, structureless peak above 450 nm grows in at the expense of the fine structured emission (Figure 3-2).

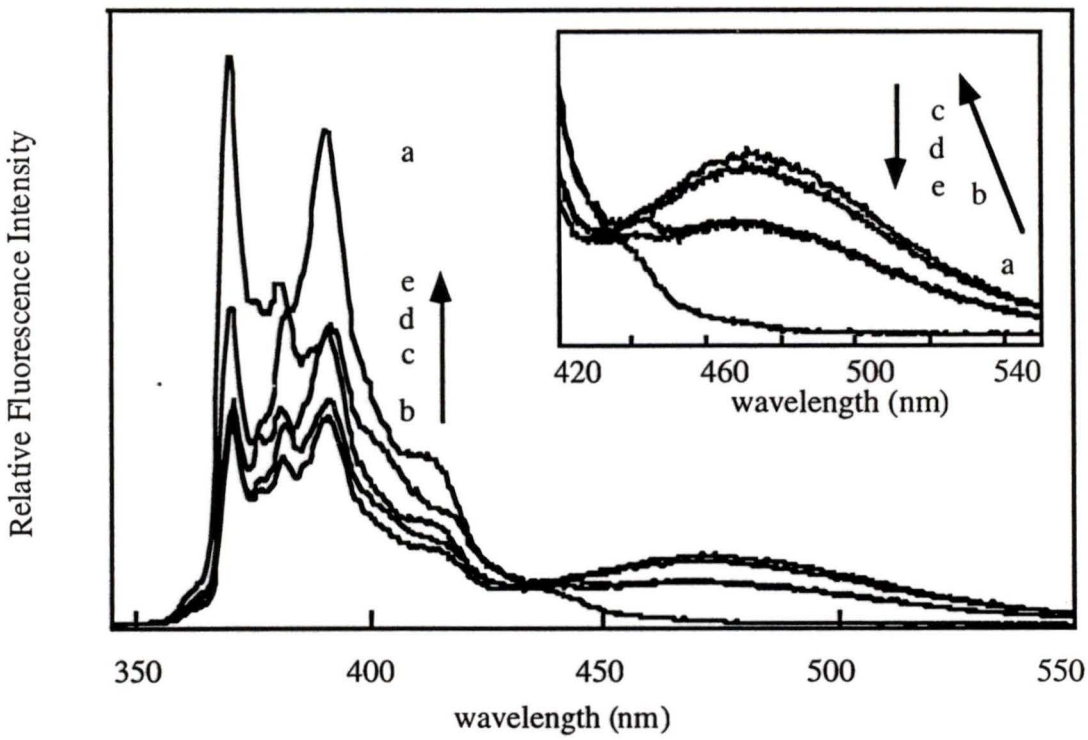

Figure 3-2: Corrected fluorescence spectra of pyrene (5.0×10^{-7} M) in the absence (a) and presence of γ-CD (2.0×10^{-3} M, (b); 5.0×10^{-3} M, (c); 10×10^{-3} M, (d); 20×10^{-3} M, (e). Inset: An enlargement of the excimer emission region at the various γ-CD concentrations is shown.

This broad, red-shifted emission is similar to that characteristic of pyrene excimer emission. At the low concentrations of pyrene used in this work, this excimer emission is absent without γ-CD in aqueous solution. The intensity of the excimer emission increases with γ-CD concentration up to 5.0×10^{-3} M γ-CD; beyond this CD concentration, the excimer emission intensity decreases. This decrease congruently correlates with a rise in intensity at the shorter (monomer) emission wavelengths (Figure 3-2 and Figure 3-3). The ratio of emission intensities at the excimer (473 nm) and

monomer (383 nm) wavelengths, i.e. the excimer-to-monomer ratio, as a function of γ-CD concentration is shown in Figure 3-3.

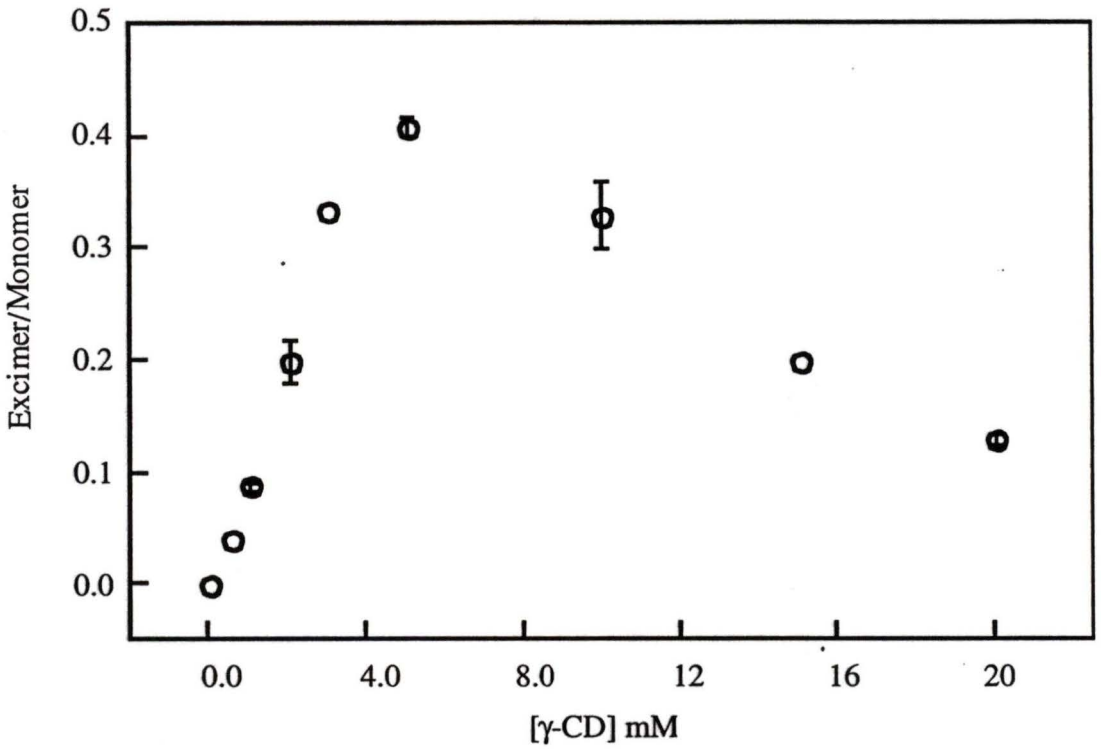

Figure 3-3: The excimer-to-monomer intensity ratio of 5.0×10^{-7} M pyrene in the presence of various γ-CD concentrations. The data have been corrected for monomer emission at the excimer emission wavelength. The excitation wavelength was 331 nm. Error bars indicate the average deviation of two trials; data with no error bars indicate data from one trial.

The excimer-to-monomer intensity ratio is calculated after correcting for monomer emission at the excimer emission wavelength, as the pyrene monomer also emits at 473 nm. The intensity of the monomer emission at 473 nm is calculated by using the monomer intensity ratio, R_m, which involves the emission intensities close to 473 nm and 383 nm of an aqueous pyrene solution, i.e. $(I_{473\ nm,\ py,aq})/(I_{383\ nm,\ py,aq})$ in the absence of

CD. The corrected excimer emission intensity is calculated by subtracting out the monomer emission at 473 nm from the experimental intensity at 473 nm (Equation 3-1). Reference to the correction is made when it is specifically used.

$$I_{excimer(corrected)} = I_{473\ nm} - I_{383\ nm}(R_m)$$

Equation 3-1

The various changes in fluorescence emission intensities indicate that pyrene forms several complexes with γ-CD at different host concentrations. The initial decrease in the intensity of the monomer emission is a result of the pyrene excimer formation. As this does not occur in aqueous solution alone, it is attributed to the formation of a complex in which two pyrene molecules are held within γ-CD. As will be discussed in this chapter, this complex is a 2:2 pyrene: γ-CD complex. The excimer intensity decrease and corresponding monomer emission increase at higher γ-CD concentrations is attributed to the formation of a doubly encapsulated pyrene monomer, i.e. a 1:2 pyrene: γ-CD complex.

The excimer-to-monomer ratio for pyrene in the presence of γ-CD is dependent on the excitation wavelength. The excimer emission intensity is dramatically increased when the excitation wavelength is red-shifted to the broadened part of the absorption spectrum of pyrene in the presence of 10×10^{-3} M γ-CD, i.e. at 350 nm. This indicates that a species other than pyrene monomer exists in the ground state in the presence of γ-CD which gives rise to excimer emission. This is attributed to the formation of a ground state dimer (see also 3.1.2.3).

3.1.2.2 pH dependence of fluorescence emission in the presence of γ-cyclodextrin

The excimer emission of dilute pyrene solutions in the presence of γ-CD is attributed to the formation of a complex with 2:2 stoichiometry. One piece of evidence for this stoichiometry is seen in the dependence of the excimer-to-monomer ratio of emission intensities as the pH varies. That is, the pK_a of the hydroxyl groups in γ-CD is 12.08. Hamai[31] previously showed that an increase in pH to the pK_a leads to a decrease of the excimer emission for the pyrene/ γ-CD system. We repeated these experiments for our experimental conditions ((0.67-1.0) x 10^{-6} M pyrene and (3.3-5.0) x 10^{-3} M γ-CD). That is, the initial concentrations of pyrene and γ-CD used were 1.0 x 10^{-6} M and 5.0 x 10^{-3} M, respectively. As a relatively large amount of base was required to increase the pH of the system to above 12, the concentration of the pyrene and γ-CD decreased throughout the experiment, i.e. to approximately 0.67 x 10^{-6} M pyrene and 3.3 x 10^{-3} M γ-CD. However, the use of the excimer-to-monomer ratio as a measure of excimer emission intensity created an internal calibration method. Thus, by knowing the excimer-to-monomer ratio in various pyrene/ γ-CD concentrations at neutral pH (i.e. Figure 3-3), it was possible to compare the ratio at increased pH with a solution of neutral pH at the same concentration. A decrease in the excimer-to-monomer ratio is observed as the pH increases (Figure 3-4). The ratio at pH 12.7 is 0.05, while it is significantly higher (0.3-0.4) in solutions of neutral pH of approximately the same concentrations. These results confirm that the excimer emission of pyrene involves two CDs.

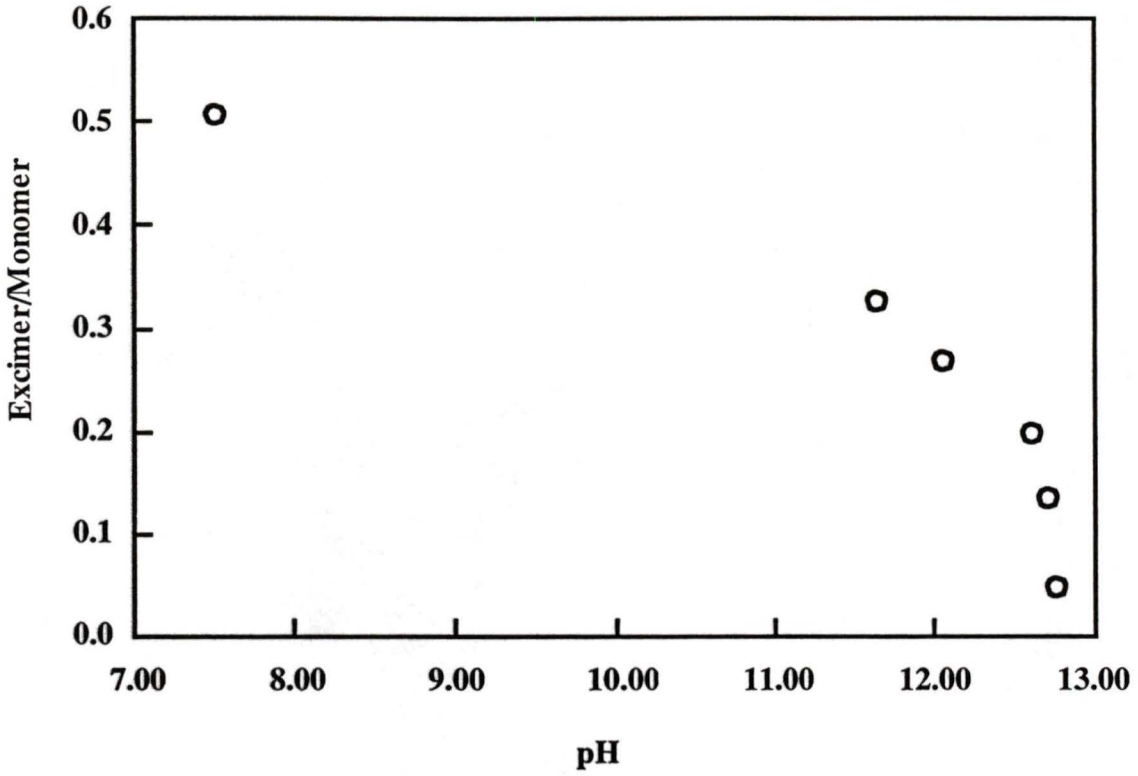

Figure 3-4: Dependence of the excimer-to-monomer ratio for pyrene ((0.67-1.0) x 10^{-6} M) in the presence of ((3.3-5.0) x 10^{-3} M) γ-CD as the pH of the solution increases. The data were corrected for monomer emission at the excimer emission wavelength (473 nm) as described in the text, using a 1.0 x 10^{-6} M pyrene, aqueous solution.

3.1.2.3 Excitation spectra

The excitation spectra of the pyrene monomer in the presence of γ-CD is slightly red-shifted relative to that in aqueous solution. The increasing red-shift from 0 M to 2.0 x 10^{-3} M to 10 x 10^{-3} M γ-CD (Figure 3-5) indicates that the pyrene responsible for the monomer emission is progressively incorporated into several different environments.

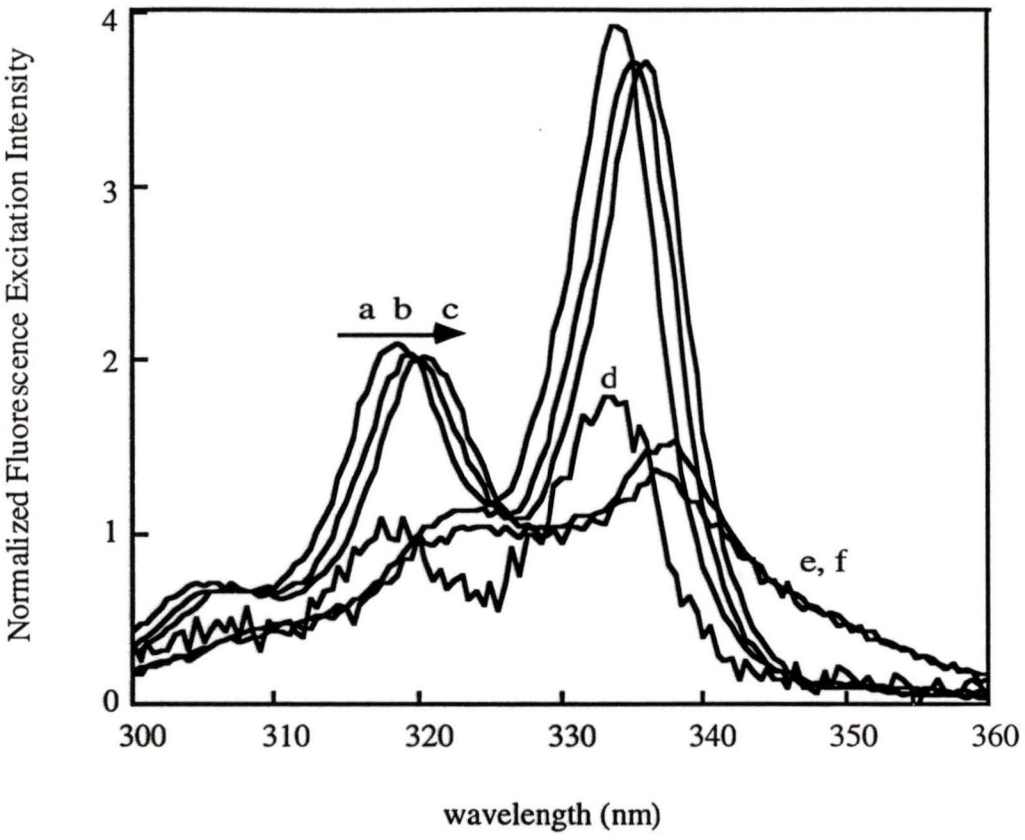

Figure 3-5: Excitation spectra of pyrene (5.0×10^{-7} M) monomer emission (λ_{em} = 383 nm; a, b, c) and excimer emission (λ_{em} = 473 nm; d, e, f) in water (a, d), and in the presence of 2.0×10^{-3} M γ-CD (b, e), and 10×10^{-3} M γ-CD (c, f). The spectra monitoring monomer and excimer emission were normalized at 320 nm to 2 and 1, respectively.

Excitation spectra of the pyrene excimer emission, i.e. monitoring at 473 nm, are red-shifted and broadened relative to the spectra of the monomer emission at each of the corresponding γ-CD concentrations. This result indicates that the emission in the excimer region is due to the excitation of a species other than the pyrene monomer. This is evidence for the formation of a ground state pyrene dimer [53,54], because in the formal excimer formation mechanism the only species present in the ground state and able to be excited are monomer species. The excitation spectrum at 473 nm in the absence of CD is

weak but quite structured, comparable to the excitation spectrum taken at the monomer emission wavelength. This indicates that pyrene monomer emits weakly in the excimer emission region.

3.1.2.4 Fluorescence quenching with iodide

3.1.2.4.1 Quenching in the absence of γ-cyclodextrin

Singlet pyrene monomer is quenched by iodide. In aqueous, aerated solutions the Stern-Volmer constant (K_{sv}) for this process was found to be 167 ± 4 M^{-1} (5 trials) using fluorescence emission measurements. A lifetime quenching study resulted in K_{sv} = 154 M^{-1}. The equal intensity and lifetime ratios indicate that quenching of singlet pyrene by iodide occurs through a dynamic mechanism rather than a static mechanism. The K_{sv} values determined are similar to the value previously reported (141 ± 5 M^{-1} [43]).

3.1.2.4.2 Quenching in the presence of γ-cyclodextrin

The degree of protection that a host provides for a guest molecule, i.e. in forming a host-guest complex, can be studied by adding a quencher to the supramolecular system. Iodide, an ionic quencher, was assumed to quench dynamically in the aqueous phase, rather than enter the hydrophobic CD cavity and cause static quenching.

The Stern-Volmer constants (K_{sv}) were determined for pyrene in several γ-CD concentrations at the monomer (383 nm) (Table 3-1) and excimer (473 nm) (Table 3-2) emission wavelengths.

Table 3-1: Stern-Volmer constants for pyrene (5.0×10^{-7} M) in the presence of various γ-CD concentrations measured at the monomer (383 nm) emission wavelengths using steady-state fluorescence emission intensities.[a]

[γ-CD] 10^{-3} **M**	K_{SV} / M^{-1} **383 nm**
0.0	167 ± 4 (5)
1.0	188 ± 5 (2)
2.0	186 ± 13 (4)
5.0	144 ± 24 (2)
10	84 ± 9 (4)
20	46 ± 5 (2)

a) The monomer emission intensity was taken as the maximum intensity in the emission spectrum near 383 nm to account for any shift in intensity due to complex formation. The number in brackets indicates the number of trials. The errors are the calculated standard deviation for cases where 3 or more trials were performed. For cases where 2 trials were performed, the errors reported are the average deviations.

The addition of γ-CD did not appear to protect the monomer species at low γ-CD concentrations, as the K_{SV} ($= k_q \times \tau_0$) was similar or greater than that without the CD. This indicates that the pyrene monomer included in the CD cavity is quite accessible to the aqueous phase quencher. That is, k_q, the quenching rate constant, appears to be constant or increasing in the presence of host, if τ_0, the lifetime in the absence of quencher, is assumed to be constant at all γ-CD concentrations. However, the lifetime of the probe within the inclusion complex in the absence of quencher may increase for well

protected probes, while k_q may remain constant or decrease as quencher is added to the pyrene/ γ-CD solution. Such a compensation effect, i.e. an increased lifetime with an equivalent or decreased quenching rate constant, may account for the slight increase in K_{SV} as γ-CD is initially added. At higher host concentrations, i.e. at 10 x 10^{-3} M and 20 x 10^{-3} M γ-CD, the linearity of the Stern-Volmer plots decreased (R = 0.9934 and 0.9866, respectively, relative to R = 1.0000 and 0.9999 for the quenching plots of aqueous pyrene and pyrene in the presence of 2.0 x 10^{-3} M γ-CD, respectively). The decrease in linearity of the Stern-Volmer plots at higher concentrations of host is an indication that the probe is present in a number of environments (Figure 3-6). However, it is clear that pyrene is in a more protected environment as the quenching efficiency decreases.

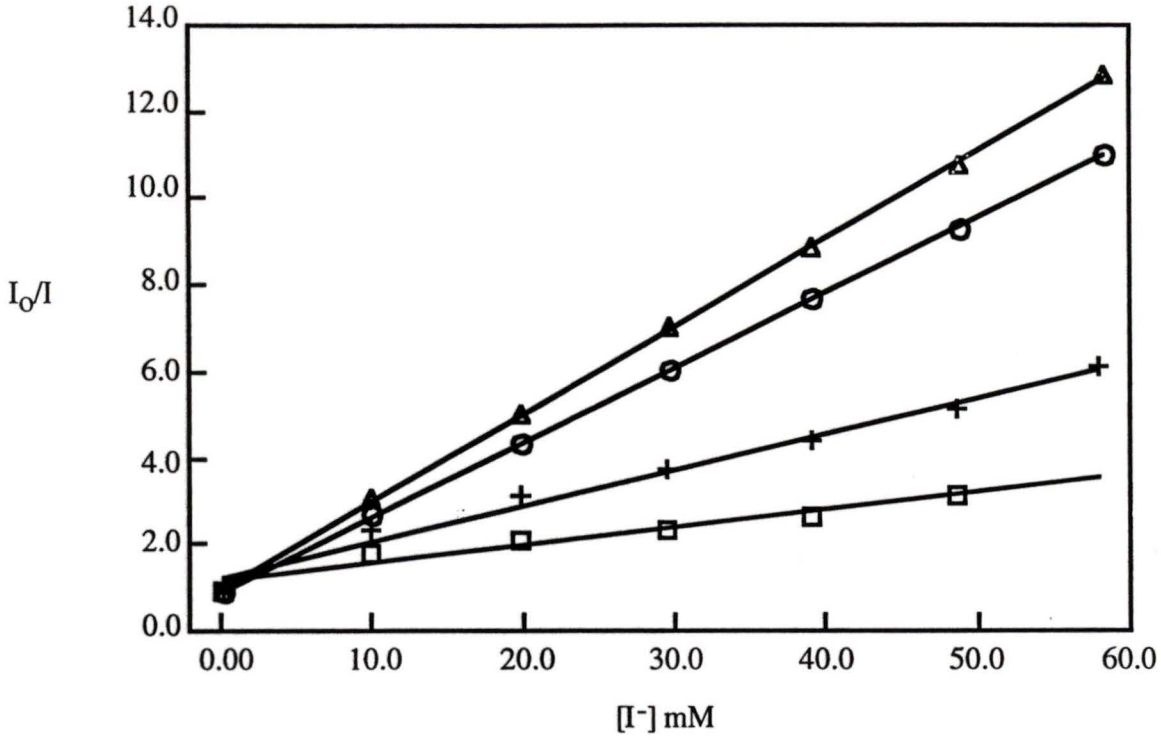

Figure 3-6: Stern-Volmer plots of pyrene (5.0×10^{-7} M) in water (O), and in the presence of 2.0×10^{-3} M γ-CD (Δ), 10×10^{-3} M γ-CD (+), and 20×10^{-3} M γ-CD (□).

Stern-Volmer analysis at the excimer emission wavelength (473 nm) generally led to less linear plots, especially at high CD concentrations (Figure 3-7). The correction for monomer emission at 473 nm (as discussed in section 3.1.2.1 and Equation 3-1) did not significantly improve linearity nor change the K_{sv} values obtained (Table 3-2). The scattering of points is likely a reflection of the very small changes in intensity as quencher is added, as indicated by the small K_{sv} values in Table 3-2.

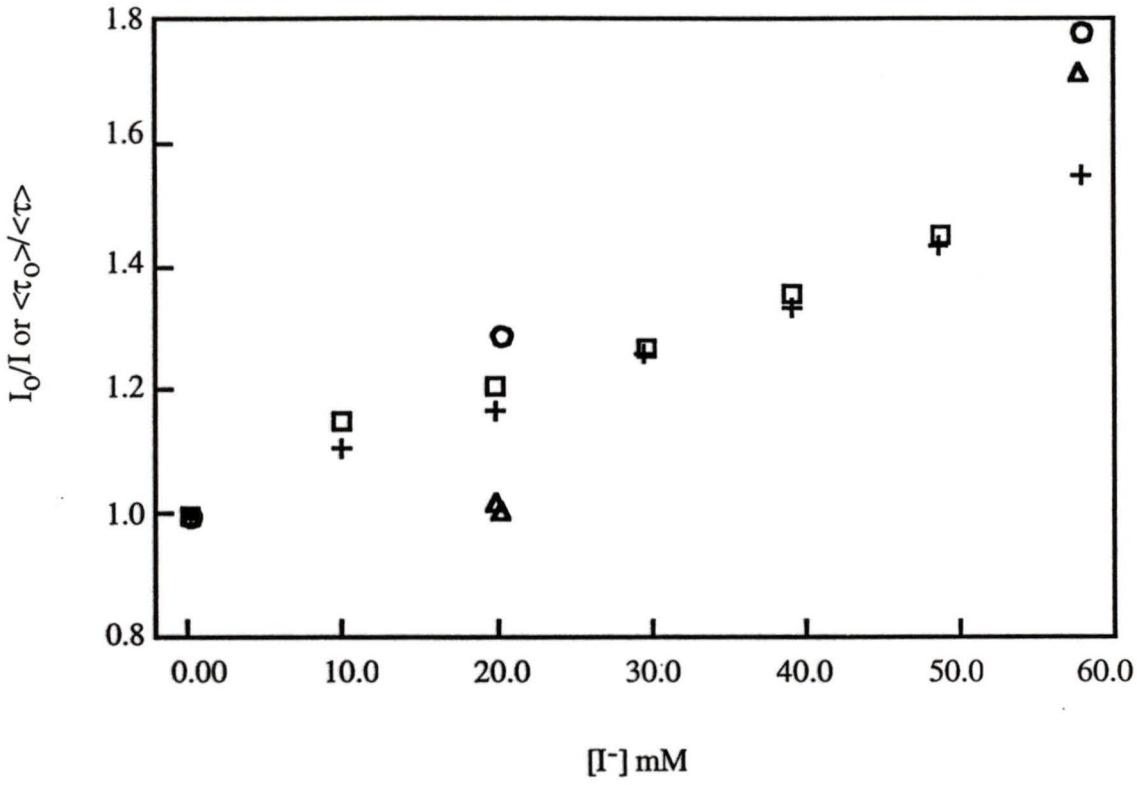

Figure 3-7: Stern-Volmer plots using steady-state and time-resolved data of pyrene (5.0×10^{-7} M) excimer in the presence of 2.0×10^{-3} M γ-CD (□ and O, respectively) and 10×10^{-3} M γ-CD (+ and Δ, respectively). The data were measured at the excimer emission wavelength of 473 nm. The steady-state data were not corrected for monomer emission at this emission wavelength.

Table 3-2: Stern-Volmer constants for pyrene excimer quenching by I^- at various γ-CD concentrations.

[γ-CD] 10^{-3} M	K_{SV} / M^{-1} [a]	K_{SV} / M^{-1} [b]
1.0	10 ± 1 (2)	6 ± 2 (2)
2.0	10 ± 2 (3)	8 ± 3 (2)
5.0	13 ± 5 (2)	17 (1)
10	15 ± 8 (3)	24 (1)

a) Values not corrected for pyrene monomer emission at 473 nm; b) Values corrected for pyrene monomer emission at 473 nm. Brackets indicate the number of trials. The errors are the calculated standard deviation for cases where 3 trials were performed. For cases where 2 trials were performed, the errors reported are the average deviations.

3.1.2.5 R(I/III) analysis

3.1.2.5.1 Influence of γ-cyclodextrin complexation

Pyrene is a favorable probe molecule due to its informative photophysical properties. For example, the relative fluorescence emission intensities of the vibronic fine structure bands are an indicator of the polarity of the environment sensed by pyrene[42] [43]. The R(I/III) ratio, where I = 371 nm and III = 383 nm, of aqueous pyrene in the absence of γ-CD was found to be 1.64 ± 0.02 (3 trials). As the concentration of γ-CD increased, the R(I/III) value continually decreased, indicating that pyrene is in a more hydrophobic environment than water, such as within the CD cavity (Figure 3-8).

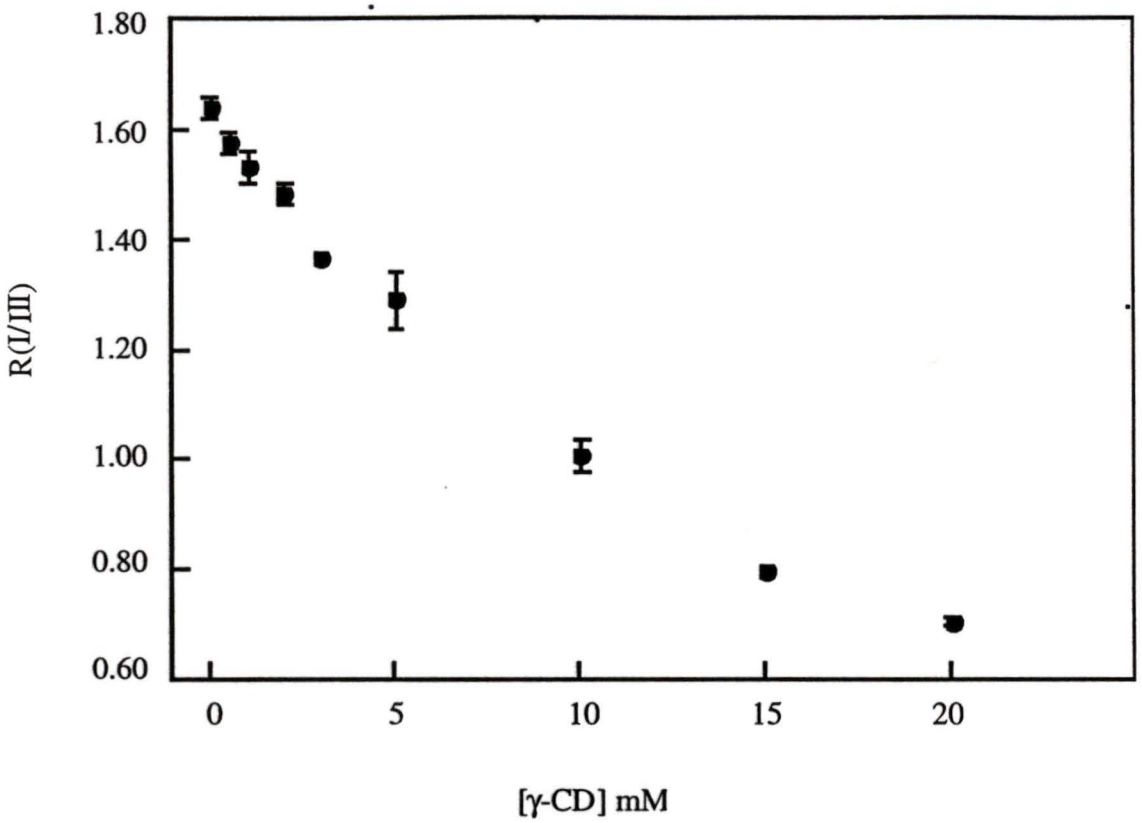

Figure 3-8: R(I/III) of pyrene (5.0×10^{-7} M) in the presence of various concentrations of γ-CD. The intensity of the peaks were taken as the maximum emission intensities near I = 371 nm and III = 383 nm. This was done so as to avoid error in calculating R(I/III) from measuring intensities at a fixed wavelength, as a shift in emission wavelength due to complexation (up to 2 nm) would appear as a change in emission intensity due to environment polarity. The error bars are the standard deviation for 3 trials.

As indicated in Figure 3-2 and Figure 3-3, the fluorescence spectra of pyrene showed increasing excimer emission with γ-CD concentration until a maximum was reached at 5×10^{-3} M γ-CD. Above this CD concentration, the intensity of excimer emission decreased with a congruent rise in monomer emission. From Figure 3-8 and Figure 3-9 it is evident there was also a dramatic drop in R(I/III) after this point. This large decrease in hydrophobicity of pyrene's environment at the expense of excimer

emission may be attributed to the formation of another monomer complex in a highly hydrophobic environment at high γ-CD concentrations, i.e. a 1:2 pyrene: γ-CD complex. The influence of pyrene excimer on the R(I/III) ratio is assumed to be negligible, as its emission does not occur in this region.

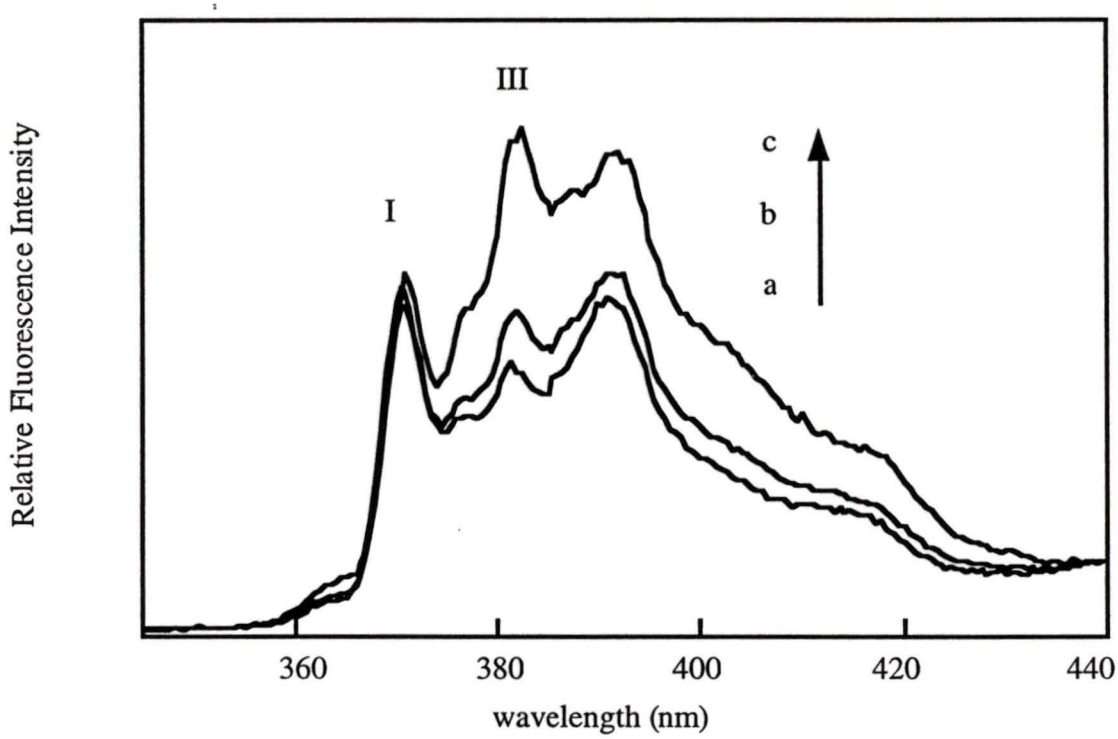

Figure 3-9: Corrected fluorescence spectra of the monomer emission region of pyrene (5.0×10^{-7} M) in the presence of 5.0×10^{-3} M, (a); 10×10^{-3} M, (b); and 20×10^{-3} M, (c) γ-CD.

3.1.2.5.2 Influence of iodide quenching on R(I/III)

The addition of iodide quencher to pyrene/ γ-CD solutions results in various R(I/III) values, depending on the concentration of CD (Figure 3-10). In aqueous solution, and at low γ-CD concentrations, the R(I/III) value is fairly high and constant as iodide is

added. This indicates that pyrene is in a relatively exposed and hydrophilic environment. As the CD concentration increases, the R(I/III) value drops with the addition of quencher, as the more exposed pyrene species are being quenched more efficiently than the protected species. At 10 x 10^{-3} M and 20 x 10^{-3} M γ-CD, R(I/III) decreases and plateaus at a value of 0.68 and 0.54, respectively, as the iodide concentration increases to the maximum value added, i.e. to 60 x 10^{-3} M. These ratios are comparable to pyrene in non-polar solvents, such as cyclohexane, which has an R(I/III) of 0.6[42]. This indicates that at high quencher concentrations any aqueous-exposed pyrene is quenched and only the pyrene that is in a very protected, hydrophobic environment is fluorescing. This well protected pyrene is likely within a doubly encapsulated 1:2 pyrene: γ-CD complex.

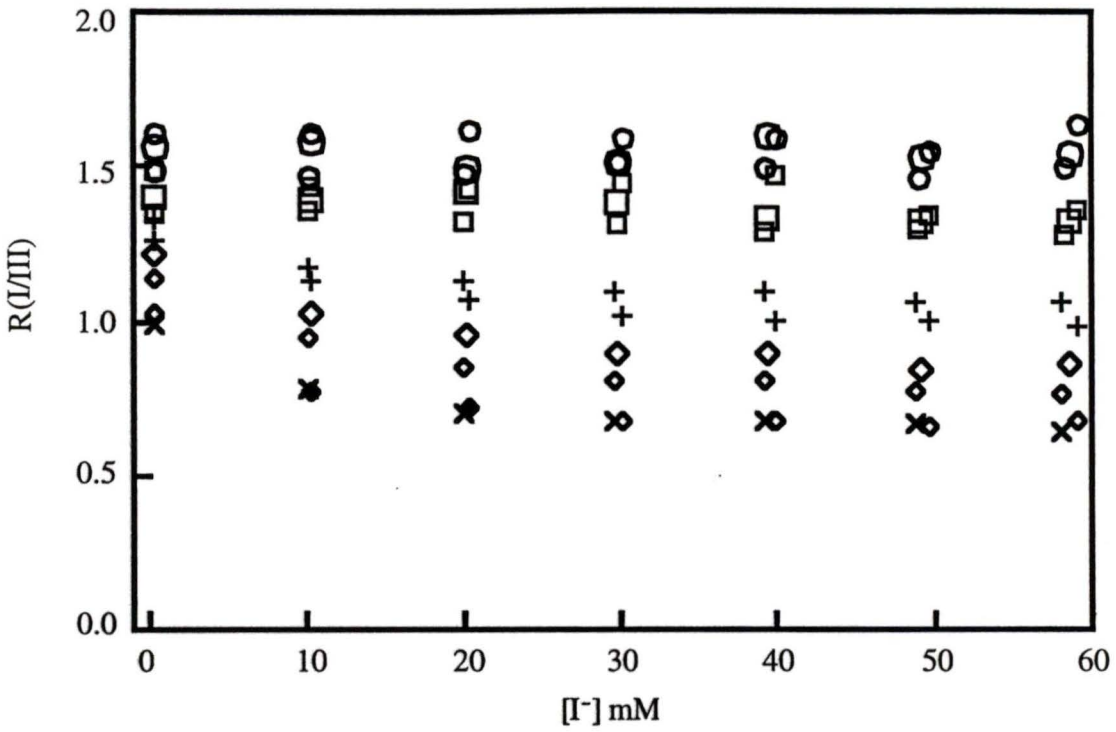

Figure 3-10: The change in R(I/III) ratio of pyrene (5.0×10^{-7} M) in water (O) and various γ-CD concentrations (□ = 2.0×10^{-3} M; + = 5.0×10^{-3} M; ◊ = 10×10^{-3} M; x = 20×10^{-3} M) with the addition of iodide quencher. The various R(I/III) values at slightly different quencher concentration for the same γ-CD concentration indicate the precision among several trials.

3.1.3 Time-resolved fluorescence spectroscopy

3.1.3.1 Excimer Kinetics

In homogenous solution, a pyrene excimer species may be formed by the bimolecular collision of an excited monomer with a ground-state pyrene molecule. As such, a growing-in phase is observed for time-resolved traces of excimer emission that corresponds to excimer formation. This is followed by the excimer decay. For the time-resolved traces of monomer emission, a mono-exponential decay is not observed under conditions where excimer formation occurs. Rather, such a trace can be fitted to the sum

of two exponentials. That is, the lifetime of the fast component corresponds to the lifetime of the growth observed for the excimer emission, as these lifetimes are attributed to the excimer formation process.

Single-photon counting experiments were performed at short time-bases (~ 170 ns) to determine whether such kinetics were present in the pyrene/ γ-CD system. No growth was observed for the excimer emission and no fast decay component was present for the monomer fluorescence decay. These results show that the excimer is formed "instantaneously" [53] [54], i.e. within the excitation pulse (typically 1 - 3 ns), suggesting that the excimer emission originates from a pyrene dimer.

In aqueous solution, pyrene excimer emission is absent due to the low concentration of probe used. The lifetime of aqueous pyrene (5.0×10^{-7} M) at the excimer emission wavelength (473 nm) is 123 ns, nearly equivalent to the lifetime of the same aqueous pyrene solution at the monomer emission wavelength, i.e. 131 ns at 383 nm (Table 3-3).

3.1.3.2 Iodide quenching results

3.1.3.2.1 In the absence of γ-cyclodextrin

Aqueous pyrene monomer was quenched by iodide giving a Stern-Volmer constant of 154 M^{-1}. As previously mentioned, this value is similar to that found using fluorescence emission intensities (167 ± 4 M^{-1}) indicating a dynamic quenching mechanism. The lifetimes at various quencher concentrations are given in Table 3-3. The quenching rate constant using the lifetime data is 1.2×10^{9} $M^{-1}s^{-1}$.

Table 3-3: Lifetimes of pyrene (5.0×10^{-7} M) in water at the monomer emission wavelength (383 nm).

[I-] (mM)	a_1 [(a)] τ_1 [(a)] (ns)
0	1.000 ± 0.001 131.22 ± 0.03
20.0	1.000 ± 0.007 32.27 ± 0.07
58.4	1.00 ± 0.01 13.1 ± 0.1

(a) The errors are specific to the data analysis of each decay, and are recovered from the PTI software.

The pyrene excimer is also quenched by iodide. In aerated acetonitrile, the lifetime of the excimer of pyrene (10×10^{-3} M) was 12.5 ns. The addition of 20×10^{-3} M iodide quencher reduced the lifetime to 11.2 ns, resulting in an estimated quenching rate constant of 5×10^{8} $M^{-1}s^{-1}$. These results are important in the interpretation of the quenching data in the presence of γ-CD.

3.1.3.2.2 In the presence of γ-cyclodextrin

The addition of quencher to supramolecular systems allows one to determine the degree of protection a host is providing for a guest. The ease with which a quencher can reach a probe, thereby reducing its lifetime, is an indicator of the probe's protection. Further, differentiation between lifetimes of the various species becomes magnified in the

presence of quencher, as some probes will be more exposed than others and therefore their lifetime will decrease more significantly. This is valid for the dynamic quenching process only, because no reduction of lifetime is observed for static quenching. As iodide is an aqueous quencher, it is not likely to enter the hydrophobic CD cavity. Also, as indicated from the steady-state and time-resolved data comparison below, quenching by iodide of the pyrene/ γ-CD system is indeed dynamic. In this work, the time-resolved quenching data are used for a qualitative analysis to determine the stoichiometries of the various species present in the complex pyrene/ γ-CD system. For this reason, the lifetime data were only collected at a few quencher concentrations.

3.1.3.2.2.1 Pyrene monomer emission

In the presence of 2.0×10^{-3} M γ-CD, the time-resolved decay trace of the pyrene monomer was fitted to the sum of two exponentials (Table 3-4). When the data were fit to the sum of three exponentials, two of the lifetimes converged to the same lifetime value, indicating that only 2 distinguishable species were present. The lifetimes recovered from the fits to the sum of two or three exponentials have considerable error. For this reason, the lifetimes of the components that are known to be present in solution were fixed in some cases, in order to determine the lifetimes of the other components. For example, in all solutions, i.e. both in the absence and in the presence of quencher and CD, free aqueous pyrene is present. As such, its lifetime was fixed in the fitting procedure.

The addition of iodide quencher to the pyrene/ γ-CD system resulted in data that were also adequately fit to a bi-exponential function, both of which had reduced lifetimes

relative to the values obtained in the absence of quencher. The estimated Stern-Volmer constant for the long-lived monomer component is 51 ± 9 M^{-1}. Based on the lifetime in the absence of quencher, i.e. 192 ns, the quenching rate constant is (2.7 ± 0.5) x 10^8 $M^{-1}s^{-1}$. This is an order of magnitude lower than kq of aqueous pyrene, i.e. 1.2 x 10^9 $M^{-1}s^{-1}$, indicating that the second monomer component that is present in γ-CD is less accessible by the quencher than the aqueous component.

Table 3-4: Lifetimes recovered from the fluorescence decay of pyrene (5.0 x 10^{-7} M) in the presence of 2.0 x 10^{-3} M γ-CD monitored at pyrene monomer emission wavelength (383 nm).

[I-] (mM)	a_1 τ_1 **(ns)**	a_2 τ_2 **(ns)**
0	0.42 ± 0.02 131.0 (*)	0.58 ± 0.02 192 ± 1
20.2	0.982 ± 0.009 33.8 ± 0.1	0.018 ± 0.001 128 ± 5
59.3	0.96 ± 0.02 13.6 ± 0.1	0.041 ± 0.006 49 ± 4

(*) indicates the lifetimes that were fixed when fitting the decay trace, as discussed in the text. The errors are specific to the data analysis of each decay, and are recovered from the PTI software.

The fitting procedure for the decays of pyrene (5.0 x 10^{-7} M) monomer emission in the presence of 10 x 10^{-3} M γ-CD and various quencher concentrations was similar to

that in the presence of 2.0 x 10^{-3} M γ-CD as described above. The results are shown in Table 3-5. In the absence of quencher, the decay trace of the pyrene monomer was fitted to the sum of two exponentials. As in case of pyrene in the presence of 2.0 x 10^{-3} M γ-CD, when the data were fit to three exponentials, two of the lifetimes converged or a negative pre-exponential value was obtained.

With the addition of quencher, the decay traces fit well to the sum of three exponentials. The lifetime of the longest lived species was recovered by fixing the lifetimes of the two shorter lived monomer species obtained previously.

Table 3-5: Lifetimes recovered from the fluorescence decay of pyrene (5.0×10^{-7} M) in the presence of 10×10^{-3} M γ-CD monitored at the monomer emission wavelength (383 nm).

$[I^-]$ mM	a_1 τ_1 (ns)	a_2 τ_2 (ns)	a_3 τ_3 (ns)
0	0.52 ± 0.02 131.0 (*)	0.48 ± 0.01 278 ± 2	
20.0	0.707 ± 0.001 32.0 (*)	0.192 ± 0.001 128.0 (*)	0.101 ± 0.001 313.2 ± 0.3
19.8	0.776 ± 0.004 32.0 (*)	0.146 ± 0.001 121.0 (*)	0.078 ± 0.001 290 ± 1
58.1	0.83 ± 0.07 13.0 (*)	0.12 ± 0.02 37 ± 4	0.054 ± 0.003 153 ± 4

(*) indicates the lifetimes that were fixed when fitting the decay trace. The errors are specific to the data analysis of each decay, and are recovered from the PTI software.

The Stern-Volmer constants of the individual components of pyrene in the presence of 10×10^{-3} M γ-CD, i.e. τ_2 and τ_3, were calculated based on the assumption that three components are present in the absence of quencher. However, experimentally these lifetimes cannot be differentiated. This is a problem that may be related to the low number of total counts collected[55]. However, data collection over longer periods of time was not technically possible. The lifetime of the intermediate component, i.e. τ_2, in the absence of quencher was assumed to be 192 ns, corresponding to the lifetime of the long-lived component in the presence of 2.0×10^{-3} M γ-CD. Using this value, K_{SV} was found

to be 77 ± 15 M^{-1}, a value that is close to that determined in the presence of 2.0 x 10^{-3} M γ-CD (i.e. 51 ± 9 M^{-1}) .

The lifetime of the third species in the absence of quencher is not known, but it is likely to be longer than 280 ns. The third lifetime becomes apparent in the presence of quencher because the difference between τ_2 and τ_3 is increased. As the differentiation between lifetimes is resolved in the presence of quencher and as the third lifetime is maintained at a higher value per quencher concentration, it may be concluded that the third species is better protected from quencher than the second species. Reinforcing this point is the observation that the degree of quenching is larger for τ_2 than it is for τ_3, i.e. there is a decrease in lifetime by a factor of 3.4 in τ_2 from 20 x 10^{-3} M I^- to 60 x 10^{-3} I^-, whereas τ_3 only decreases by a factor of 2.0 under the same conditions (Table 3-4).

The comparison between time-resolved and steady-state Stern-Volmer analysis is an issue that has been debated in the past[7 8 43], as both static quenching and dynamic quenching may be involved. The amplitude average lifetime leads to average lifetime values that can be directly compared to the intensity ratios in the steady-state experiments[8]. If there is an element of static quenching occuring in the system, the value of $\langle\tau_o\rangle / \langle\tau\rangle$ would lie below that of I_o/I[6]. The Stern-Volmer constant derived for pyrene monomer in 2.0 x 10^{-3} M γ-CD using the amplitude average lifetimes was 169 M^{-1}. This value was slightly, but not significantly lower than the value obtained from steady-state fluorescence (186 ± 13 M^{-1}). However, considering that the lifetime measurements were done at only two quencher concentration, the agreement between the two methods is good. As such, the two values may be considered equivalent and therefore no significant static quenching is occuring.

Using the amplitude average lifetimes from the time-resolved data obtained for the pyrene monomer species in the presence of 10 x 10^{-3} M γ-CD, the Stern-Volmer constant was calculated to be 135 M^{-1}. This value is higher than that found from steady-state analysis (84 ± 9 M^{-1}); however, the Stern-Volmer plot began to lose linearity, and the data should be taken qualitatively rather than quantitatively. In any case, both values are lower than that obtained in the absence of CD suggesting that some of the pyrene monomer species are protected from iodide quenching.

3.1.3.2.2.2 Pyrene excimer emission

In the presence of 2.0 x 10^{-3} M γ-CD, two components were obtained from the time-resolved decay traces at the pyrene excimer emission wavelength (473 nm), both in the absence and presence of quencher (Table 3-6). In the absence of quencher, an attempt was made to fit the lifetime data to three exponentials, but only a very short lived (1 ns) third component was present that had a very small pre-exponential factor (0.02). This short lifetime is due to a fitting artifact. At the highest quencher concentration (~ 60 x 10^{-3} M I^-), a fit to the sum of three exponentials resulted in the convergence of two lifetimes, indicating only two species were distinguishable. The lifetime of the short-lived species did not change appreciably upon the addition of quencher. However, the initially longer lived component was quenched in a similar fashion to the long-lived monomer species (Table 3-6). This species corresponds to the monomer emission at 473 nm.

Table 3-6: Lifetimes obtained from the fluorescence decay traces of pyrene (5.0×10^{-7} M) in the presence of 2.0×10^{-3} M γ-CD and various iodide quencher concentrations; λ_{ex} = 331 nm.

$[I^-]$ mM[(a)]	a_1 τ_1 (ns)[(a)]	a_2 τ_2 (ns)[(a)]	$[I^-]$ mM[(b)]	τ_2 (ns)[(b)]
0	0.922 ± 0.001 77.99 ± 0.01	0.078 ± 0.001 171.8 ± 0.1	0	192 ± 1
20.0	0.949 ± 0.007 62.4 ± 0.2	0.051 ± 0.004 132 ± 3	20.1	128 ± 5
57.8	0.235 ± 0.001 69.4 ± 0.1	0.765 ± 0.001 41.2 ± 0.1	59.3	49 ± 4

(a) Lifetimes obtained at the excimer emission wavelength, 473 nm; (b) Lifetimes of the long-lived component obtained at the monomer emission wavelength, 383 nm, under similar conditions, i.e. similar host and quencher concentrations. The errors are specific to the data analysis of each decay, and are recovered from the PTI software.

In the presence of 10×10^{-3} M γ-CD, the decay traces at the excimer emission wavelength were fit to the sum of two exponentials at all quencher concentrations. The lifetime values obtained are listed in Table 3-7. Attempts were made to fit the decay traces to the sum of three exponentials, but in the absence of quencher two of the lifetimes converged indicating only two species were distinguishable. Similarly, upon the addition of quencher, the best fits were to the sum of two exponentials.

As discussed earlier, the decay of pyrene in 2.0×10^{-3} M γ-CD measured at 473 nm included a component due to monomer emission as well as excimer emission.

Further, in traces at this concentration of CD and various quencher concentrations, one of the lifetimes recovered at an emission wavelength of 473 nm corresponded closely to one of the lifetimes measured at 383 nm (at all equivalent quencher concentrations). Such a correspondence of lifetimes at the two emission wavelengths is not seen in the presence of 10 x 10^{-3} M γ-CD and at various quencher concentrations (Table 3-7). This is likely due to the lower number of counts obtained for the traces. Further, the emission quantum yield of monomer emitting in the excimer region is very low and therefore differentiation between monomer species may not have been possible. The lifetime of the initially longer-lived component in the excimer emission region of pyrene in the presence of 10 x 10^{-3} M γ-CD (column 3 in Table 3-7) is likely the lifetime of a combination of the monomer species present, i.e. a combination of the lifetimes in columns 5 and 6 in Table 3-7.

Table 3-7: Lifetimes recovered from the decay traces of pyrene (5.0×10^{-7} M) in the presence of 10×10^{-3} M γ-CD and various iodide concentrations; $\lambda_{ex} = 331$ nm.

$[I^-]$ mM[(a)]	a_1 τ_1 (ns) [(a)]	a_2 τ_2 (ns) [(a)]	$[I^-]$ mM [(b)]	τ_2 (ns) [(b)]	τ_3 (ns) [(b)]
0	0.926 ± 0.007 93.6 ± 0.7	0.074 ± 0.007 260 ± 10	0	278 ± 2	
19.8	0.88 ± 0.02 90 ± 1	0.12 ± 0.02 205 ± 9	19.8	121.0 (*)	290 ± 1
20.0	0.900 ± 0.002 90.4 ± 0.2	0.100 ± 0.001 233 ± 1	20.0	128.0 (*)	313.2 ± 0.3
57.5	0.33 ± 0.04 94 ± 3	0.67 ± 0.04 46 ± 2	58.1	37 ± 4	153 ± 4

(a) Lifetimes taken at the excimer emission wavelength, 473 nm; (b) Lifetimes of the long-lived components taken at the monomer emission wavelength, 383 nm. (*) represents fixed lifetimes in the fitting procedure, as discussed in the text. The errors are specific to the data analysis of each decay, and are recovered from the PTI software.

To compare time-resolved data to steady-state data for excimer emission, amplitude average calculations were used, as described above. For pyrene in 2.0×10^{-3} M γ-CD, K_{SV} was found to be 13.5 M^{-1}. This is quite comparable to the low value obtained from steady-state fluorescence emission, i.e. 10 ± 2 M^{-1}. This value did not involve the correction for monomer emission at 473 nm, i.e. Equation 3-1, as the lifetime average includes the monomer component(s) emitting in this region (Figure 3-7).

In the presence of 10 x 10^{-3} M γ-CD, the Stern-Volmer constant estimated using the average lifetimes was 13.7 M^{-1}. This is very close to the K_{sv} obtained using fluorescence intensity data, i.e. 15 M^{-1}. As mentioned above, calculation of this latter value did not involve correction of monomer emission at 473 nm, as the lifetime average analysis also factors in monomer emission at 473 nm.

3.2 Discussion

3.2.1 Species present in the pyrene/ γ-cyclodextrin system

As discussed in the Introduction, previous studies involving the characterization of pyrene in the presence of γ-CD have led to inconsistent results. For example, the stoichiometries of the complexes present as well as their proposed equilibrium constants vary quite significantly (Table 1-2). However, before a study of the dynamics of a system can be initiated, it is necessary to know the stoichiometry and amount of each complex present under various experimental conditions. This information is required so that a dynamic mechanism of the system may be proposed and verified. From the characterization results of this work, the equilibria in the pyrene/γ-CD system are presented in Scheme 3-1.

$$py + CD \underset{}{\overset{K_{1:1}}{\rightleftharpoons}} py\text{-}CD$$

$$py\text{-}CD + CD \underset{}{\overset{K_{1:2}}{\rightleftharpoons}} CD\text{-}py\text{-}CD$$

$$py\text{-}CD + py\text{-}CD \underset{}{\overset{K_{2:2}}{\rightleftharpoons}} CD\text{-}py\text{-}py\text{-}CD$$

Scheme 3-1: Equilibria present in the pyrene/ γ-CD system.

The equilibrium constants in Scheme 3-1 are defined in terms of the components based on the step-wise formation mechanism in Equation 3-2, Equation 3-3, and Equation 3-4.

$$K_{1:1} = \frac{[Py\text{-}\gamma\text{-}CD]}{[Py]_{free}[\gamma\text{-}CD]}$$

Equation 3-2

$$K_{1:2} = \frac{[\gamma\text{-}CD\text{-}Py\text{-}\gamma\text{-}CD]}{[\gamma\text{-}CD][Py\text{-}\gamma\text{-}CD]}$$

Equation 3-3

$$K_{2:2} = \frac{[(Py\text{-}\gamma\text{-}CD)_2]}{[(Py\text{-}\gamma\text{-}CD)]^2}$$

Equation 3-4

The physical sizes of pyrene and γ-CD are reported as the following: i) pyrene: 10.4 Å long, 8.2 Å wide[25] and ii) the γ-CD cavity has a diameter ranging from 7.5 – 8.3 Å, and is 7.8 Å long[10]. From these values, each of the proposed complexes are feasible, although the various orientations may vary. Further, it should be realized that the CD cavities are not rigid structures, and therefore their dimensions may vary somewhat, in order to accommodate the guest.

Qualitative evidence for the presence of these species include the absorption spectra, steady-state spectra, time-resolved traces, and the quenching data obtained from the latter two techniques. The equilibrium constants of these species can be determined using equations that incorporate steady-state fluorescence data (see below).

The lack of isosbestic points in the absorption spectra of pyrene in the presence of γ-CD indicates that more than two species are present in equilibrium. The steady-state fluorescence data indicate that pyrene is in various environments as the γ-CD concentration varies. For example, as the concentration of host increases, the R(I/III) ratio decreases to about 0.6, similar to the value of pyrene in cyclohexane. This indicates that the pyrene monomer is incorporated into an increasingly hydrophobic environment. On the addition of quencher, there is a decrease and plateau of the R(I/III) ratio at the higher γ-CD concentrations. This indicates that only a well protected monomer species is left to emit. This decrease in R(I/III) does not occur at the lower γ-CD concentrations indicating that only an equally exposed monomer is present. These results are consistent with the fact that at higher γ-CD concentrations, a double encapsulated 1:2 pyrene: γ-CD species is present, whereas a 1:1 pyrene: γ-CD species dominates at the lower host concentrations. As one of the driving forces for supramolecular complex formation is the

hydrophobic effect[11], that is, removing water from the hydrophobic interior of the CD cavity and replacing it with the hydrophobic guest molecule, this explanation is feasable.

The different lifetimes obtained from the time-resolved data at the monomer emission wavelengths also indicate that more than one monomer species is present. The fact that one of the multiple lifetimes obtained in the presence of higher γ-CD concentration (Table 3-5) was longer than that at lower CD concentration (Table 3-4) indicates that two different CD-included pyrene monomers are present. Further proof of the presence of various monomers is seen in the quenching experiments. The degree of reduction of lifetimes as a result of a dynamic quenching mechanism indicates the degree of protection provided by the host. From the Stern-Volmer constants obtained for the individual components (using lifetimes), it is evident that in the presence of 2.0×10^{-3} M γ-CD and 10×10^{-3} M γ-CD, there are two common species, i.e. two species quenched to the same degree. The most exposed is aqueous or free pyrene ($k_q = 1.2 \times 10^9$ $M^{-1}s^{-1}$). The second component that is more protected ($k_q = (2.7 \pm 0.5) \times 10^8$ $M^{-1}s^{-1}$ and $(4.0 \pm 0.8) \times 10^8$ $M^{-1}s^{-1}$ in 2.0×10^{-3} M γ-CD and 10×10^{-3} M γ-CD, respectively) is attributed to a 1:1 pyrene: γ-CD complex. The third component in 10×10^{-3} M γ-CD had a longer lifetime and was quenched less efficiently than the other two components. This species, which is even more protected from the quencher, is attributed to a doubly-encapsulated 1:2 pyrene: γ-CD complex.

Further evidence of a 1:2 pyrene: γ-CD complex is seen from the change in excimer-to-monomer ratio as the concentration of host is increased. As Figure 3-3 shows, the ratio maximizes and then begins to decrease above 5×10^{-3} M γ-CD. That is, the amount of excimer formed decreases as host is added, at the expense of the formation

of a monomer species. As this occurs at high host concentrations, it is likely due to the formation of a monomer species within more than one CD, i.e. the 1:2 pyrene: γ-CD complex.

The complex that gives rise to pyrene excimer emission in the presence of γ-CD has previously been proposed to be either a 2:1 and/or a 2:2 pyrene: γ-CD complex[13,31,32]. However, the single photon counting data, the pH experiment, and the fitting procedure for determining equilibrium constants (below) point to the formation of a 2:2 pyrene: γ-CD complex. Several pieces of evidence indicate that the pyrene excimer emission seen in the presence of γ-CD is due to the formation of a pyrene dimer in the ground state rather than via the formal dynamic mechanism of excimer formation described in the Introduction. For example, the very broadened and red-shifted excitation emission spectrum indicates that a species other than the pyrene monomer is being excited. Secondly, single photon counting traces at the excimer emission band do not show the growth curve that would be present due to bimolecular excimer formation. Further, the monomer does not show a fast decay component which would complement the excimer growth, as excimer formation is a quenching mechanism of the monomer.

As previously mentioned, the excimer emitting species is a 2:2 pyrene: γ-CD complex which is formed in the ground state. The lifetime of pyrene excimer in the presence of γ-CD is 86 ± 8 ns, corresponding well to 77 ns, which has been reported in the literature for 4.9×10^{-7} M pyrene in 10×10^{-3} M γ-CD [44]. The lifetime of pyrene excimer has also been reported in various solvents as 65 ns (cyclohexane), 43.5 ns (acetone), 50 ns (95% ethanol), and 113 ns (for the pyrene excimer crystal)[9]. The relatively long lifetime recovered for the excimer in γ-CD indicates that the pyrene dimer

is in a rigid environment, as the rate of deactivation is decreased. The lifetime of the excimer is quite constant with the addition of quencher, indicating that this species is not quenched by iodide. From lifetime data of pyrene excimer in the absence of cyclodextrin, i.e. in organic solvent where the solubility of pyrene is high enough such that excimer formation is possible, the quenching rate constant of the pyrene excimer by iodide is $5 \times 10^8\ M^{-1}s^{-1}$. If, in the presence of γ-CD, the excimer emitting complex was a 2:1 pyrene: γ-CD complex, it is likely that the quenching rate constant would be quite similar to the value obtained in acetonitrile ($5 \times 10^8\ M^{-1}s^{-1}$), or to that of the 1:1 pyrene: γ-CD complex ($(2.7 \pm 0.5) \times 10^8\ M^{-1}s^{-1}$, see section 3.1.3.2.2.1), oweing to its exposure to quencher at the open-sided CD faces. As a result, the expected lifetimes on the addition of quencher would be substantially lower than they are found to be experimentally (Table 3-6 and Table 3-7). That is, using Equation 1-15 and the quenching rate constant of pyrene excimer by iodide as $(2 - 5) \times 10^8\ M^{-1}s^{-1}$, the lifetimes of the pyrene dimer at 20×10^{-3} M I^- and 60×10^{-3} M I^- quencher concentrations are calculated to be 46-64 ns and 24-42 ns, respectively. Such a decrease in lifetime is not observed upon quenching (Table 3-6 and Table 3-7) and is therefore an indication that the pyrene dimer is in a well protected environment, such as within two CDs as a 2:2 guest: host complex. Stern-Volmer analysis of fluorescence data also indicate the excimer is not quenched by iodide (Figure 3-7).

As discussed in the Introduction, several authors have proposed that if the pH of a solution containing an excimer emitting CD complex rises above the pK_a of the CD hydroxyl groups (i.e. to a pH greater than ~ 12), the excimer emission intensity will decrease if the complex giving rise to the excimer emission is a 2:2 guest: CD complex.

This is because the deprotonated hydroxyl groups of the two facing "barrel-type"[31] CDs that form the 2:2 complex repel each other, resulting in the complex falling apart. As such, the intensity of excimer emission would decrease. This is what is seen for the pyrene/ γ-CD system. As the pH increases above 11, the excimer-to-monomer ratio begins to drop dramatically indicating that the 2:2 excimer emitting species is falling apart while the amount of pyrene monomer increases. This result has been reported in the literature[31]. The authors that disregard the 2:2 complex[13], or include the 2:1 complex[13,32] did not report a pH-dependent fluorescence experiment.

3.2.2 Determination of equilibrium constants for the multiple stoichiometric equilibria

The method employed to calculate the equilibrium constants of solutions containing multiple stoichiometric equilibria has been used by several authors[17-19]. It involves knowing which species are present in the system. This may be based on other experimental analysis, although the goodness of fits for the equilibrium constants to experimental data themselves also reinforce the presence of species of various stoichiometries. The model used to determine the equilibrium constants for the pyrene: γ-CD follows the sequential formation of the 1:1, 1:2 and 2:2 pyrene: γ-CD complexes, as shown in Scheme 3-1. The determination of equilibrium constants for the multi-component pyrene/ γ-CD system is based on the assumption that the amount of excimer species present is proportional to the intensity of its emission at a wavelength where only that species emits. As some monomer does emit at 473 nm, the excimer emission intensity was corrected for as described by Equation 3-1. It is this corrected excimer

emission intensity that was taken as being proportional to the concentration of excimer present in the solution. An equation was formulated based on the relation of the 2:2 concentration to the concentration of all other species present in solution (Equation 3-5).

$$\left[(\text{Py-}\gamma\text{-CD})_2\right] = \left(\frac{[\text{Py}]_{total} - [\text{Py}]_{free} - [\text{Py-}\gamma\text{-CD}] - [\gamma\text{-CD-Py-}\gamma\text{-CD}]}{2}\right)$$

Equation 3-5

The equation is divided by two to account for the fact that there are two pyrene molecules within one 2:2 complex. The concentrations of the complexes in Equation 3-5 are defined in Scheme 3-1 and in terms of equilibrium constants based on the step-wise formation mechanism as defined in Equation 3-2, Equation 3-3, and Equation 3-4; $[\text{Py}]_{free}$, is given by Equation 3-6.

$$[\text{Py}]_{\text{free}} = \frac{A \pm \sqrt{B}}{C}$$

Equation 3-6

where A, B, and C are defined as:

$$A = -\left(1 + K_{1:1}[\gamma - \text{CD}] + K_{1:1}K_{1:2}[\gamma - \text{CD}]^2\right)$$

Equation 3-7

$$B = \left(1 + K_{1:1}[\gamma - CD] + K_{1:1}K_{1:2}[\gamma - CD]^2\right)^2 + 4\left(2K_{2:2}K_{1:1}{}^2[\gamma - CD]^2\right)\left([Py]_{total}\right)$$

Equation 3-8

$$C = 2\left(2K_{2:2}K_{1:1}{}^2[\gamma - CD]^2\right)$$

Equation 3-9

This was formulated by solving the terms in Equation 3-5 in terms of the equilibrium constants from the step-wise formation mechanism (Scheme 3-1), equating the equation to zero (see Equation 3-10), and solving for $[Py]_{free}$ using the quadratic equation.

$$2K_{2:2}K_{1:1}{}^2[Py]_{free}^2[\gamma - CD]^2 + [Py]_{free}\left(1 + K_{1:1}[\gamma - CD] + K_{1:2}K_{1:1}[\gamma - CD]^2\right) - [Py]_{total} = 0$$

Equation 3-10

The use of Equation 3-5 was only valid upon normalization of the experimental excimer fluorescence emission intensity as well as the calculated 2:2 complex concentration. This is because the emission quantum yield of this complex is not known, and therefore it's absolute concentration cannot be determined. However, by normalizing the experimental emission intensity and the calculated 2:2 concentration to one at the maximum intensity and concentration, respectively, the values at the various γ-CD concentrations may be directly compared.

Based on the proposed mechanism (Scheme 3-1) and equations (Equation 3-5 to Equation 3-10) values of 2:2 concentration were calculated at different γ-CD concentrations by varying the equilibrium constants present in the equations. The equilibrium constants based on the calculations were considered acceptable by visual inspection, i.e. by how well each normalized calculated point corresponded to the normalized experimental value at each γ-CD concentration. Once a data set of the three K_{eq} values gave reasonable correspondance to the experimental data, two of the K_{eq} values were fixed (within their acceptable range), while the third value varied. The variation in this K_{eq} value that maintained a reasonable comparison to all experimental values at each γ-CD concentration was used to estimate the error in the equilibrium constant. The ranges for the equilibrium constants for the pyrene/ γ-CD are found to be $K_{1:1}$ = 300 - 350 M^{-1}, $K_{1:2}$ = 80 – 140 M^{-1}, and $K_{2:2}$ = (1-2) x 10^6 M^{-1}. These ranges of values were obtained from separate experiments involving 5.0 x 10^{-7} M pyrene and 2.5 x 10^{-7} M pyrene (U. Kisiel, personal communication). Figure 3-11 shows the comparison between the normalized calculated values and the normalized (corrected) excimer emission intensities for one experiment, with $K_{1:1}$ = 310 M^{-1}, $K_{1:2}$ = 85 M^{-1}, and $K_{2:2}$ = 1.3 x 10^6 M^{-1}. Further, these equilibrium constant ranges correspond well with the equilibrium constants reported by Hamai[31]($K_{1:1}$ = 300 M^{-1}, $K_{1:2}$ = 170 M^{-1}, and $K_{2:2}$ = 1.3 x 10^6 M^{-1}).

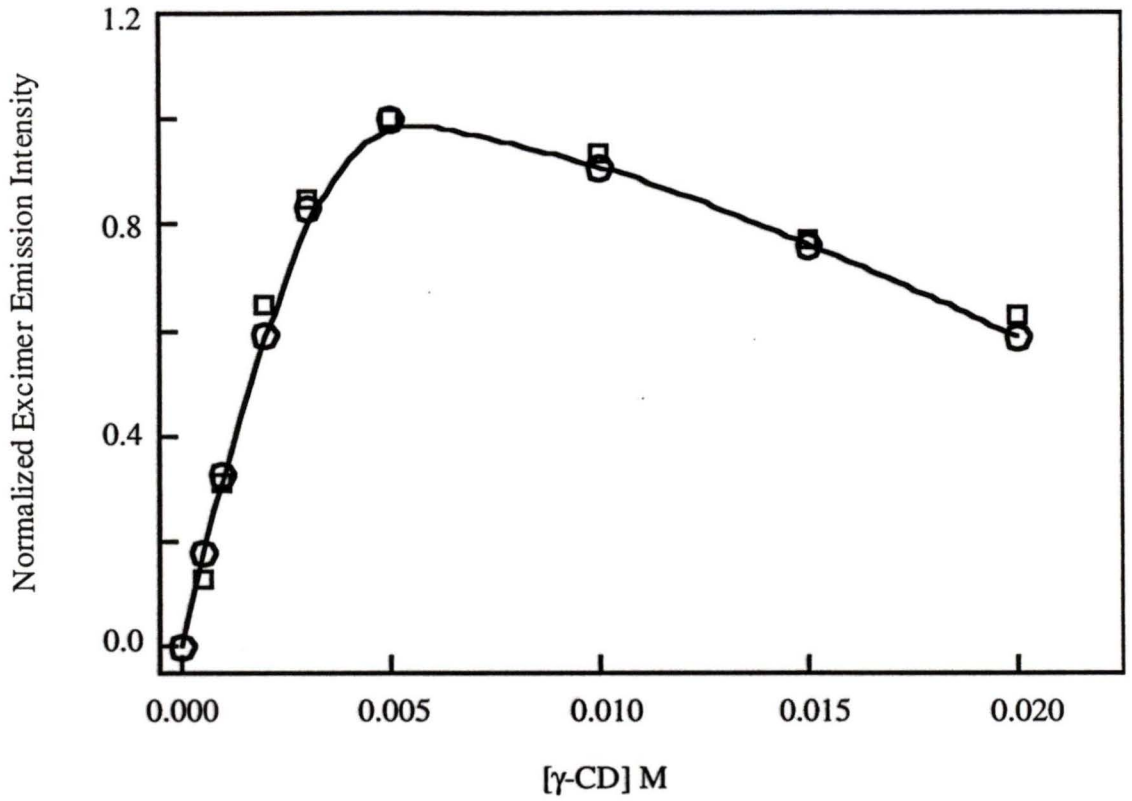

Figure 3-11: Comparison of normalized experimental excimer emission intensity (O) to calculated values (□) based on the formation mechanism (**Scheme 3-1**) and the corresponding equations as described in the text. The equilibrium constants used in the calculation were $K_{1:1} = 310\ M^{-1}$, $K_{1:2} = 85\ M^{-1}$, and $K_{1:1} = 1.3 \times 10^{6}\ M^{-1}$. The line through the experimental data points is not a fit, but rather a smoothed line through the data points to facilitate the comparison of points.

It is interesting to compare the experimental intensity data to other proposed equilibria and equilibrium constants reported in the literature. For example, from Table 1-2, Kobayashi proposed the presence of four complexes, i.e. a 1:1, 1:2, 2:1, and a 2:2 complex, and Kano proposed the formation of three pyrene/ γ-CD complexes, including a 2:1 pyrene: γ-CD complex rather than the 2:2 complex. By modifying Equation 3-5,

Equation 3-6, and Equation 3-10 to incorporate these complexes, it is possible to compare values based on their proposed equilibrium constants of the various species to our normalized experimental data. This is shown in Figure 3-12. Clearly, a poorer fit is obtained when using these published values.

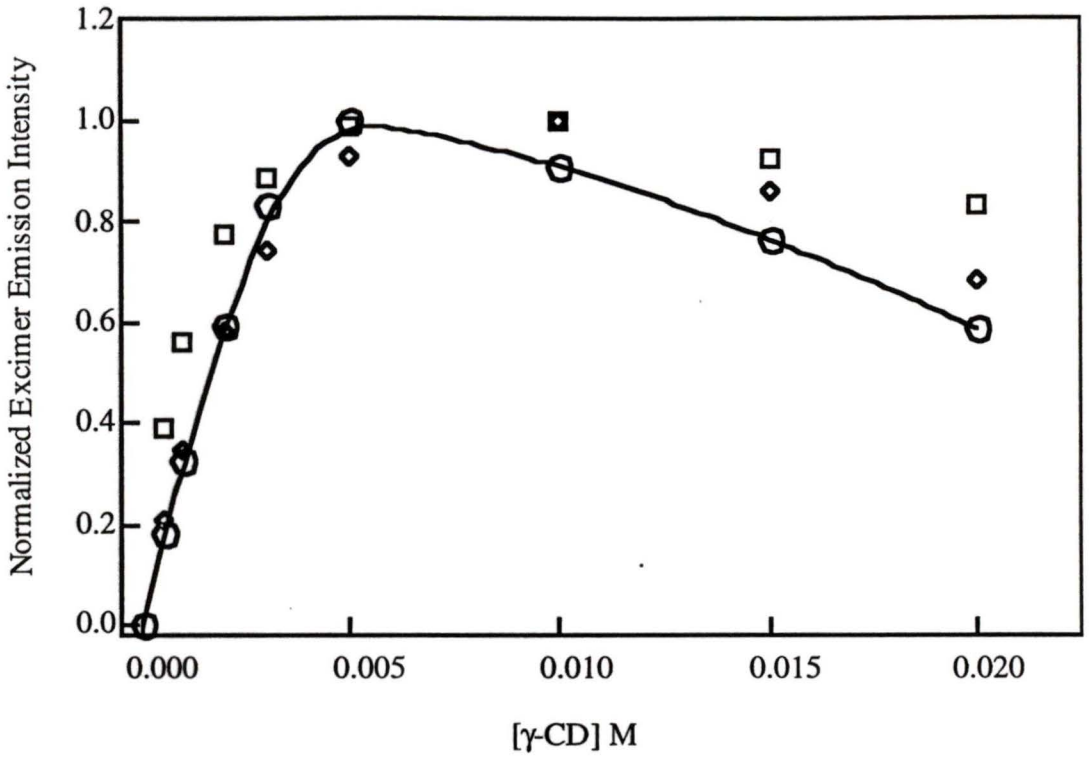

Figure 3-12: Comparison of normalized experimental excimer emission intensity values (O) to calculated values as calculated based on a step-wise formation mechanism similar to **Scheme 3-1** and on the equilibrium constants proposed by Kobayashi[32]: $K_{1:1} = 35\ M^{-1}$, $K_{1:2} = 310\ M^{-1}$, and $K_{2:1} = 1.9 \times 10^{7}\ M^{-1}$, and , $K_{2:2} = 1.1 \times 10^{8}\ M^{-1}$ (□) and Kano[13]: $K_{1:1} = 20\ M^{-1}$, $K_{1:2} = 200\ M^{-1}$, and $K_{2:1} = 5 \times 10^{6}\ M^{-1}$ (◊). The calculated values were normalized at 10×10^{-3} M γ-CD, as this was the value of highest 2:2 concentration, whereas the experimental data was normalized to one at 5.0×10^{-3} M γ-CD. The line through the experimental data is not a fit, but rather a smoothed line through the data points to facilitate the comparison of points.

Based on the equilibrium constants of the pyrene/ γ-CD system, the concentrations of each species at several different γ-CD concentrations can be calculated based on a total pyrene concentration of 5.0×10^{-7} M. These theoretical concentrations

help formulate and verify the dynamic mechanism as presented by the stopped flow data (Chapter 4).

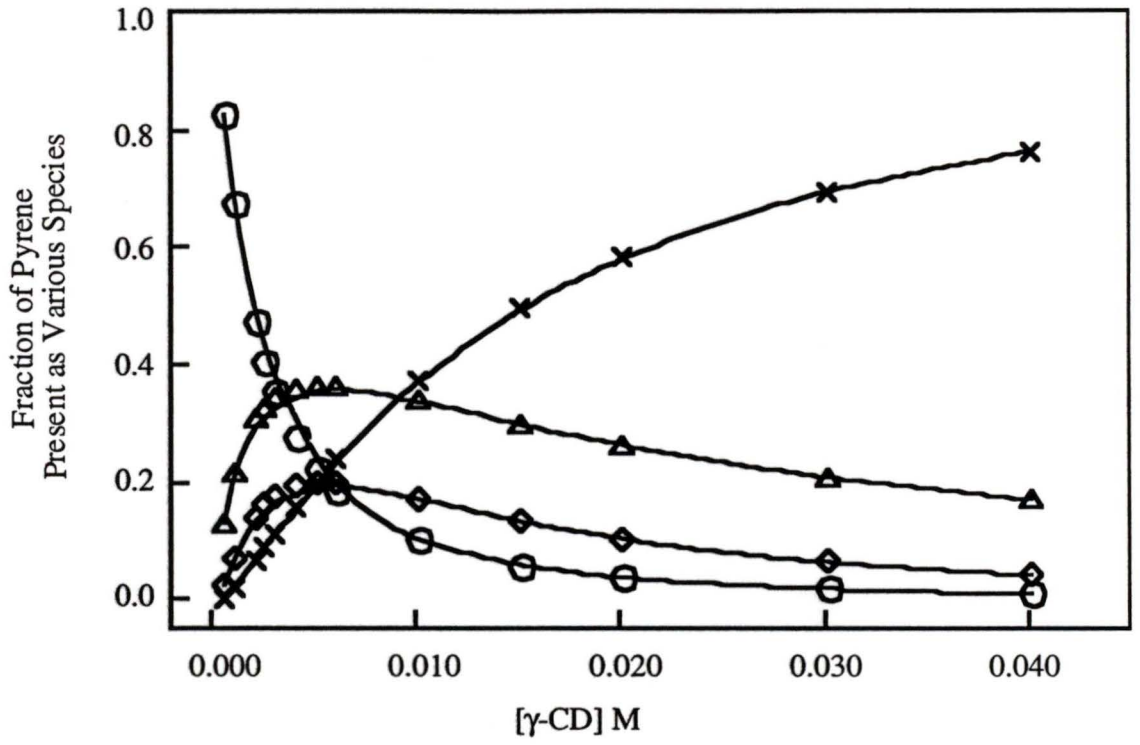

Figure 3-13: The calculated fractions of the pyrene species in a 5 x 10^{-7} M pyrene solution in the presence of various γ-CD concentrations. The calculated values are based on **Scheme 3-1** and **Equation 3-5** to **Equation 3-10** and the equilibrium constants $K_{1:1}$ = 325 M^{-1}, $K_{1:2}$ = 110 M^{-1}, $K_{2:2}$ = 1.5 x 10^{6} M^{-1} and 5.0 x 10^{-7} M pyrene in γ-CD. The pyrene species are free aqueous pyrene (O), and the pyrene: γ-CD complexes of the stoichiometries 1:1 (Δ), 1:2 (X), and 2:2 (◊). The lines through the data points do not show a fit, but are included only to aid in following the trends.

4. Dynamics of the pyrene/ γ-cyclodextrin system

The dynamics of the pyrene/ γ-CD system were measured using a stopped flow apparatus which is capable of monitoring dynamic events that occur on the millisecond time-scale. As such, events that occur faster than ~2 ms cannot be detected by this method (see Chapter 1 and Chapter 2). Processes that occur within this time-frame are therefore not directly involved in the analysis of the data.

4.1 What is chemical relaxation?

As discussed in Chapters 1 and 2, the stopped-flow technique is also known as the concentration jump method, as it involves changes in concentration of the species present in a system. The rapid mixing together of two solutions results in the change in concentration, or a 'perturbation' of the system. The re-equilibration process, or self-adjusting process of the perturbed system back to (a new) equilibrium, is known as chemical relaxation. The relaxation lifetime is the time taken by the system to re-equilibrate to this point, and represents the sum of all dynamic processes that are occuring in the system on that time scale, including a term for both the forward and reverse reactions[56].

The stopped-flow technique is referred to as a 'transient relaxation method', as it measures the rate of change in the concentration of any one or several species directly following the perturbation. Distinct from this method is the 'stationary relaxation method', where the perturbation is brought about by an oscillating force.[56] In the pyrene/ γ-CD system, the species that were monitored were the 2:2 excimer-emitting complex, and the monomer species. From steady-state fluorescence results (Chapter 3, Figure 3-2),

it is evident that the fluorescence emission of pyrene (monomer and excimer) varies as the γ-CD concentration varies. This change in intensity is directly related to the amount of each species present in the system, as indicated by Figure 3-11, from which the equilibrium constants of the system are derived. As such, it is possible to study the dynamics of the system by monitoring the change in fluorescence emission intensity, i.e. the concentrations of the species, using this chemical relaxation technique.

From the thermodynamic characterization results, a scheme of all of the species present and their corresponding equilibrium constants (at 20° C) is presented in Scheme 4-1.

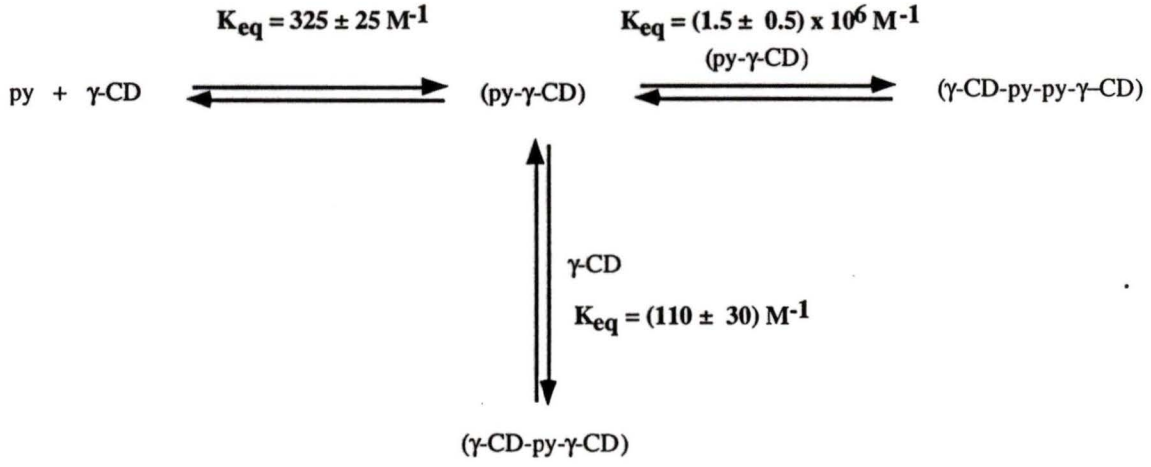

Scheme 4-1: Equilibria present in the pyrene/γ-CD system as described in Chapter 3.

Based on this scheme and the K_{eq} values, the concentrations of the various species may be calculated under various conditions of pyrene and γ-CD concentrations. For example, Figure 3-13 shows the calculated fraction of the various species present at 5.0×10^{-7} M pyrene at several γ-CD concentrations. With this data, it is possible to evaluate the

observed rate constants obtained from the stopped-flow experiments in terms of re-equilibrated (calculated) concentrations. This analysis and correlation allow the dynamic mechanism and some rate constants of the processes involved in Scheme 4-1 to be extracted.

4.1.1 Influence of the size of concentration perturbation: Theoretical and experimental considerations

Relaxation kinetics usually deals with systems where the changes in concentration of the species is small, i.e. the change in concentration is not far from the final equilibrium concentration. This allows for the rate equation to be simplified as it eliminates the presence of a term, resulting in a rate equation that follows first order kinetics [56]. For example, for the system $A + B \rightleftarrows C$, the rate equation is given by Equation 4-1[56], where Δc_n is the change in concentration of species, n, i.e. A or B, k_+ is the rate constant for the forward reaction, k_- is the rate constant for the reverse reaction, and c_A and c_B are the final equlibrium concentrations of reactants A and B.

$$\frac{d\Delta c_n}{dt} = -[k_+(c_A + c_B) + k_-]\Delta c_n - k_+(\Delta c_n)^2$$

Equation 4-1

When $(k_+(c_A + c_B) + k_-)\ \Delta c_n$ is much larger than $k_+(\Delta c_n)^2$, i.e. when the change in concentration, Δc_n, is very small, the final term may be eliminated. The deletion of this term results in linearization of the rate equation. Further, the relaxation time, τ, may replace the first term as shown in Equation 4-2[56]

$$\frac{dx}{dt} = -(\frac{1}{\tau})x$$

Equation 4-2

where $1/\tau$ is defined in Equation 4-3 and x is Δc_n, where n is species A, B, *or* C, as for small perturbations, the linearized equation is independent of the sign of x. That is, it does not matter whether the equilibrium is shifted to the right or to the left; the rate of approach is the same[56].

$$\frac{1}{\tau} = k_+(c_A + c_B) + k_-$$

Equation 4-3

After integration of Equation 4-2, it is possible to see that the relaxation time is the time taken for the concentration of species, n (i.e. A, B, or C), to decrease by a factor of *e* (Equation 4-4).

$$\Delta c_n = \Delta c_n^o \exp(-\frac{t}{\tau})$$

Equation 4-4

The terms in Equation 4-4 are defined such that Δc_n is the change in concentration of species, n, to 1/e of the total concentration change, and Δc_n° is the total change in concentration of species, n.

The above discussion is only relevant to bimolecular or higher order reactions. This is because only these reactions give rise to the higher order terms in the rate equation, i.e. $k_+(\Delta c_n)^2$. Reactions that are first-order or pseudo-first order (in both directions) do not require small perturbations, as the chemical relaxation is a first order process, irrespective of the size of the perturbation[56].

Theoretically, a small change in concentration is required in order to facilitate data analysis. Experimentally, however, a larger perturbation or change in concentration is preferred, as it leads to higher precision [56] and accuracy. That is, the signal-to-noise ratio improves as the signal becomes stronger with a larger perturbation.

4.2 Results

4.2.1 Comparison of stopped-flow and steady-state fluorescence data

In order to determine the dynamics mechanism of the pyrene/ γ-CD system, several mixing scenarios were tested. One scenario (i) involved mixing two solutions such that no pyrene/ γ-CD complex was initially present, i.e. there was a relatively large perturbation of the system. In other mixing scenarios, the complexes were present before the perturbation occurred, i.e. the concentration perturbation was relatively smaller. In order to verify that the stopped-flow results were valid, a comparison of the change in excimer emission intensity was made between steady-state fluorescence spectra and stopped-flow traces for all of the scenarios above. In the first case, an overall increase in excimer emission is observed, as no excimer emitting species is initially present. Stopped-flow traces for this example are shown in Figure 4-1.

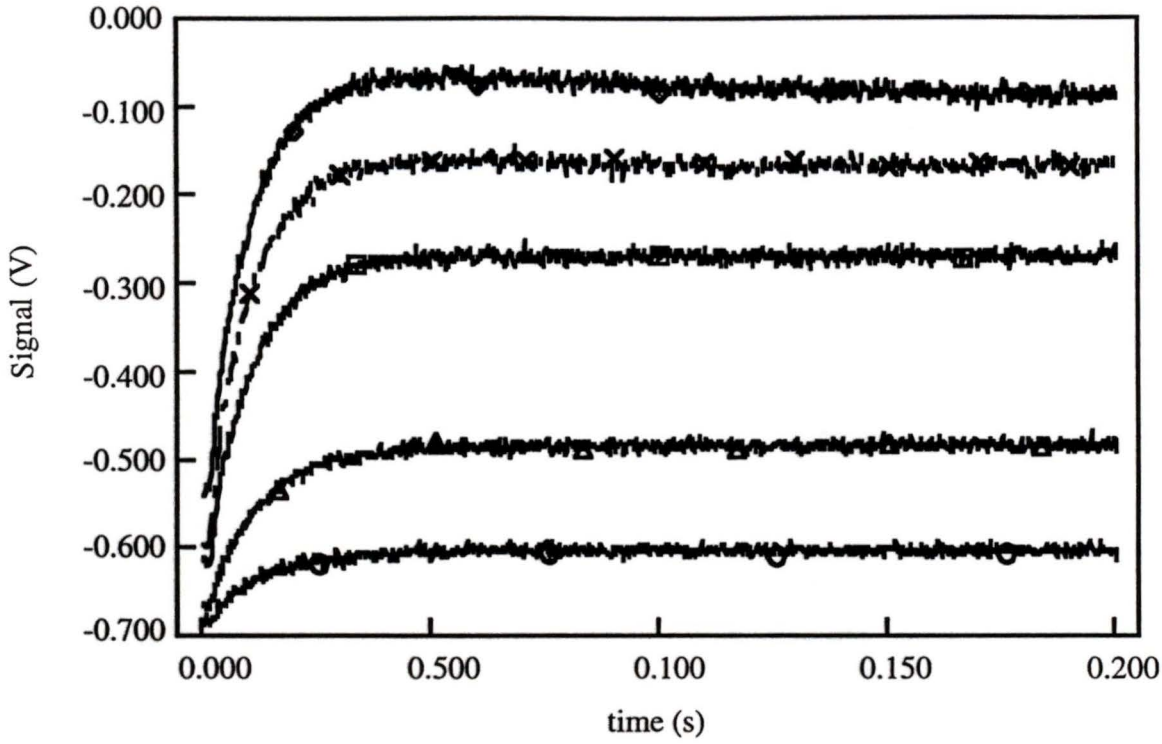

Figure 4-1: Stopped-flow traces monitoring the change in excimer emission intensity upon mixing aqueous pyrene (5 x 10^{-7} M, initial concentration) with aqueous γ-CD of the following initial concentrations: O = 1 x 10^{-3} M; Δ = 2 x 10^{-3} M; □ = 5 x 10^{-3} M; X = 10 x 10^{-3} M; ◊ = 20 x 10^{-3} M. Note that the final concentrations are half of the initial concentrations. The PMT setting for these traces was 400.0 V and the off-set was 1.10 V.

The second mixing scenario (ii) initially contained all of the pyrene/ γ-CD complexes, i.e. in a previously prepared pyrene/ γ-CD solution. Upon mixing this solution with water, there was an overall decrease in excimer emission intensity in the stopped flow system. This corresponds to steady-state fluorescence results, where the excimer-to-monomer ratio decreases from 0.2 upon diluting the system in 5.0 x 10^{-7} M pyrene in 2.0 x 10^{-3} M γ-CD to 0.07 at the final concentration of the re-equilibrated system of 2.5 x 10^{-7} M pyrene in 1.0 x 10^{-3} M γ-CD. Stopped-flow traces under these conditions are shown in Figure 4-2.

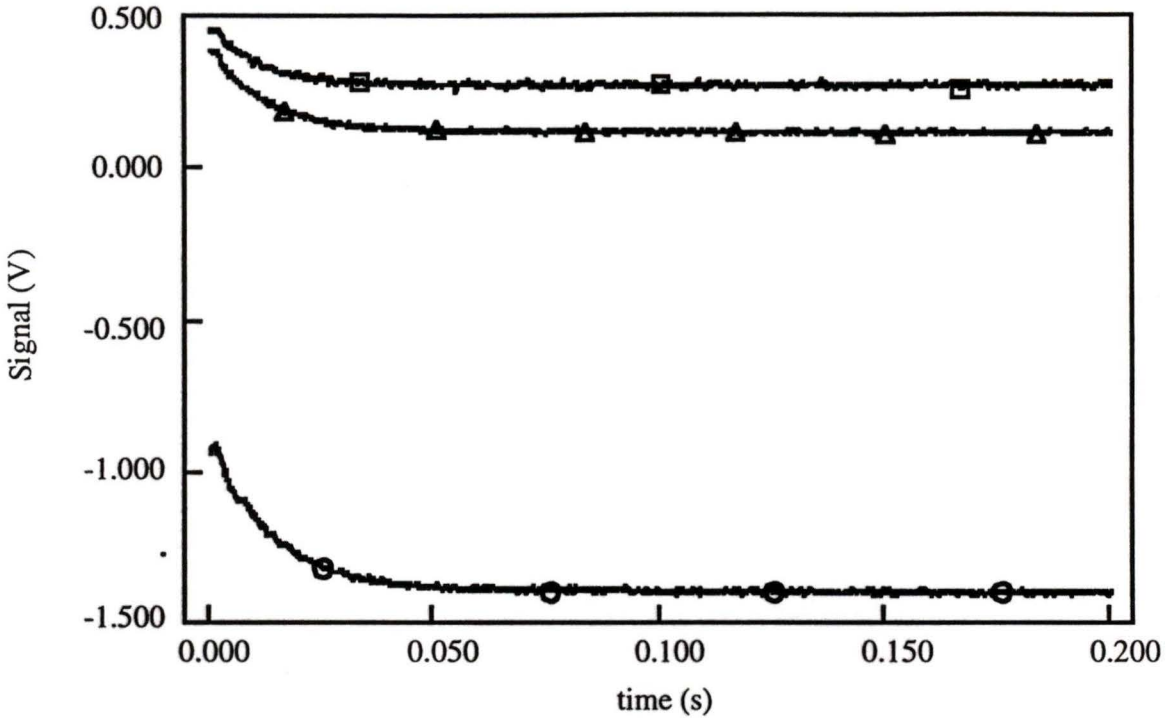

Figure 4-2: Stopped-flow traces monitoring the change in excimer emission intensity upon mixing pyrene (5×10^{-7} M) in γ-CD (O = 1×10^{-3} M; Δ = 2×10^{-3} M; □ = 5×10^{-3} M) with water. Traces Δ and □ were performed on the same day, with a PMT setting of 400.0 V and an off-set of 1.00 V; the trace O was taken on a different day with a PMT setting of 440.0 V and an off-set of 3.00 V.

A third stopped-flow mixing condition (iii) involved the addition of 5.0×10^{-7} M pyrene to a solution that already contained the pyrene/ γ-CD complexes, i.e. a previously prepared pyrene/ γ-CD solution. The result (at initial concentrations larger than 1×10^{-3} M γ-CD) was an overall increase in excimer emission intensity in the stopped-flow traces (Figure 4-3).

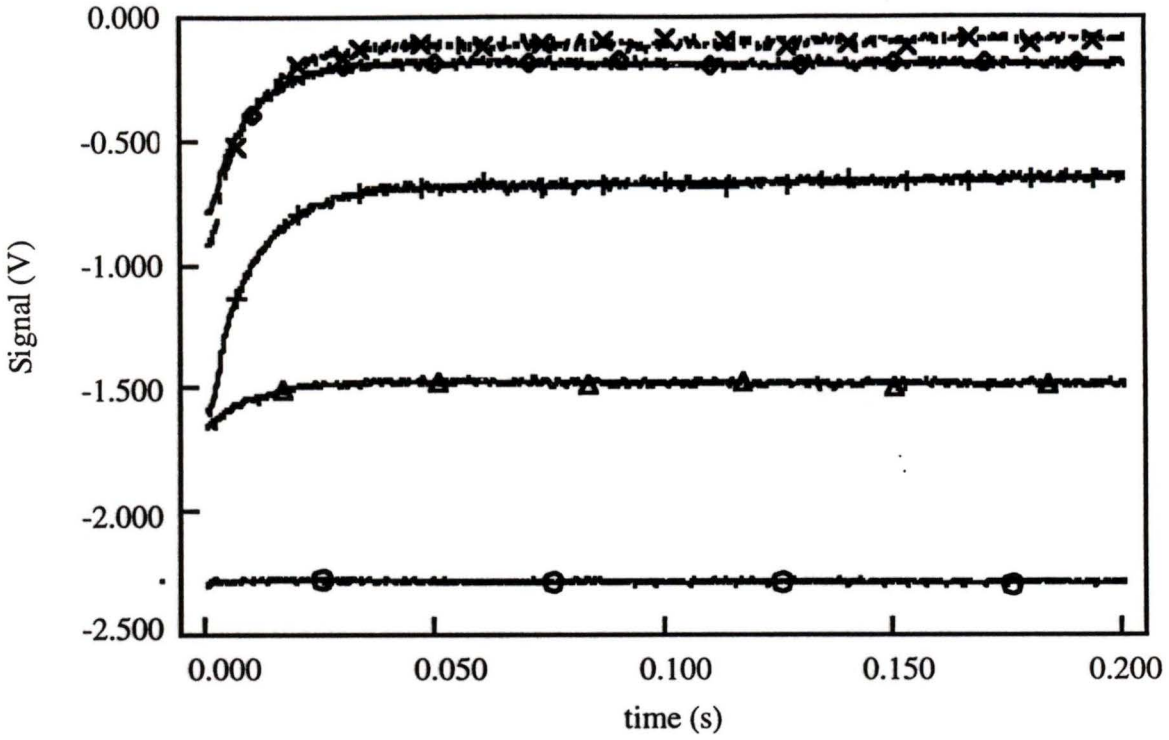

Figure 4-3: Stopped-flow traces monitoring the change in excimer emission intensity upon mixing pyrene (5×10^{-7} M) in γ-CD (O = 1×10^{-3} M; Δ = 2×10^{-3} M; ◊ = 5×10^{-3} M; + = 10×10^{-3} M; X = 20×10^{-3} M) with pyrene (5×10^{-7} M). The PMT setting for these traces was 420.0 V and the off-set was 3.90 V.

These stopped-flow traces agree with steady-state fluorescence data. That is, after dividing the excimer fluorescence emission intensity of a solution of 5.0×10^{-7} M pyrene in 10×10^{-3} M γ-CD in half (i.e. to account for initial dilution of the system immediately after mixing, at time $t \leq 2$ ms), there is an increase in emission intensity to reach the final equilibrium concentration of excimer emitting species, i.e. 5.0×10^{-7} M pyrene in the presence of 5.0×10^{-3} M γ-CD. Further, there is a larger increase in excimer emission intensity at 10×10^{-3} M γ-CD (initial) than when pyrene is in the presence of 2.0×10^{-3} M

γ-CD (initial) (Figure 4-4). This relative difference in emission intensity is also seen in the amplitude of the stopped-flow traces (Figure 4-3).

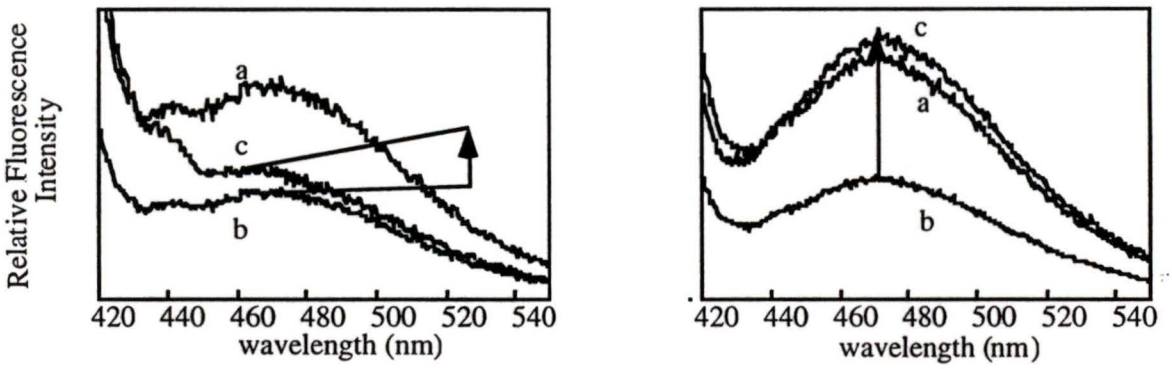

Figure 4-4: Steady-state fluorescence spectra used to compare the change (i.e. relative increase) in excimer emission intensity to the direction of change of the excimer emission intensity in the stopped-flow traces of corresponding final concentrations (after mixing). Left spectrum: pyrene (5.0×10^{-7} M) in γ-CD (a = 2.0×10^{-3} M; b = (intensity of spectrum, a)/2 to account for initial dilution in the stopped-flow system; c = 1.0×10^{-3} M). Right spectrum: pyrene (5.0×10^{-7} M) in γ-CD (a = 10×10^{-3} M; b = (intensity of spectrum, a)/2 to account for initial dilution in the stopped-flow system; c = 5.0×10^{-3} M).

The above data describes excimer emission only. However, stopped flow traces were also collected using an interference filter such that the change in monomer fluorescence emission intensity could be monitored (Figure 4-5). In nearly all cases tested, the shape of the monomer emission traces mirrored that of the excimer emission, reinforcing the validity of the mixing process as well as the kinetic process.

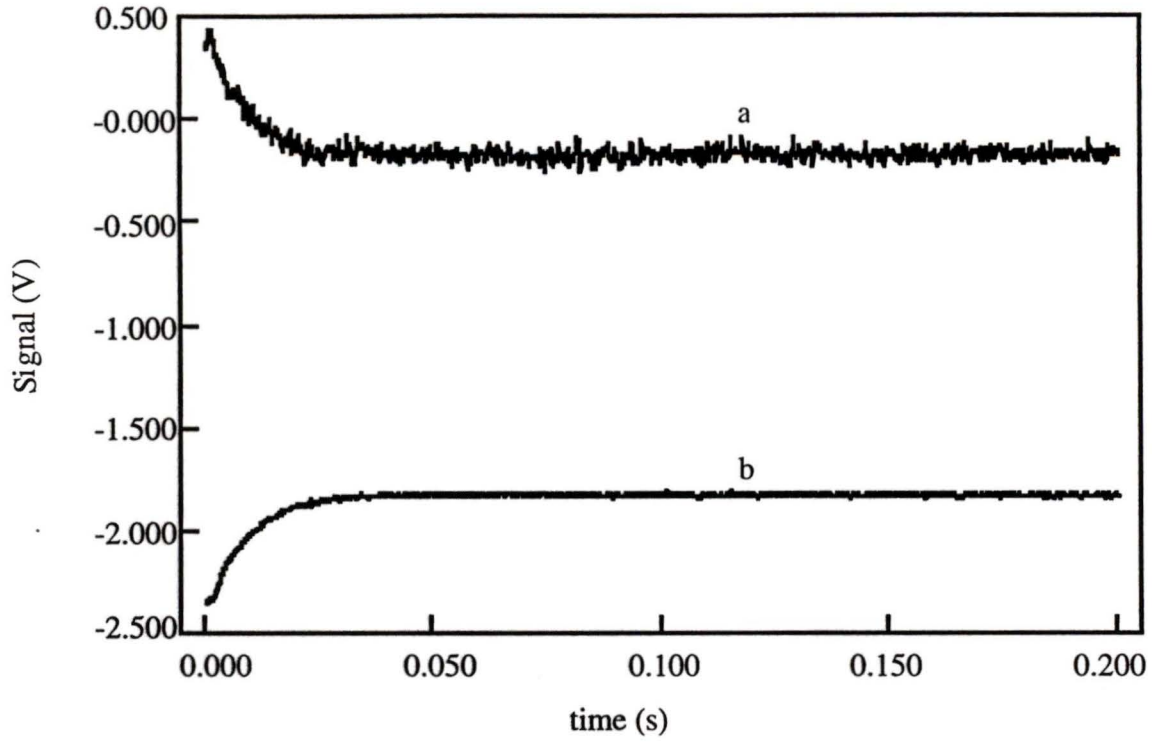

Figure 4-5: Stopped-flow traces monitoring the change in monomer (a) and excimer (b) emission intensity upon mixing 5 x 10^{-7} M pyrene (aq) with 10 x 10^{-3} M γ-CD. The traces were collected on different days; the PMT setting of (a) was 525.0 V with an off-set of 3.00 V, while the settings of trace (b) were 450.0 V and 3.00 V, respectively.

Stopped-flow kinetics results at low γ-cyclodextrin concentrations

At low γ-CD concentrations, i.e. an initial concentration below 10 x 10^{-3} M γ-CD, in the stopped-flow mixing scenarios (i) and (ii) described above, the stopped flow traces were fit to a single exponential equation (Equation 2-1). At higher host concentrations, some of the traces were fit to the sum of two exponentials (Equation 2-2, see below). The observed rate constants obtained on the 200 ms time scale were seen to depend on the (final) pyrene-γ-CD 1:1 complex concentration (**Figure 4-6**).

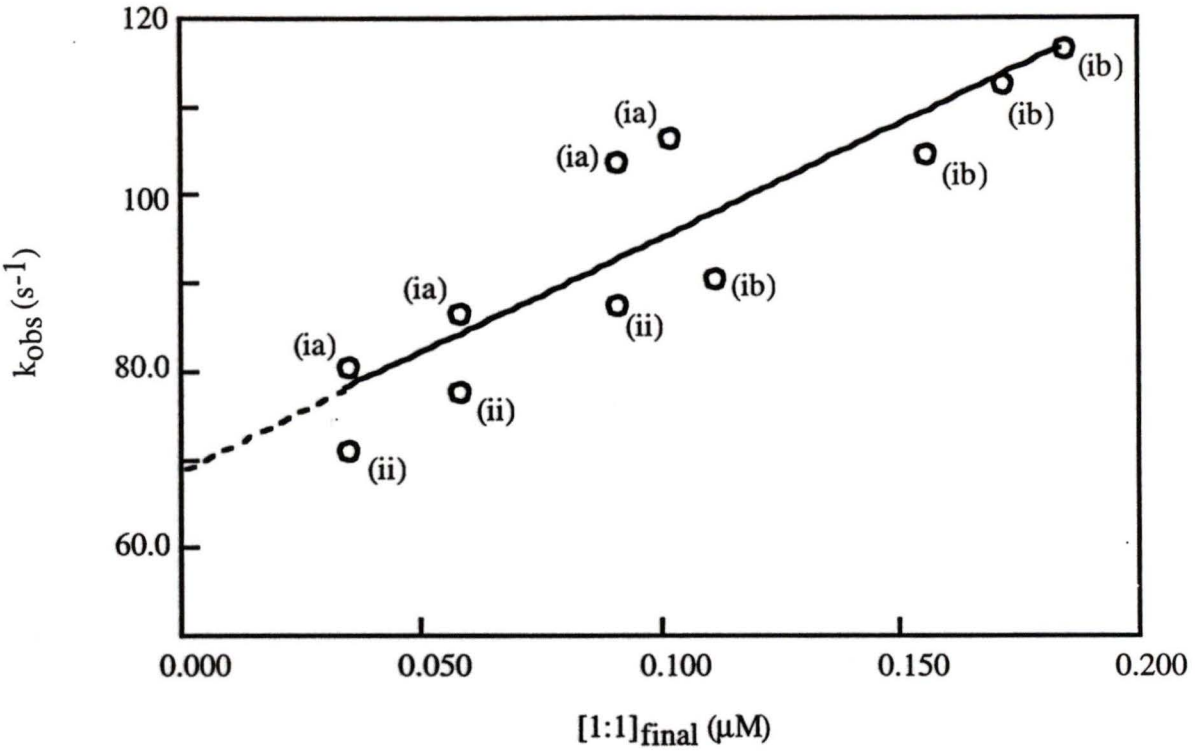

Figure 4-6: The observed rate constants (k_{obs}) of several mixing scenarios depend on the final 1:1 pyrene: γ-CD concentration, as calculated based on steady-state equilibrium constants ($K_{1:1}$ = 325 M^{-1}, $K_{1:2}$ = 110 M^{-1}, $K_{2:2}$ = 1.5 x 10^6 M^{-1}). The various mixing scenarios include: (ia) 5 x 10^{-7} M pyrene (aq) with γ-CD (aq); (ib) 1 x 10^{-6} M pyrene (aq) with γ-CD (aq); (ii) 5 x 10^{-7} M pyrene in γ-CD with water. The solid line corresponds to the fit of the data to Equation 4-5.

The initial concentrations of γ-CD used in this plot range from 1 x 10^{-3} M to 20 x 10^{-3} M. The stopped-flow trace for which pyrene was mixed with 20 x 10^{-3} M γ-CD was fit to the sum of two exponentials (on the 200 ms time-based scan). The second observed rate constant was determined independently on a longer time-scale, and was a fixed parameter

in the short time-scale fit. This latter (faster) observed rate constant fit in well with the 1:1 final concentration dependence (as the second highest point in **Figure 4-6**).

The dependence shown in **Figure 4-6** is indicative of a dimerization reaction, i.e. two 1:1 complexes coming together to form the 2:2 excimer emitting species. The relaxation time for this dimerization process to occur is given in Equation 4-5[56]. The derivation of this equation is similar to that shown in section 4.1.1 for the reaction $A + B \rightleftarrows C$, where A = B.

$$k_{obs} = 4k_{+}[(py-\gamma-CD)] + k_{-}$$

Equation 4-5

In this equation, k_+ and k_- are the association and dissociation rate constants of dimerization, respectively, and [(py-γ-CD)] is the final equilibrium concentration of the 1:1 complex. Thus, in order for this equation to be used, the final equilibrium concentration of the reagent, i.e. the 1:1 pyrene: γ-CD complex, must be directly measureable or known from equilibrium constants[56]. In this case, the concentrations were calculated based on the equilibrium constants from steady-state results as described in Chapter 3. The factor of 4 is necessary to account for the stoichiometry of the dimerization process, i.e. 2(1:1)→ (2:2).

As discussed in section 4.1.1, Equation 4-5 can be used for stopped flow results when the change in equilibrium concentrations is small, i.e. so linearization of the rate equation is possible. This is the case for scenario (ii) above. However, the observed rate constants obtained using mixing scenario (i) (for initial pyrene concentrations of 0.5 x 10

^{6} M and 1 x 10^{-6} M) were plotted on the same graph as the data mixing scenario (ii) (**Figure 4-6**). As all the data points fall fairly close together on the same line, it is reasonable to assume the use of Equation 4-5 for the mixing scenario (i) is valid as a first approximation. The reasonable fit of the combined data also indicate that the model used to describe the kinetics of the system, i.e. dimerization, is correct to a first approximation, as will be discussed.

From Equation 4-5, it is evident that the slope of the curve is equal to $4k_+$ and the y-intercept is equal to k_-. The slope, k_+, and k_- obtained from **Figure 4-6** are given in Table 4-1.

Table 4-1: The association and dissociation rate constants, and equilibrium constants (a) of the dimerization process of pyrene (5 x 10^{-7} M and 1 x 10^{-6} M) based on stopped-flow results. (b) The equilibrium constant for the dimerization process from steady-state analysis.

slope ($\mu M^{-1} s^{-1}$) = **4** k_+	k_+ ($M^{-1}s^{-1}$)	k_- (s^{-1})	K_{eq} (M^{-1})[a]	K_{eq} (M^{-1})[b]
260 ± 40	(7 ± 1) x 10^7	69 ± 5	(1.0 ± 0.2) x 10^6	(1.5 ± 0.5) x 10^6

Calculation of the equilibrium constant, K_{eq}, of the dimerization process is possible using the kinetic data, as indicated by Equation 4-6.

$$K_{eq} = \frac{k_+}{k_-}$$

Equation 4-6

The value of the equilibrium constant using stopped-flow kinetic data is given in Table 4-1, and is compared to the value found using steady-state analysis. Correlation between these values verify that the kinetic model used for the analysis is correct.

4.2.2 Kinetics at high γ-cyclodextrin concentrations

At high γ-CD concentrations, i.e. greater than or equal to 10×10^{-3} M, the kinetics of the pyrene: γ-CD system becomes more complex. For example, in the mixing scenario (i) above, where no pyrene/γ-CD complex is present intially, the influence of a second process is evident at time scales greater than 200 ms. Figure 4-7 shows traces of mixing scenario (i), where the initial concentration of γ-CD varied from 10×10^{-3} M to 40×10^{-3} M.

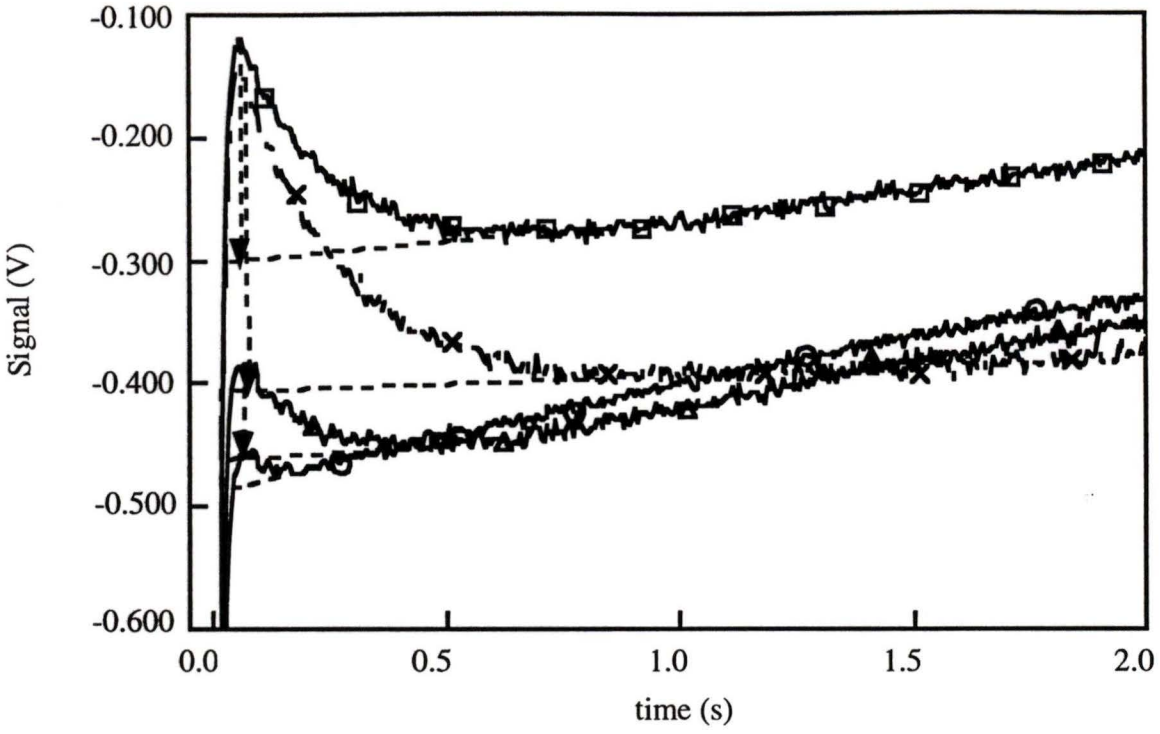

Figure 4-7: Stopped-flow traces monitoring pyrene excimer emission upon mixing aqueous pyrene (5 x 10^{-7} M) with γ-CD of initial concentrations (before mixing): O = 10 x 10^{-3} M; Δ = 20 x 10^{-3} M; □ = 30 x 10^{-3} M; X = 40 x 10^{-3} M. See text below for significance of dashed lines and arrows.

As the γ-CD concentration increases, the relative decrease in amplitude of the emission signal from t ~ 100 ms to around 1000 ms increases. This relative amplitude was measured after extrapolating back from the plateau of the decrease in signal to the initial fast rise in emission intensity, i.e. the dashed lines in Figure 4-7. The difference in emission intensity signal between the top of the fast initial rise to this extrapolated line was taken as the relative amplitude of this slow process, i.e. the arrows in Figure 4-7. This decrease in emission intensity is labelled as the slow process, as it appears after a longer time-base than the initial (fast) process that gives rise to the initial increase in signal as in Figure 4-1. The decrease in emission intensity corresponds to a decrease in

concentration of the excimer emitting species, which is equivalent to an increase in the concentration of the pyrene monomer species. When this change in amplitude is plotted against the final 1:2 (pyrene: γ-CD) concentration (as calculated from steady-state data), there appears to be a qualitative correlation (Figure 4-8).

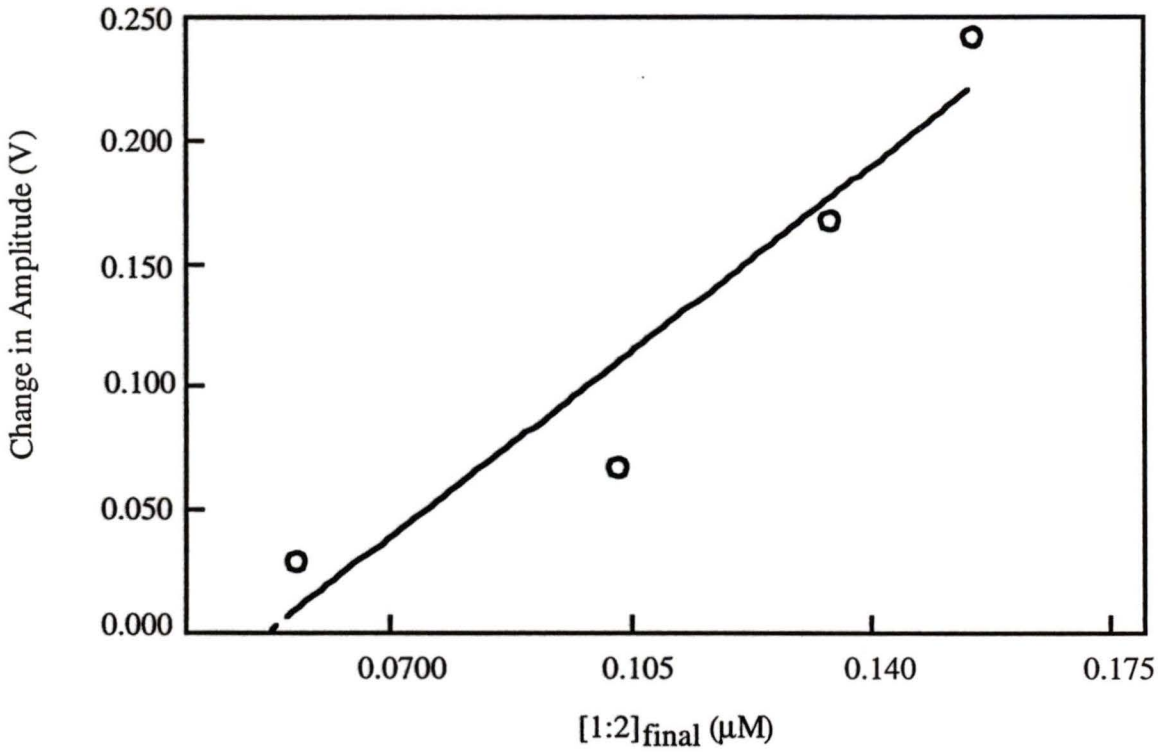

Figure 4-8: The change in amplitude that occurs in the stopped-flow traces monitoring excimer emission intensity upon mixing 5 x 10^{-7} M pyrene with γ-CD (10 x 10^{-3} M to 40 x 10^{-3} M before mixing) between ~ 0.100 s and < 1.0 s (**Figure 4-7**) depends on the final concentration of the 1:2 pyrene: γ-CD complex.

It is interesting to note that the x-intercept of the line is at 5.1 x 10^{-8} M (of the 1:2 complex). This corresponds to a γ-CD concentration of around 5 x 10^{-3} M (based on calculated concentrations of 2.5 x 10^{-7} M pyrene in γ-CD solutions), before which very

little of the doubly encapsulated monomer is present. As such, the increased complexity of the stopped flow traces occuring on longer time scales appears to involve the 1:2 pyrene: γ-CD monomer species.

4.2.3 Kinetics on long-time scales at high γ-cyclodextrin concentrations

4.2.3.1 Stopped-flow results

The stopped-flow apparatus can measure kinetic events happening over a time-scale of up to 1000 s. From Figure 4-9, it is evident kinetic events are continuously occuring beyond 500 s in the pyrene/ γ-CD system.

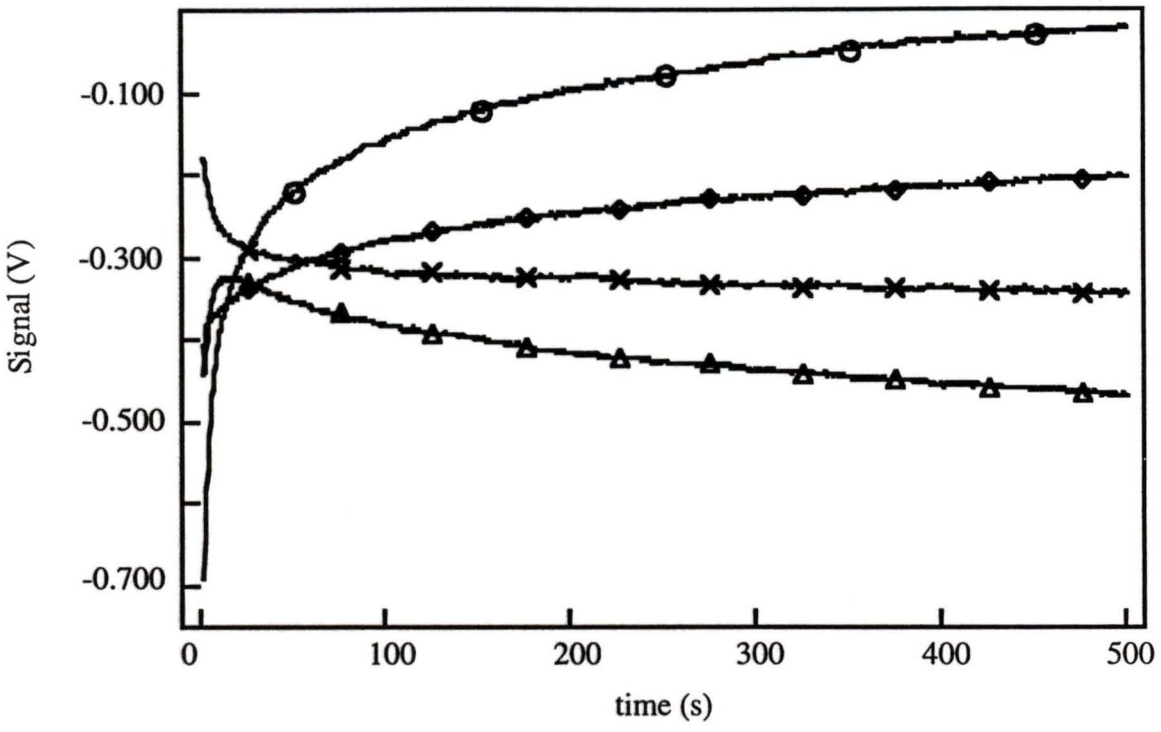

Figure 4-9: Stopped-flow traces monitoring pyrene excimer and monomer emission upon mixing aqueous pyrene (5×10^{-7} M) with γ-CD of initial concentrations of 10×10^{-3} M (O = excimer emission; X = monomer emission) and 30×10^{-3} M (Δ = excimer emission; ◊ = monomer emission).

Both the monomer and the excimer emission was monitored in these traces. On the long time scale, the trend in monomer and excimer emission intensity is complementary, i.e. inversely related, for solutions of the same γ-CD concentration. However, the direction of emission is opposite between the two host concentrations. That is, the excimer emission increases as pyrene is mixed with 10×10^{-3} M γ-CD (initial concentration), whereas it decreases from ~20 s to 500 s when pyrene is mixed with 30×10^{-3} M γ-CD. Similarly, the monomer emission shows a continous decrease when pyrene is mixed with 10×10^{-3} M γ-CD (initial concentration), and it increases when the probe is

mixed with 30 x 10^{-3} M γ-CD (initial concentration). These results are further evidence that the dynamics of the 1:2 pyrene: γ-CD monomer-emitting complex occur on a slower time-scale than that of the dimerization process. That is, the stopped-flow traces represent the sum of all kinetic processes that are occuring in the system. As such, the continuous increase in monomer emission intensity over 500 s at 15 x 10^{-3} M γ-CD, i.e. a high final equilibrium concentration, indicates a dominant monomer influence, whereas this trend is not evident at 5 x 10^{-3} M γ-CD, i.e. a lower final equilibrium concentration, over the long time-base where less of the species is present. This argument is reinforced by comparing the calculated fractions of pyrene present as the various pyrene: γ-CD complexes based on 2.5 x 10^{-7} M pyrene and equilibrium constants as described in Chapter 3. The values given in Table 4-2 relate to the concentrations of the aforementioned example. That is, at the higher final host concentration (15 x 10^{-3} M γ-CD), there is a much larger fraction of 1:2 monomer species relative to the fraction of this species present at 5 x 10^{-3} M γ-CD. Conversely, there is a larger increase in the fraction of excimer emitting 2:2 complex at the low host concentration relative to the higher γ-CD concentration. The fractions of these two pyrene: γ-CD complexes correlate well with the observed changes in excimer and monomer emission intensity.

Table 4-2: Fraction of pyrene present in the multiple stoichiometric pyrene: γ-CD complexes.

$[\gamma\text{-CD}]_{final}$ M	fraction of pyrene as py_{free}	fraction of pyrene as 1:1	fraction of pyrene as 1:2	fraction of pyrene as 2:2
5×10^{-3}	0.25	0.40	0.22	0.12
15×10^{-3}	0.07	0.32	0.53	0.08

a) The fractions are calculated based on 0.25×10^{-6} M pyrene and the equilibrium constants as described in Chapter 3.

4.2.3.2 Time-based steady-state fluorescence results

The time-scale of kinetic events in the pyrene/ γ-CD system appears to occur over the minute time scale. As such, it should be possible to monitor events occuring in real time using time-based steady-state fluorescence. Experiments were performed by manually mixing pyrene (5×10^{-7} M) and γ-CD (10×10^{-3} M and 30×10^{-3} M) in a 1:1 ratio, and monitoring the emission under similar conditions as the stopped flow system (e.g. emission range, excitation wavelength, and temperature) in order to simulate the stopped-flow experiments. The control experiments involved mixing two solutions together of the same final concentration, such as two aliquots of 2.5×10^{-7} M pyrene in 5×10^{-3} M γ-CD in a 1:1 ratio, and monitoring the time-based scan under the same conditions as those for the manual mixing stopped-flow simulation experiment described above. The time-based scans were started within 30 s after mixing the solutions, and

were monitored for 60 min. As shown in Figure 4-10, the overall trends correspond with the stopped-flow results.

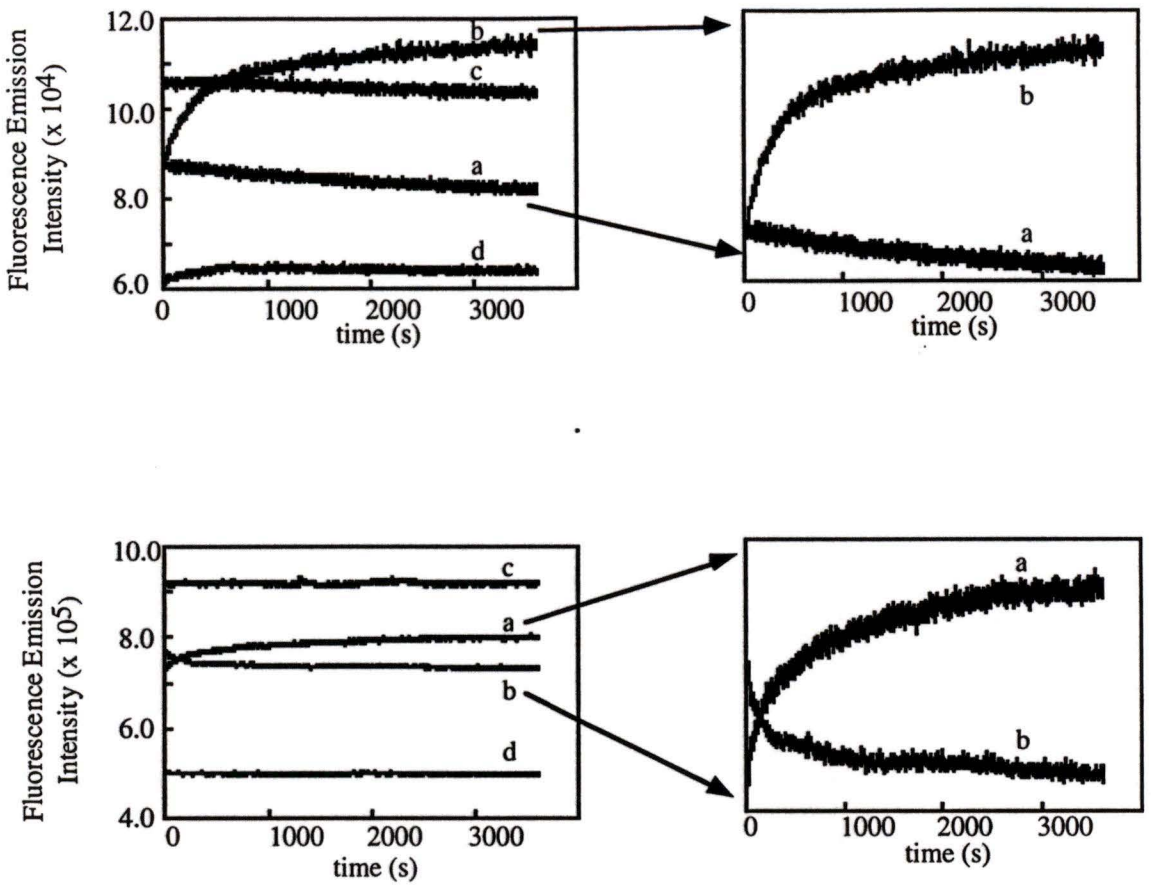

Figure 4-10: Time-based fluorescence traces of solutions that were manually mixed in a 1:1 ratio to simulate the stopped-flow experiments on long-time scales. The top traces monitor excimer emission; the bottom traces monitor monomer emission. The mixing scenarios include: a = 5 x 10^{-7} M pyrene (aq) + (30 x 10^{-3} M) γ-CD (aq); b = 5 x 10^{-7} M pyrene (aq) + (10 x 10^{-3} M) γ-CD (aq). The control experiments include mixing two solutions of the final equilibrium concentrations together: c = 2.5 x 10^{-7} M pyrene (aq) + (15 x 10^{-3} M) γ-CD (aq); d = 2.5 x 10^{-7} M pyrene (aq) + (5 x 10^{-3} M) γ-CD (aq). The traces on the right emphasize the relative change in monomer or excimer emission intensity with time.

That is, when pyrene (5×10^{-7} M) is mixed with 10×10^{-3} M γ-CD (initial), the monomer emission decreases whereas the excimer emission continuously increases. In the same conditions, the monomer emission of pyrene (5×10^{-7} M) mixed with 30×10^{-3} M γ-CD (initial) shows a continous increase in emission intensity whereas the excimer emission decreases over the time range. Ideally, the relative fluorescence intensity of the control experiments should correspond to the final emission intensity of the stopped-flow simulated mixing experiments, as the final concentrations of the two solutions are the same. Although this was not observed experimentally, the relative change in emission intensity was not as great for the control experiments as it was for the stopped-flow simulated traces. As such, the change in emission intensity seen in the time-based scans run on the fluorimeter were taken as significant, and not due to experimental artifacts such as temperature effects. The discrepency seen in final emission intensity values between the control solutions and the experimental solutions may be due to kinetics occuring on longer time-scales than one hour (as the control solutions had equilibrated over night). Secondly, a small change in concentration of the control solutions would have a large influence on where the emission intensity lies relative to the time-based curve, as the change in emission intensity that is being monitored is quite small, i.e. less than a 10 % change in total intensity.

4.3 Discussion

4.3.1 The use of a linearized rate equation in the pyrene/ γ-cyclodextrin system

As disucussed in section 4.1.1, chemical relaxation analysis is facilitated by linearization of the rate equation. Such a process is equivalent to analysis of first order

kinetic events that follow monoexponential behaviour. However, linearization is valid for changes in the system that are very small, i.e. the system remains fairly close to equilibrium. This is not the case in the experimental mixing scenario (i), however, where there are initially no pyrene/ γ-CD complexes present. Although this is so, several points indicate the linearized equation is appropriate for the analysis. (1) The rate equation for the dimerization process is given in Equation 4-7. This equation and the defined terms are similar to Equation 4-1 for the bimolecular process involving two different reagents.

$$\frac{d\Delta c_A}{dt} = -(4k_+c_A + k_-)(\Delta c_A) - 2k_+(\Delta c_A)^2$$

Equation 4-7

Linearization of the rate equation is valid when $|(4k_+c_A+k_-)(\Delta c_A)| >> |2(k_+(\Delta c_A)^2|$. In the pyrene/ γ-CD system, k_+ of the dimerization process is $(7 \pm 1) \times 10^7\ M^{-1}s^{-1}$, the final equilibrium concentration of the 1:1 complex is around 1×10^{-7} M, and k_- is $70\ s^{-1}$. The change in 1:1 concentration is equal to the final equilibrium concentration in mixing scenario (i), as no complex is formed initially. Substituting these values into Equation 4-7, we find that $(1 \times 10^{-5}\ Ms^{-1}) > (1 \times 10^{-6}\ Ms^{-1})$. Although the first term is not much larger than the square term, linearization of the rate equation is valid as a first approximation. (2) Integration of the linearized rate equation, as shown by Equation 4-2, Equation 4-3, and Equation 4-4, shows the decay follows an exponential function, a common equation for first-order kinetic processes. The stopped-flow data are fit to a single exponential function at low γ-CD concentrations. If the perturbed system did not correspond to the linearized rate equation, the data would not be fit as a first-order

function as it would have second-order dependence. (3) The observed rate constants from mixing scenario (i), i.e. from the relatively large perturbation, are similar to those from mixing scenario (ii), where the perturbation is small, i.e. within accepted values[56] (see **Figure 4-6**). Further, analysis of this data leads to a calculated equilibrium constant of $(1.0 \pm 0.2) \times 10^6\ M^{-1}$, which agrees within experimental error with the value determine from steady-state measurements $(1.5 \pm 0.5) \times 10^6\ M^{-1}$. These agreements are good indication that the (linearized) relaxation kinetics equation and analysis model are valid.

4.3.2 Kinetic and thermodynamic model of the pyrene/ γ-cyclodextrin system

The thermodynamic equilibrium constants of the pyrene/ γ-CD system that were determined in Chapter 3 are shown in Scheme 4-1. Kinetic parameters may be added to this and compared to the thermodynamic data, as shown in Scheme 4-2.

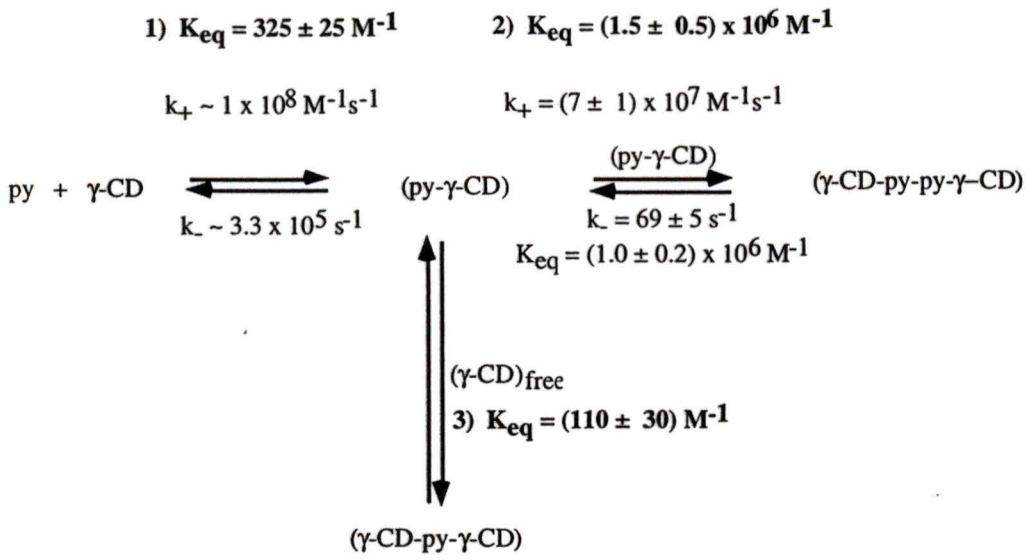

Scheme 4-2: Thermodynamic and kinetic parameters of the pyrene/ γ-CD system based on stopped-flow kinetic data (normal font), and compared to thermodynamic equilibrium constants (bold font, Chapter 3).

The formation of the 1:1 complex (step (1) in Scheme 4-2) is assumed to occur faster than the time-resolution of the stopped-flow system. There are several pieces of evidence that indicate that this assumption is correct: i) No excimer emitting species is involved in this first step. However, as the change in excimer emission intensity in the stopped-flow experiments corresponds to the direction and relative degree of change in excimer emission intensity in steady-state measurements, the dominant process being monitored (within 500 ms) are those involving excimer emission, i.e. dimerization kinetics (see below). It should be noted that although kinetics occur on much longer time-scales than 500 ms in the pyrene/ γ-CD system, the comparison between the direction of the change in emission intensity between stopped-flow traces and steady-state spectra are consistent in the analysis range studied. As a result, only the direction rather than the magnitude of amplitude change may be compared between steady-state

spectra and stopped-flow traces. ii) Values of formation rate constants of 1:1 probe: CD inclusion complexes involving large organic molecules in aqueous systems have been reported as being in the range of 10^7 $M^{-1}s^{-1}$ to 10^8 $M^{-1}s^{-1}$ [19,33,35,36], and have even been considered to be "diffusion controlled" [34]. Under such an assumption, the dissociation rate constant, k_-, can be calculated by substituting the equilibrium constant of 1:1 formation (Chapter 3) and the assumed association rate constant, k_+, into Equation 4-6. The resulting values are $k_+ = 1 \times 10^8$ $M^{-1}s^{-1}$ and $k_- = 3.3 \times 10^5$ s^{-1}. Substituting these values into Equation 4-3, and noting that step (1) is under pseudo-first order conditions, i.e. [CD] ~ 10^{-3} M >> [py], the observed rate constant is ~ 4×10^5 s^{-1}. As the stopped-flow monitors processes occuring in the ms time-range, the fast association process occuring in the μs time-scale is not measureable.

Step (2) in Scheme 4-2 is the dimerization process. The analysis of this step may be considered semi-quantitative, as it partially represents the full complexities of the system. For example, kinetic events occur on a much longer time scale than that from which the kinetic rate constants were determined. Also, the analysis was done based on the steady-state data from which the final 1:1 pyrene: γ-CD monomer concentrations were calculated. Although this is the case, the analysis was done only at low CD concentrations where the slow component, i.e. the presence of the 1:2 monomer, is not very significant. The ratio of the association ($(7 \pm 1) \times 10^7$ M^{-1} s^{-1}) and dissociation rate constants (69 ± 5 s^{-1}) obtained using the dimerization analysis method ($(1.0 \pm 0.2) \times 10^6$ M^{-1}) agree within experimental error with the equilibrium constant obtained from steady-state analysis ($(1.5 \pm 0.5) \times 10^6$ M^{-1}). Although the association rate constant of the dimerization process is of the same order of magnitude as the association rate constant

assumed for the 1:1 complex (step (1)), the stopped-flow apparatus can be used to measure the kinetics of the dimerization process. This is because the observed rate constant depends on the (low) concentration of the 1:1 inclusion complex, i.e. ~ 1 x 10^{-7} M. That is, by substituting the dimerization rate constants and the 1:1 concentration into Equation 4-5, the observed rate constant is ~ 100 s^{-1}. As the summed association and dissociation processes occurs in approximately 10 ms, the dynamics are indeed measureable on the stopped-flow apparatus. These results and analyses verify that the dimerization model, the final equilibrium concentrations used, and the obtained kinetic parameters are valid as a first-approximation.

Contrasting the high association rate constant for the dimerization process, the dissociation rate constant is quite low. The tendency for the 2:2 complex to fall apart relatively slowly may be a result of the high stability of this complex. For example, a doubly encapsulated species is likely more protected from the aqueous phase; thus, encapsulating two pyrene molecules into two CD cavities is likely due to the hydrophobic effect, or protection of the hydrophobic guests from the aqueous phase. Further, two pyrene molecules would fill the two CD cavities to a larger capacity than would a single pyrene molecule. As such, other non-covalent interactions are present to a larger extent in the doubly occupied complex than in a single-pyrene 1:2 complex.

Step (3) involves the formation of the 1:2 pyrene: γ-CD monomer. This monomer species is significant at host concentrations greater than 5 x 10^{-3} M. Congruently, complex kinetics are seen in the stopped-flow traces at higher CD concentrations. These events appear at time-scales greater than approximately 150 ms, i.e. on longer time-scales than that over which the dimerization processes occur. For example, a decrease in the

excimer emission intensity is seen in the stopped-flow traces (Figure 4-7). The fact that the proportion of this decrease in amplitude of excimer emission intensity corresponds the the concentration of 1:2 monomer (Figure 4-8) qualitatively indicates that these kinetic events are due to this complex, and that they are slower than the dynamics of the dimerization process. Before this system can be analyzed quantitatively, however, it is necessary to realize that all of the processes in Scheme 4-2 are linked to some degree. This is because the reactions, i.e. steps (1), (2) and (3), are coupled by a common reagent [56]. In this case, the common reagent is the 1:1 pyrene: γ-CD complex. Reaction mechanisms involving more than one step are often characterized by more than one relaxation time. The number of relaxation times is equal to the number of states (or equilibrium complexes) minus one[56]. However, when certain species are not present in large enough concentration to be detected some of the relaxation times are not detectable [56]. This is likely the case at low CD concentrations where the concentration of the 1:2 monomer complex is relatively low. However, at higher host concentrations, the slow decrease in excimer emission intensity (of mixing scenario (i)) does have a second relaxation time. These two relaxation times are likely due to step (2) and step (3) in Scheme 4-2, as step (1) occurs faster than the time resolution of the instrument. Although this is the case, this first step may still contribute to the overall kinetics of the system. As such, a fully quantitative analysis must consider such a coupling or dependence among all of the reactions, and will require studies where the pyrene concentration is varied over a wider range. Qualitatively, however, a valid observation is that the dimerization of the 1:1 process occurs on a faster time scale than the dynamics involving the 1:2 complex.

4.3.3 Implications of kinetic results

The results of the kinetic study of the pyrene/ γ-CD system indicate that the dimerization process is fast, whereas the 1:2 pyrene: γ-CD monomer complex kinetics are relatively slower. That is, the 2:2 complex is the kinetically driven product, whereas the doubly encapsulated monomer is the thermodynamic mass balance product. This concept is expressed on a larger scale in Scheme 4-3.

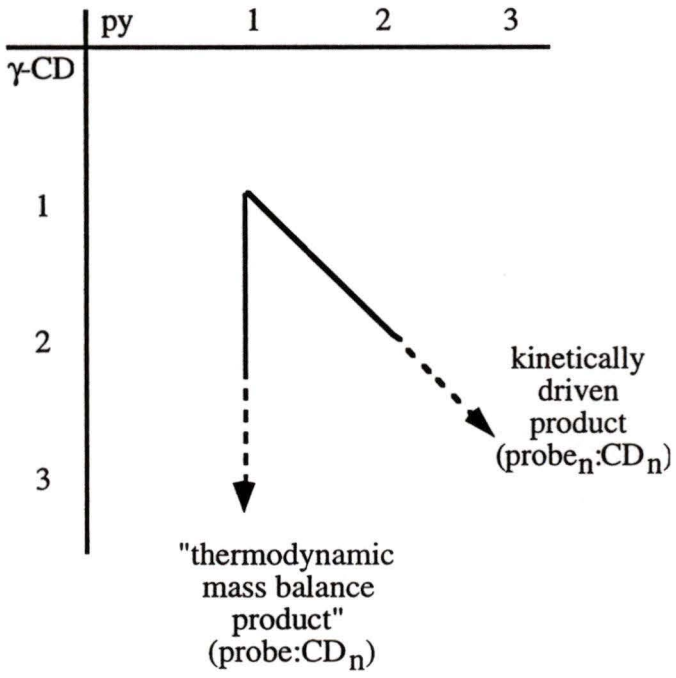

Scheme 4-3: Possible implication of the kinetic results of the pyrene/ γ-CD system. Of the multiple stoichiometric complexes present, the kinetically driven product is of the stoichiometric ratio (probe$_n$- CD$_n$), while that of the thermodynamic mass balance product is (probe-CD$_n$) where $n \geq 2$.

The kinetically driven product seems to be more dependent on the structure of the probe molecule(s) than does the "thermodynamic mass balance" product. For example, for the pyrene/ γ-CD system, the multiple stoichiometric complex in which a larger amount of the hydrophobic CD cavities are filled with hydrophobic moieties forms faster than the complex that contains a smaller amount of hydrophobic species. This may be because the water within the cavity and solvating the hydrophobic pyrene is rapidly removed upon the interaction of the two molecules, thereby driving the n:n complex together. Another driving force for this rapid formation step may be a result of the higher degree of non-covalent interactions involved in an inclusion complex of reduced empty space.

The thermodynamic mass balance product, however, is less dependent on the probe molecule. It involves encapsulation of a probe, but its formation is driven by mass balance, i.e. the excess CD concentration compared to the pyrene concentration, rather than host- guest interactions. This is evident as this product forms more slowly than the n:n complex, i.e. the driving force of formation is not as strong (e.g. lower equilibrium constants), yet it is an important equilibrium at high CD concentrations.

This concept has important implications for cyclodextrin applications and their use as models of supramolecular systems. For example, cyclodextrins may be used as hosts in supramolecular systems to form and perhaps trap products at a higher concentration than expected from a thermodynamic analysis. This is because the kinetic product is transiently at higher concentrations than at the final equilibrium position. Conversely, the stability of the aggregated CDs has implications on how much CD is required for various applications.

4.3.4 Comparison between the pyrene/ γ-cyclodextrin kinetic study and other probe/ cyclodextrin literature results

As discussed in the Introduction, kinetic studies of other probe: CD inclusion complexes have been studied, and the rate constants obtained have been shown to vary quite substantially. In most of these cases, the stoichiometries of the probe: host complexes and their stability constants were determined before the kinetic study was undertaken. In the case of α-CD encapsulating various azo dyes, the stoichiometry is consistently 1:1[33,34]. However, although the observed rate constant varied with CD concentration, the fit of this data to the kinetic model improved when a two-step binding model was considered. This included a fast inclusion process followed by a slow conformational change in the complex, resulting in the (relatively stable) 1:1 complex.

In systems involving larger guest molecules, kinetic studies involving multiple stoichiometric species within β–CD and γ-CD hosts have been investigated. In the case of Crystal Violet[23] (containing three benzyl groups) and Tropaeolin 000 No. 2 [37](containing a naphthyl group), 1:1 and 2:1 probe: γ-CD complexes have been proposed; in the latter system, a 2:2 complex was also proposed, although its dynamics are considered to be fast, i.e. faster than the time resolution of the measuring technique. The perturbation method used in these studies are dominantly the temperature-jump technique using an absorption detection system. In these two systems, the kinetics involving the 2:1 probe: CD complexes were considered slow, and the observed data was analysed as such. It is interesting to note, however, that both of these probe molecules are known to dimerize independently of the host molecule in the aqueous phase. Further, most of these

probe molecules (including the azo dyes in the α-CD complexes) were ionic under the conditions of the studies. As such, the driving force for the 2:2 probe: CD complex is reduced, as the probe is not as hydrophobic. Rather, the 2:1 probe: CD complex would be a more stable complex (and therefore have a slow dissociation step) as the hydrophobic portion of the dimer could be encorporated into the cavity, while the ionic portion is open to the aqueous phase.

Other studies have also proposed the formation of extended CD aggregates with the aid of probe molecules. For example, a naphthyl-substituted β-CD system was found to form non-excimer emitting dimer complexes[57]. That is, rather than self-including the naphthyl moiety, an extended aggregate forms whereby the naphthyl group is encorporated into the β-CD portion of another naphthyl-substituted β-CD molecule. This study also noted that measurements made with freshly prepared solutions did not resemble the equilibrium conditions, i.e. slow dynamics were involved. Another example of probe/CD interactions resulting in CD aggregates involved the probe molecule 2,5-Diphenyloxazole (PPO). Linear aggregates of the repeating unit (2PPO: γ-CD)$_n$ was proposed[58,59].

4.4 Conclusions of kinetic analysis

Although the above examples from the literature are substantially different from the pyrene/ γ-CD system, some interesting comparisons and conclusions can be made. For example, although the characterization of the system should be known before kinetic studies are undertaken, i.e. so that an initial kinetic model may be proposed, the kinetic model employed to analyse the kinetic results can also be used to reinforce and/or alter

the characterization results. Secondly, the probe molecule appears to influence the kinetics of multiple stoichiometric probe: CD complexes. The size, hydrophobicity, ionic character, and (internal) dimerization properties of the probe all influence not only which complexes form, but also the kinetics of the various complexes. This is so, as it appears the stability of the complex influences the kinetic role it has in the total system. For example, the "mass balance product", i.e. a probe: CD complex that contains one probe molecule and two or more CD molecules, does not appear in the literature studies (involving chemical perturbation) discussed above involving ionic probe molecules. It appears that encapsulation by more than one (hydrophobic) CD cavity is not favored in such cases. As such, the probe molecule appears to be very influential in the stability and dynamic processes occuring in the mulitiple stoichiometric CD systems, including both the CD aggregated and probe-driven n:n complexes.

5. Conclusions

The pyrene/ γ-CD supramolecular guest: host system was characterized to facilitate an investigation into the dynamics of a supramolecular system containing multiple stoichiometric complexes. Thermodynamic characterization of this system has been reported by several authors while its dynamic characterization has not. As the previously reported thermodynamic characterization results are ambiguous and inconsistent, we reinvestigated this aspect of the system using several techniques, such as quenching, steady-state fluorescence, and time-resolved fluorescence. The data obtained by the combination of the various techniques allowed for a comparative and complementary analysis. For example, using various host and quencher concentrations, the steady-state fluorescence data (e.g. the pyrene hydrophobicity indicator, the R(I/III) ratio, and the excimer-to-monomer intensity ratio) together with the time-resolved fluorescence data analysis indicated that a fairly protected monomer in a relatively hydrophobic environment is present in the system at higher γ-CD concentrations. That is, a 1:2 pyrene: γ-CD monomer exists in solution in addition to free aqueous pyrene and that within a 1:1 pyrene: γ-CD complex. Excimer fluorescence emission indicated the presence of a complex containing two pyrene molecules. The decrease in the excimer-to-monomer intensity ratio upon increasing the pH of the system to above the pK_a of the CD hydroxyl groups indicated that the complex that gives rise to the excimer emission is a 2:2 complex, as the repulsion between the deprotonated hydroxyl groups forces the two 1:1 components apart. Further, the inability of the (aqueous) iodide quencher to reduce the lifetime of the excimer emitting complex to the degree expected indicates that this complex is fairly protected from the aqueous phase, such as within two CD cavities.

The kinetics of the pyrene/ γ-CD system are quite complex, and appear to occur over the minute time-scale. However, the relatively fast kinetics, i.e. the events occuring in the ms time-scale, may be analyzed in terms of a dimerization process where two 1:1 complexes come together to form the 2:2 pyrene: γ-CD complex. This complex is considered the kinetic product, as it is the first of the mulitiple stoichiometric complexes to form when solutions containing aqueous pyrene and γ-CD are mixed. The relatively slow dissociation of this complex, however, should be noted. The 1:2 complex is proposed to be the "mass balance product". Its formation is delayed relative to the initial formation of the 2:2 complex, and the complexation process is proposed to be driven by the presence of excess CD. The formation of a doubly encapsulated pyrene monomer is a reasonable hypothesis as the hydrophobic pyrene molecule is likely to be quite stable within the hydrophobic environment of two CDs. Thus, the kinetic events of the supramolecular system involving multiple stoichiometric complexes depends on both the properties of the probe (e.g. structure, hydrophobicity, size), as well as on the aggregation of CDs. This latter step seems to occur with the aid of the probe.

The concepts and methodologies proposed in this study contribute to the field of supramolecular dynamics, and could influence the way CDs are used in applications and as models of supramolecular systems. Further, they could be important in the way future studies are undertaken to further investigate the interesting dynamics involved in guest: CD supramolecular systems containing multiple stoichiometric complexes.

6. References

(1) Gilbert, A.; Baggott, J. *Essentials of Molecular Photochemistry*; Blackwell Scientific Publications: Oxford, 1991.

(2) Klessinger, M.; Michl, J. *Excited States and Photochemistry of Organic Molecules*; VCH Publishers, Inc.: New York, New York, 1995.

(3) Bohne, C.; Redmond, R. W.; Scaiano, J. C. In *Photochemistry in Organized & Constrained Media*; Ramamurthy, V., Ed.; VCH Publishers, Inc.: New York, 1991; pp 79-132.

(4) Laidler, K. J. *Chemical Kinetics, Third Edition*; Third ed.; Harper & Row, Publishers, Inc.: New York, 1987.

(5) Lakowicz, J. R. In *Principles of Fluorescence Spectroscopy*; I ed.; Plenum Press: New York, 1983; pp 257-295.

(6) Clements, J. H.; Webber, S. E. *J. Phys. Chem. A* **1999**, *103*, 2513-2523.

(7) Sillen, A.; Engelborghs, Y. *Photochem. Photobiol.* **1998**, *67*, 475-486.

(8) Webber, S. E. *Photochem. Photobiol.* **1997**, *65*, 33-38.

(9) Birks, J. B. *Photophysics of Aromatic Molecules*; Wiley- Interscience: London, 1969.

(10) Saenger, W. *Angew. Chem. Int. Ed. Engl.* **1980**, *19*, 344-362.

(11) Connors, K. A. *Chem. Rev.* **1997**, *97*, 1325-1357.

(12) Wenz, G. *Angew. Chem. Int. Ed. Engl.* **1994**, *33*, 803-822.

(13) Kano, K.; Takenoshita, I.; Ogawa, T. *Chem. Lett.* **1982**, 321- 324.

(14) Kano, K.; Takenoshita, I.; Ogawa, T. *J. Phys. Chem.* **1982**, *86*, 1833-1838.

(15) Herkstroeter, W. G.; Martic, P. A.; Evans, T. R.; Farid, S. *J. Am. Chem. Soc.* **1986**, *108*, 3275-3280.

(16) Yang, H.; Bohne, C. *J. Photochem. Photobiol. A: Chem.* **1995**, *86*, 209-217.

(17) Hamai, S. *Bull. Chem. Soc. Jpn.* **1996**, *69*, 543- 549.

(18) Hamai, S.; Hatamiya, A. *Bull. Chem. Soc. Jpn.* **1996**, *69*, 2469- 2476.

(19) Barros, T. C.; Stefaniak, K.; Holzwarth, J. F.; Bohne, C. *J. Phys. Chem. A* **1998**, *102*, 5639- 5651.

(20) Schneider, H.-J.; Blatter, T.; Simova, S. *J. Am. Chem. Soc.* **1991**, *113*, 1996-2000.

(21) Herkstroeter, W. G.; Martic, P. A.; Farid, S. *J. Chem. Soc. Perkin Trans. 2* **1984**, 1453-1457.

(22) Balabai, N.; Linton, B.; Napper, A.; Priyadarshy, S.; Sukharevsky, A. P.; Waldeck, D. H. *J. Phys. Chem. B* **1998**, *102*, 9617-9624.

(23) Schiller, R. L.; Coates, J. H.; Lincoln, S. F. *J. Chem. Soc. Faraday Trans.* **1984**, *80*, 1257-1266.

(24) Villani, R. P.; Lincoln, S. F.; Coates, J. H. *J. Chem. Soc. Faraday Trans.* **1987**, *83*, 2751-2756.

(25) Hollas, M.; Chung, M.-A.; Adams, J. *J. Phys. Chem. B* **1998**, *102*, 2947-2953.

(26) Xu, W.; Demas, J. N.; DeGraff, B.; Whaley, M. *J. Phys. Chem.* **1993**, *97*, 6546-6554.

(27) Hamai, S. *J. Phys. Chem.* **1990**, *94*, 2595- 2600.

(28) De Feyter, S.; van Stam, J.; Boens, N.; De Schryver, F. *Chem. Phys. Lett.* **1996**, *249*, 46-52.

(29) Benesi, H. A.; Hildebrand, J. H. *J. Am. Chem. Soc.* **1949**, *71*, 2703-2707.

(30) Hamai, S. *Bull. Chem. Soc. Jpn.* **1982**, *55*, 2721-2729.

(31) Hamai, S. *J. Phys. Chem.* **1989**, *93*, 6527-6529.

(32) Kobayashi, N.; Saito, R.; Hino, H.; Hino, Y.; Ueno, A.; Osa, T. *J. Chem. Soc. Perkin Trans. 2* **1983**, 1031- 1035.

(33) Cramer, F.; Saenger, W.; Spatz, H.-C. *J. Am. Chem. Soc.* **1967**, *89*, 14-20.

(34) Hersey, A.; Robinson, B. *J. Chem. Soc. Faraday Trans.* **1984**, *80*, 2039-2052.

(35) Liao, Y.; Frank, J.; Holzwarth, J. F.; Bohne, C. *J. Chem. Soc. Chem. Commun.* **1995**, 199-200.

(36) Hashimoto, S.; Thomas, J. K. *J. Am. Chem. Soc.* **1985**, *107*, 4655-4662.

(37) Clarke, R. J.; Coates, J. H.; Lincoln, S. F. *J. Chem. Soc. Faraday Trans.* **1984**, *80*, 3119-3133.

(38) Munoz de la Pena, A.; Ndou, T.; Zung, J. B.; Warner, I. M. *J. Phys. Chem.* **1991**, *95*, 3330-3334.

(39) Keehn, P. M.; Rosenfeld, S. M. *Cyclophanes*; Academic Press: New York, 1983; Vol. 1.

(40) Mathews, C. K.; van Holde, K. E. *Biochemistry*; The Benjamin/ Cummings Publishing Company, Inc.: New York, 1990.

(41) Van Dyke, D.; Pryor, B. A.; Smith, P.; Topp, M. *J. Chem. Educ.* **1998**, *75*, 615-620.

(42) Kalyanasundaram, K.; Thomas, J. K. *J. Am. Chem. Soc.* **1977**, *99*, 2039-2044.

(43) Ju, C.; Bohne, C. *Photochem. Photobiol.* **1996**, *63*, 60-67.

(44) Yorozu, T.; Hoshino, M.; Imamura, M. *J. Phys. Chem.* **1982**, *86*, 4426-4429.

(45) Elliott, N.; Ndou, T. T.; Warner, I. M. *J. Inclusion Phenom. Mol. Recognit. Chem.* **1993**, *16*, 99-112.

(46) Ju, C. M. Sc. Thesis, University of Victoria: Victoria, 1995; p 122.

(47) Nelson, G.; Warner, I. M. *J. Phys. Chem.* **1990**, *94*, 576-581.

(48) Ueno, A.; Suzuki, I.; Osa, T. *J. Chem. Soc. Chem. Commun.* **1988**, 1373-1374.

(49) Ueno, A.; Suzuki, I.; Osa, T. *J. Am. Chem. Soc.* **1989**, *111*, 6391- 6397.

(50) De Feyter, S.; van Stam, J.; Imans, F.; Viaene, L.; De Schryver, F.; Evans, C. *Chem. Phys. Lett.* **1997**, *277*, 44-50.

(51) Agnew, K. A.; McCarley, T. D.; Agbaria, R. A.; Warner, I. M. *J. Photochem. Photobiol. A: Chem.* **1995**, *91*, 205-210.

(52) Patonay, G.; Rollie, M. E.; Warner, I. M. *Anal. Chem.* **1985**, *57*, 569- 571.

(53) Winnik, F. M. *Chem. Rev.* **1993**, *93*, 587-614.

(54) Barros, T. C.; Adronov, A.; Winnik, F. M.; Bohne, C. *Langmuir* **1997**, *13*, 6089-6094.

(55) Ware, W. R.; James, D. R. *Chem. Phys. Lett.* **1985**, *120*, 455-459.

(56) Bernasconi, C. F. *Relaxation Kinetics*; Academic Press, Inc.: New York, 1976.

(57) McAlpine, S. R.; Garcia-Garibay, M. A. *J. Am. Chem. Soc.* **1998**, *120*, 4269-4275.

(58) Agbaria, R. A.; Gill, D. *J. Phys. Chem.* **1988**, *92*, 1052-1055.

(59) Agbaria, R. A.; Gill, D. *J. Photochem. Photobiol. A: Chem.* **1994**, *78*, 161-167.

VITA

Surname: Dyck Given Names: Andria Sara Marie

Place of Birth: Saskatoon, Saskatchewan, Canada

Educational Institutions Attended:

University of Victoria	1998 to 2001
University of Saskatchewan	1994 to 1998

Degrees Awarded:

B.Sc. (Honours), University of Saskatchewan	1998

Honours and Awards:

NSERC Postgraduate Scholarship	1998 to 2000
President's Research Scholarship (University of Victoria)	1998, 1999
Department of Chemistry (University of Saskatchewan)	
Convocation Award	1998
Canada Scholarship in Science and Engineering	1994 to 1998
Hypercube Award	1998
Society of Chemical Industry (Canadian Section) Merit Award	1998
Canadian Society for Chemistry Award	1996
Thorvaldson Undergraduate Scholarship	1996
Introductory Chemistry Award	1996
CRC Press Freshman Chemistry Achievement Award	1995
NSERC Student Research Award	1995

Partial Copyright License

I hereby grant the right to lend my thesis to users of the University of Victoria Library, and to make single copies only for such users or in response to a request from the Library of any other university, or similar institution, on its behalf or for one of its users. I further agree that permission for extensive copying of this thesis for scholarly purposes may be granted by me or a member of the University designated by me. It is understood that copying or publication of this thesis for financial gain shall not be allowed without my written permission.

Title of Thesis:

Characterization and Dynamics of Pyrene and Gamma-Cyclodextrin Complexes of Multiple Stoichiometries

Author: [redacted]

Andria Sara Marie Dyck

January 17, 2001